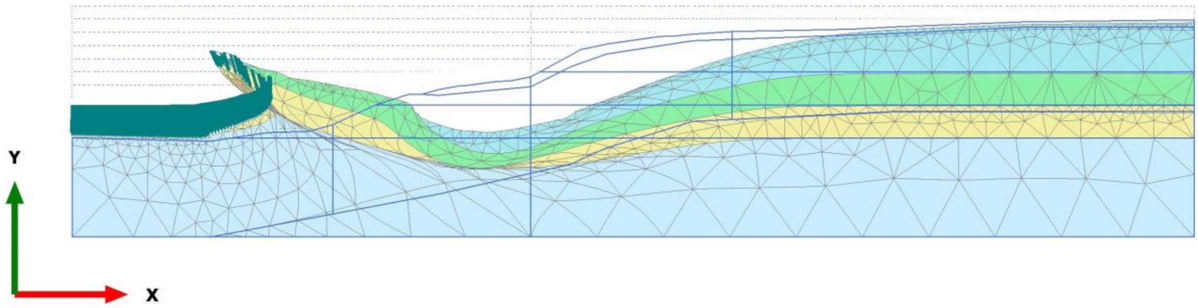

Modelling of Anisotropy in Slope Stability Problems

A study about slope stability in Göta Älv valley

Master's thesis in Infrastructure and Environmental Engineering

ANDREA SVENSSON

DEPARTMENT OF ARCHITECTURE AND CIVIL ENGINEERING

CHALMERS UNIVERSITY OF TECHNOLOGY
Gothenburg, Sweden 2020
www.chalmers.se

Master's thesis ACEX30

Modelling of Anisotropy in Slope Stability problems

A study about slope stability in Göta Älv valley

ANDREA SVENSSON

CHALMERS
UNIVERSITY OF TECHNOLOGY

Department of Architecture and Civil Engineering
Division of Geology and Geotechnics
Chalmers University of Technology
Gothenburg, Sweden 2020

Modelling of Anisotropy in Slope Stability Problems
A study about slope stability in Göta Älv valley
ANDREA SVENSSON

Supervisors: Carolina Sellin, Architecture and Civil Engineering
Khaled Alaydi, WSP
Examiner: Minna Karstunen, Architecture and Civil Engineering

Department of Architecture and Civil Engineering
Division of Geology and Geotechnics
Chalmers University of Technology
SE-412 96 Gothenburg
Telephone +46 31 772 1000

Cover: An illustration of a slope in failure.

Printed by Chalmers Reproservice
Gothenburg, Sweden 2020

Modelling of Anisotropy in Slope Stability Problems
A study about slope stability in Göta Älv valley
ANDREA SVENSSON
Department of Architecture and Civil Engineering
Chalmers University of Technology

Abstract

The purpose of this Master's thesis is to analyse the effects of considerations for anisotropy in slope stability problems using two different calculation models. The slope stability is investigated for a slope located in Göta Älv valley with high representation of quick clay. From Göta Älv valley are field and laboratory test data retrieved and evaluated. The retrieved test results from laboratory are from Triaxial, Oedometer and CRS tests. All data are used for the purpose of modelling in two different softwares: Geostudio SLOPE/W and PLAXIS 2D. In PLAXIS 2D the Creep-SCLAY1S model is used for the calculation of the slope stability. Results retrieved defines different slip surfaces and factors of safety. For the same slope section, the factors of safety are calculated to be between 1.15-1.18 in Geostudio SLOPE/W and between 1.36-3.0 in PLAXIS 2D. All laboratory test results are used to model anisotropy when using Creep-SCLAY1S since the model uses input parameters such as stress ratio, state variable for anisotropy and evaluation of anisotropy. For the calculation in Geostudio SLOPE/W anisotropy is considered through dividing the soil into vertical layers. The main conclusion is that Creep-SCLAY1S considers anisotropy in a more detailed way meanwhile are more assumptions and simplifications used for Geostudio SLOPE/W. The certainty of the factor of safety is important for slope stability analyses both for research and ethical purposes.

Keywords: Slope stability, Creep-SCLAY1S, PLAXIS 2D, Geostudio SLOPE/W, Göta Älv.

Acknowledgements

I would like to thank my examiner Minna Karstunen for all inputs during the work. I would also like to thank my supervisor Carolina Sellin for all valuable help with the modelling and report writing. I wish to thank all of my colleagues at WSP for the support and especially I would like to thank my supervisor, Khaled Alaydi, at WSP for all help. Finally, I would like to thank the department of Delegation for Göta Älv at Swedish Geotechnical Institute for letting me participate in meetings connected to Smådala.

Andrea Svensson, Gothenburg, June 2020

Contents

List of Figures

List of Tables

Nomenclature

Greek letters

α_0	Initial inclination of reference yield surface
γ_{sat}	Unit weight saturated soil
γ_w	Unit weight water
ϵ_a	Axial strain
ϵ_q	Deviatoric strain
ϵ_r	Radial strain
ϵ_v	Volumetric strain
ϵ_q^c	Creep deviatoric strain
ϵ_q^e	Elastic deviatoric strain
ϵ_v^c	Creep volumetric strain
ϵ_v^e	Elastic volumetric strain
η	Stress ratio
κ*	Modified swelling index
λ*	Modified compression index
λ_i*	Intrinsic modified compression index
μ_i^*	Modified creep index
ν'	Poisson's ratio
ξ	Rate of destructuration
σ	Total stress
σ'	Effective stress
σ'_1	Effective stress, axial direction
σ'_3	Effective stress, radial direction
σ'_p	Pre-consolidation pressure
σ'_{v0}	Vertical effective stress
τ	Reference time
ϕ'	Friction angle
χ_0	Initial amount of bonding
ω	Absolute effectiveness of rotational hardening
ω_d	Relative effectiveness of rotational hardening

Roman letters

a	Absolute rate of destructuration
b	Relative rate of destructuration
c	Cohesion
G	Elastic shear modulus
K	Elastic bulk modulus
K_0^{nc}	Stress ratio, normally consolidated state
M_c	Critical state line in compression
M_e	Critical state line in extension
p'	Mean effective stress
p'_{eq}	Equivalent mean stress
p'_p	Isotropic preconsolidation pressure
q	Deviatoric stress
S_t	Sensitivity
u	Pore water pressure
z	Depth

Abbrevations

CSS	Current stress surface
ICS	Intrinsic compression surface
NCS	Normal consolidation surface
OCR	Overconsolidation ratio
POP	Preoverburden pressure
FS	Factor of safety

1

Introduction

1.1 Background

Göta Älv valley consists of slopes towards the river created by years of erosion. The geology of the slopes are mainly represented by clay on top of a friction material layer and bedrock (SGU, 2019). Anisotropy has an impact on slope stability as the undrained shear mobilises differently for different parts of the slope. The anisotropy can be tested in the laboratory with triaxial tests, considering the two extremes of triaxial compression and extension. Normally undrained shear strength is determined from tests and empirical values (IVA, 1995). The empirical behaviour for anisotropy in a slope is based on that the shear strength is decreased in the passive zone and increased in the active zone, when basing the estimated in field vane test restults. When SGI (Swedish Geotechnical Institute) and WSP have investigated the slope stability for an area in Göta Älv valley, it was discovered that the empirical values do not apply at high OCR. The tests that have been performed do not agree with the expectations for the undrained shear strength in extension. Retrieved results indicate that the values for the undrained shear strength in direct shear are lower than for shearing in extension. Because of this behaviour can the results from shear strength in extension not be used for further work (WSP, personal communication, December 2, 2019).

1.2 Purpose

The main aim is to evaluate the topography, soil condition and stability of a slope in Göta Älv valley by applying two different calculation methods/soil models. The aim is also to analyse the use of all laboratory data for the slope stability calculation in the Göta Älv valley that represents anisotropy. This is done through collecting data from the old and new field- and laboratory tests performed on soil sample from different parts of Göta Älv valley. The slope stability should be evaluated through analysing anisotropy at different soil characteristics (OCR, sensitivity and critical state lines).

1.3 Limitation

This Master's thesis is considering a problem that appears along the complete Göta Älv valley. The analysis will be, however, limited to one slope profile located in Göta Älv valley as a representation for that specific geological site.

The evaluation of data regarding finding a deviation to empirical values will primary be neglected. If there is time, more analyses can be performed to define new possible deviations of empirical values. This could be done by modelling several slope sections.

The modelling will be limited to perform basic modelling in Geostudio SLOPE/W and use PLAXIS 2D for an advanced model (Creep-SCLAY1S).

1.4 Research questions

Research questions to be answered in this project:

- How is the anisotropy considered in the different modelling methods (Geostudio SLOPE/W and Creep-SCLAY1S)?
- Is it possible to consider anisotropy in the zone of extension (passive zone) of the slope?
- How is the factor of safety affected by considerations for anisotropy in both zone of compression and extension of the slope?
- Is it possible to consider all retrieved data from laboratory tests?

1.5 Ethical considerations

Ethical aspects need to be considered when choosing which part of the Göta Älv valley that should be analysed. To get a more conservative result regarding the factor of safety is it most effective to choose the worst-case scenario both in slope topography and when evaluating data.

A good method/model for evaluating slope stability is important for ecology and society since unwanted failure of slopes can be predicted. The optimisation of a method/model can contribute to a reduction of mitigation measurements which leads to financial savings. With less need for measurements, the natural environment can be more preserved.

Göta Älv river is a source for drinking water for several municipalities along the river. If a slope fails it can contribute to major problems in the drinking water treatment and distribution. Göta Älv is also an important resource for marine transportation between the Western Sweden and the sea (Kattegat) (SGI, 2012).

2

Theory

In this chapter, information about the analysed site described is considering both geography, geology and hydrogeology. Basic information about geotechnical parameters and the models used for the calculation are described for further understanding of the analysis.

2.1 Göta Älv river

Göta Älv is a river located in the western part of Sweden, see Figure 2.1. The river starts in lake Vänern in Vänersborg and flows towards Gothenburg where it flows out in Kattegat, see Figure . With a catchment area of about 50 000 km^2 and a flow from lake Väner, Göta Älv is one of Swedens most abundant rivers. Along the Göta Älv river there are five other rivers that influents; Mölndals ån, Säveån, Lärejån, Grönån and Slumpån (SGI, 2012).

The river is approximately 93 km long from Vänersborg to Gothenburg and has a height difference of 44 meters where dams and power stations are included. The dams and power stations are located in Vargön, Trollhättan and Lilla Edet (SGI, 2012). These power stations can regulate the flow in the river from lake Vänern which can affect the risk for landslides along Göta Älv valley (Andree, 2006). Approximately 17 km northeast of Gothenburg in Bohus is Göta Älv river divided into two streams where the river that flows north of the island Hisingen is named Nordre Älv and the river south of Hisingen is still named Göta Älv. In this fork, about 70% of the total flow of the Göta Älv river is flowing into the Nordre Älv branch and the rest flows through Gothenburg to Kattegat (SGI, 2012).

Göta Älv river is an important source for drinking water, transport and power. The river acts both as a recipient and a source of the drinking water for eight municipalities along the river. The bigger cities like Vänersborg, Trollhättan and Gothenburg are three of these eight municipalities that are dependent on the drinking water from Göta Älv. The water from Göta Älv is also used in some industries for cooling or processing systems. Hydroelectric power is received from the three power stations along Göta Älv and represents about 4-5% of the total amount of hydroelectrical power produced in Sweden per year (SGI, 2012).

Figure 2.1: *Map over Göta Älv river. Flowing from Vänersborg to Göteborg along the highway E45 on the western side (Eniro, 2020)*

2.2 Geology

The geology in Sweden was formed during the last ice age which happened about 115 000 to 10 000 years ago. During the beginning of this time, a big mass of ice was formed to a glacier and covered bigger parts of northern Europe. The glacier did slowly move and collected the materials lying in connection to the central parts of the ice which could have a magnitude up to a couple of kilometres. The material from the central part of the ice was due to movements of the ice transported to the edge of the glacier where it got deposited. This material is today known as till and can be found on top of the bedrock (SGU (a), n.d.).

Next process of the ice age was when the glacier started to melt from south to north. During this time a large amount of meltwater was flowing in under the glacier mainly in meltwater tunnels. The meltwater was the main transportation of eroded materials and materials from the glacier. Depending on the velocity of the melting water and the grain size of the material, different soils could be created at different locations and shapes. When there was a higher velocity of the melting water the larger sediments got deposited. This material is today represented by sand and gravel. The more fine-grained materials like silt and clay got deposited when the velocity of the melting water was slower. This happened mostly where the melting water was reaching lakes or oceans. The shape of the soils today depends on the location of the ice at the time that the material got deposited (SGU (a), n.d.). Depending on the movements of the glacier and the flow of the water, different shapes were created. When glacier rivers reached the lake created from the melting water at the edge of the glacier a delta formation could be created by deposition of material in a triangular-shaped area (Knappett and Craig, 2012).

During the glacial period was the earth crust compressed from the heavy mass of the glacial ice. This contributed to that larger parts of today's land areas were covered in water (SGU (a), n.d.). The level that this water line reached during the ice age is named the highest coastline and is about 100 meters above the current sea level in Gothenburg (SGI, 2012). After the glacial ice had melted, the earth crust did slowly extend to today's topography and water levels, this process is still ongoing.

The geology in Göta Älv valley consists of bedrock at the bottom, followed by a layer of till in varying thickness. On top of this is mainly clay found with elements of glaciofluvial sediments. In some parts of the valley, wave-washed materials can be found in the slopes towards Göta Älv. The clay can be divided into glacial clay and post-glacial clay (SGI, 2012). A quarternary map with the materials found at the ground surface can be seen in Appendix A.1.

2.2.1 Clay

There are two different types of clay that have been formed either during or after the glacier existed. The clay formed when the glacial ice was still melting is the glacial clay. Here the fractions in the water settled when the melting water reached slower velocities. In many parts of Sweden, it is common that the glacial sediment soils consist of layering with clay and silt but in the western part of Sweden, the clay and silt got deposited at the same time due to the marine environment. The glacial clay is often found in deeper locations in the soil. The clay formed after the glacial ice melted is the post-glacial clay and can be found on top of the glacial clay at more shallow locations in the soil. The post-glacial clay was created through sedimentation of materials in lakes and seas. The material that got deposited and created post-glacial clay was often from eroded glacial clay located in shallow waters (SGU (a), n.d.).

Clays that got deposited in the marine environment could consist of salt from the salt in the seawater. When the glacial ice had melted and the earth crust slowly expanded the groundwater flow in the soils could contribute to that the salt in the clay leached out. When this type of clay is vibrated or stirred the connection between the particles can break and the clay reaches failure where the strength in the soil is lost. The term of this type of clay is quick clay and is common in the areas around Gothenburg and coastlines (SGI, 2012). Quick clay can be recognised through the value of sensitivity which can be retrieved from laboratory tests (Karstunen and Amavasai, 2017). Sensitivity is a measurement of the natural ratio of strength in a soil (Sivasithamparam, 2012).

2.3 Groundwater conditions

Groundwater is water that flows within the pores shaped between the solid particles that a soil is made of. The groundwater in a soil has a certain pressure defined as the pore pressure. The pore pressure is one influencing factor to stiffness and strength of a soil. Pore water pressure is measured compared to the atmospheric pressure and the zero level starts where the water table is located. The water table or phreatic surface is normally defined as the measured groundwater level. Below the water surface, the pressure is in most cases assumed to be hydrostatic with depth. Normally an increase of 10 kPa per meter below the water table is used in hydrostatic conditions. The pore water pressure can have artesian conditions if a layer with high permeability is confined by a layer of low permeability. The artesian conditions can be noticed when the pore water pressures are higher than hydrostatic conditions (Knappett and Craig, 2012).

The groundwater conditions in the Göta Älv valley are mainly affected by the geology and topography. The geology affects the groundwater due to the characteristics of the soils in the valley. As mentioned before consists the valley of clay on top of till and bedrock. The clay found in Göta Älv valley has normally a quite low permeability which contributes to low groundwater flow. Therefore, are the groundwater conditions dependent on layers of other friction materials or cracks within the clay layer. The occurrence of groundwater can be divided into four zones. The first zone is in the first layer represented by a dry crust which has high permeability and contributes to the occurrence of groundwater in some locations along the valley. The second zone is the upper part of the clay layer which consist of cracks where the water can be transported. These cracks contribute to a higher permeability than in the third zone which is the deeper part of the clay layer without cracks. The fourth and last zone for groundwater is the layer of friction material/till located on top of the bedrock. This layer has a high permeability. The pressures through the different zones can be assumed to be hydrostatic with some deviation in zone three (Persson, Bengtsson, Lundström and Karlsson, 2011).

2.4 Geotechnical parameters

The structure of a soil can be described as solid particles enclosing voids which can be filled with either water or air. There is a force acting between every particle in a soil. When an unsaturated soil is under compression it is the air that is compressed, since the solid particles and the water has low compressibility or are incompressible. The compression contributes to change in volume of the mass through rolling and sliding of the particles in the soil. These new positions of the particles contribute to change in forces between the particles. When the voids are only filled with water and no air the soil can be defined as fully saturated and the mass can only change in volume if the water can dissipate during compression (Knappett and Craig, 2012). An example of the principle of a soil structure can be seen in Figure 2.2.

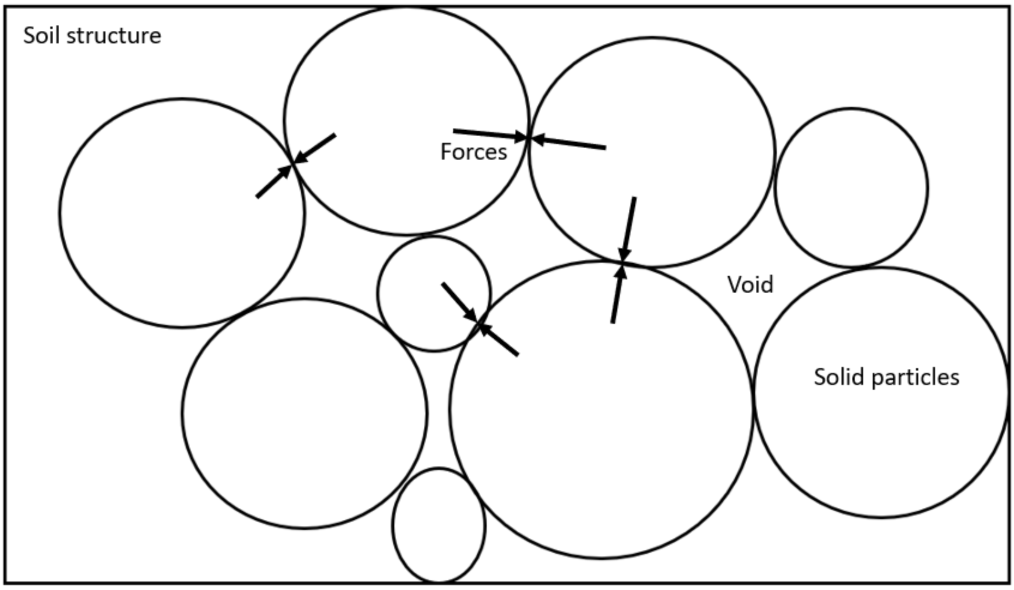

Figure 2.2: *Visualisation of a soil structure with internal forces between particles.*

2.4.1 Effective stress

The principle of effective stress of a soil was first defined by Terzaghi in 1943. When creating the principle a plane through a soil with particles and voids were considered. In every connection between the particles, there appears certain stress due to a force divided over an area. When summing up all these connection over the plane and considering the impact of pore pressures a principle of effective stress could be determined. This principle considers the effective stress in a fully saturated soil (Knappett and Craig, 2012). The relationship is described in equation (2.1).

$$\sigma = \sigma' + u \tag{2.1}$$

Here the σ is represented by the total normal stress that acts on a plane in the soil. The unit of the total normal stress is force per unit area. The u is represented by the pore water pressure which is the pressure of the water in the voids. Lastly, the σ' is defined as the effective normal stress. This is the stress that is transmitted through the structure of the soil (Knappett and Craig, 2012).

The total stress can be calculated by considering a soil with a horizontal surface, a water table and a depth z. This is defined as the total vertical stress and can be calculated using the unit weight (γ_{sat}) of the soil where both solids and water are included, see equation (2.2) (Knappett and Craig, 2012).

$$\sigma_v = \gamma_{sat} z \tag{2.2}$$

With the same principle can the hydrostatic pore water pressure be calculated using the unit weight of water (γ_w) and the depth z using the water surface as level zero, see equation (2.3) (Knappett and Craig, 2012).

$$u = \gamma_w z \tag{2.3}$$

2.4.2 Consolidation

When a fully saturated soil gradually reduces in volume due to a change in effective stress the term consolidation is used. This occurs when the pore water drains from the soil or when there is a reduction of pore water pressure due to groundwater pumping. The opposite of consolidation is swelling and appears when the volume increases due to negative excess pore pressure. When consolidation takes place it happens that there are vertical displacements of the soil surface, this is defined as consolidation settlement (Knappett and Craig, 2012). Depending on the permeability of the soil the volume change can happen immediately or with a delay. For soils like clay or silt with low permeability are the volume changes delayed or slowed and contributes therefore to time-dependent behaviour of the settlements (Sällfors, 2013).

Consolidation can define stress history. In geotechnical terms there are usually two different consolidation designations of a soil: Normally consolidated or overconsolidated. The difference between these terms is if the present effective stress is equal or lower than the historical maximum effective stress that the soil has been subjected to. If the effective stress is higher or equal to the historically subjected stresses, the soil is normally consolidated. If the effective stress is lower, the soil is overconsolidated. The consolidation can be defined with an overconsolidation ratio (OCR) where the pre-consolidation pressure (σ'_p) is divided with present vertical effective stress (σ'_{v0}) (Knappett and Craig, 2012), see equation (2.4).

$$OCR = \frac{\sigma'_p}{\sigma'_{v0}} \tag{2.4}$$

2.4.3 Drained and undrained conditions

A soil can be considered to have drained or undrained conditions. When a soil due to dissipation has high permeability and the pore water pressure does not change during loading, the conditions are considered to be drained. The drained conditions can in some cases appear in soils with low permeability due to slow loading rate which contributes to no change in pore pressure. Undrained conditions appear in soils with low permeability or during fast loading. In these situations can the water in the soil not flow into or out of the soil which leads to a build-up of excess pore pressure. An example of a soil type that often is considered undrained is clay (Abed, Korkiala-Tanttu, 2018).

2.5 Slope stability

When the failure surface is in both horizontal and vertical direction the concept slope stability is used. Slope stability problems are therefore considered to be two-dimensional (Knappett and Craig, 2012). To describe the stability in a slope three zones of stresses are defined. In the upper part of the slope defined as the active zone is the soil affected by compression stresses. In the lower part of the slope defined as the passive zone is the soil affected by extension stresses. The third zone that appears is the transition zone between compression and extension (Sällfors, 2013). The three zones are used to model anisotropic behaviour in models that are not created to consider anisotropy. The instability of a natural slope depends on the weight of the soil in the slope section (Knappett and Craig, 2012).

The analysis of a slip surface can be divided into three different behaviours; rotational, translational or compound slip. The rotational slip surface can appear circular or non-circular. The circular slip surface is often due to soil conditions that are homogeneous and assumed isotropic, meanwhile non-circular slip surface is due to non-homogeneous anisotropic soil conditions. Translational and compound slip surface appear when there are discontinuities in the soil considering the strength. The discontinuity can be adjacent to the soil or cross the soil which affects the shape of the slip surface (Knappett and Craig, 2012).

The slope stability is defined with a factor of safety which indicates if there is a failure or not in the slope. If the value is lower than one the slope stability may reach failure. When the factor of safety is determined it is common to divide undrained and drained calculations due to the differences in strengths of the soil in the different conditions. A combined analysis is possible and is often used for clay. The combined analysis uses the lowest strength in the soil from either drained or undrained for every specific case (Sällfors, 2013).

Isotropy and anisotropy are important considerations in slope stability analyses. Isotropy is when the soil has the same characteristics in all direction and anisotropy is when the soil has different characteristics in different directions (Knappett and Craig, 2012).

2.5.1 Limit equilibrium methods

The limit equilibrium method is a method used for analysing slope stability. The method assumes that the soil behaves perfectly plastic and the failure behaviour follows the Mohr-Coulomb failure criterion.

Based on the limit equilibrium method there are several improved methods by Morgenstern and Price, Bishop, Janbu and Spencer developed in the 1960s. All of the refined methods use vertical slices for analysing the slope stability (Yu, Salgado, Sloan and Kim, 1998). The principle of the forces acting on a slice in a slope is presented in Figure 2.3. Normal and shear forces are acting on all edges of the slice which is within the soil. The main difference between the refined methods is which equations of static equilibrium that are used to describe the relationship between the slices shear and normal forces (Krahn, 2003).

The limit equilibrium method requires that the slip surface is assumed and in most cases, it is assumed to have a circular shape, see slip surface in Figure 2.3. In reality, the slip surface is not always circular. Due to non-homogeneity in the soil, it is more reasonable for the slip surface to be non-circular. Hence this is the case, the minimum factor of safety is often connected to non-circular surfaces. The non-homogeneity can be due to differences in pore water pressures or strength parameters (Morgenstern and Price, 1965).

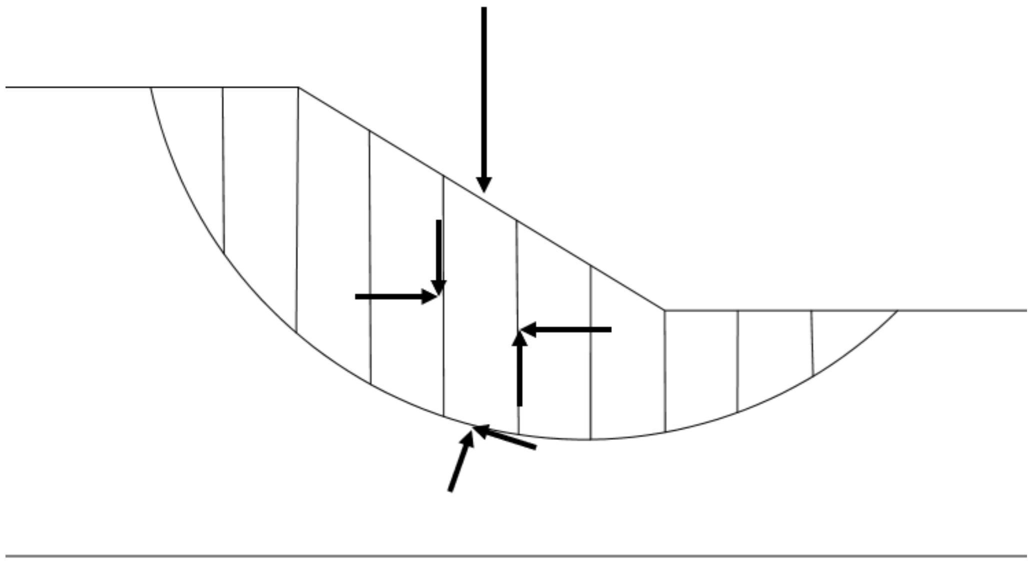

Figure 2.3: *Normal and shear forces of a slice in a slope due to limit equilibrium.*

2.5.2 Finite element method

The finite element method is a numerical method and can simulate the slope stability behaviour. The main difference from the limit equilibrium method is that the problem analysed needs fewer simplifications. In this method, the soil is divided into small regions in the shape of triangles or rectangles. These regions are called finite elements and are connected through nodes. Each element is represented with a certain geometry and value of parameters. The unknown parameters that are solved with the method are defined in the nodes. All variables in the nodes are solved using mathematically analyses where the value of each node from the elements are represented in a matrix. The element matrices are then combined to algebraic equations that represent the total soil system analysed. To solve the problem and the unknown variables the algebraic equations are solved (Abed and Korkiala-Tanttu, 2018).

2.6 Data collection

For the evaluation and calculation of different parameters mentioned in the Geotechnical chapter, there is a need for data collection through field and laboratory testing of the soil from the specific site. In the following chapters, the methods of retrieving data through different laboratory tests are described. There are several methods performed in the laboratory for testing the strength of a soil. Three common laboratory tests to perform when evaluating the strength of clay are Triaxial test, Oedometer test and CRS test.

2.6.1 Triaxial test

The Triaxial test is one of the most common laboratory tests for measuring the behaviour of soil during shear. The most common method is the direct shear test. The Triaxial test apparatus works for all types of soils. During a Triaxial test, it is possible to control the drainage conditions and also to measure pore water pressures. The control of drainage contributes to the advantage that saturated soils can be consolidated. A cylindrical shape of the soil specimen is placed in the apparatus and covered with a waterproof membrane. The apparatus is then filled with fluid surrounding the specimen. See an example of a specimen and the Triaxial test apparatus in Figure 2.4. The loading of the soil is applied axially and radially is the specimen stressed by the confining fluid pressure (Knappett and Craig, 2012).

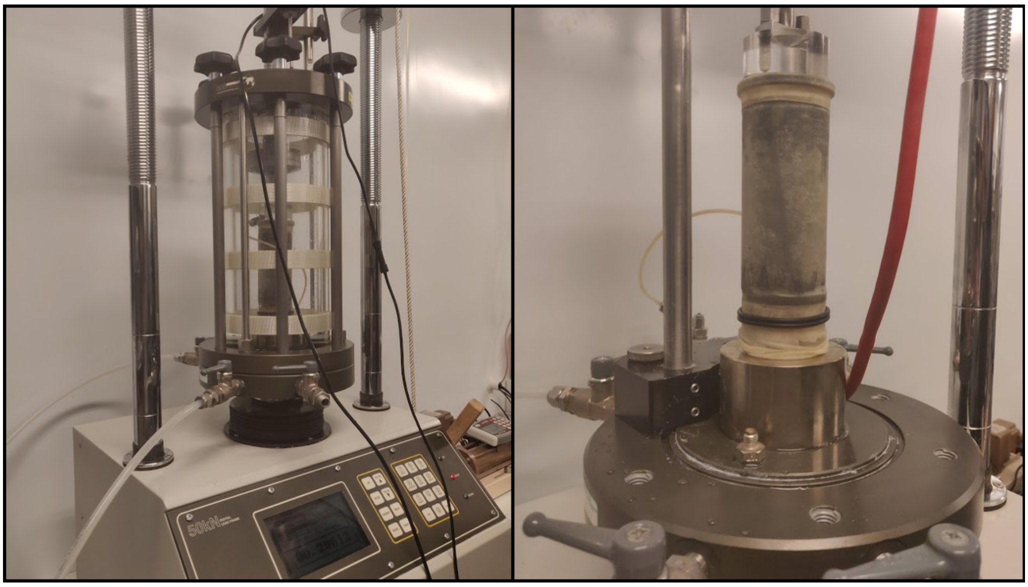

Figure 2.4: *A Triaxial test apparatus to the left and the specimen with membrane before test to the right.*

There are several test procedures for Triaxial tests but there are three different types that are normally being performed. The first is an unconsolidated undrained test (UU) where the principal stress difference is immediately applied under certain confining pressure on the specimen. There is no drainage or consolidation during the complete test time. The second type of test procedure is to perform a consolidated but undrained Triaxial test (CU). The specimen is then subjected with drained conditions until the consolidation is finished under certain confining pressure. After the consolidation is complete is the principal stress difference applied with undrained conditions. During the stage of consolidation, it is most common to perform isotropic testing but it is possible to retrieve anisotropic stresses if a condition of no-lateral strain is retrieved by using hydraulic pressure control. During the undrained stage, it is possible to measure the pore water pressure to control the effective stress. The third type of test procedure is by using consolidated and drained conditions (CD). With a confining pressure and drained conditions is the consolidation finished before the principal stress difference is applied to the specimen still using drained conditions. The stress rate is slowly applied to maintain a zero excess pore water pressure (Knappett and Craig, 2012).

From a Triaxial test data of max shear stress, effective axial stress, effective radial stress, axial strain and pore pressures can be retrieved. From this, it is possible to evaluate further parameters such as the deviatoric stress (q), also known as the principal stress difference, and mean effective stress (p') (Knappett and Craig, 2012).

2.6.2 Oedometer test

An Oedometer test is a laboratory test where one-dimensional swelling or consolidation can be performed to define the characteristics of a soil. The specimen of soil used for an Oedometer test has a cylindrical shape. This cylinder of soil is placed in the Oedometer apparatus between two porous stones. The specimen and the stones are surrounded by a metal ring where the lower stone is fixed and the upper stone has a small clearance for movements. On top of the upper stone is a loading cap in metal placed which can apply loading to the soil specimen. The metal ring with the specimen and the stones are placed in a water cell which the specimens has access to. The purpose of the water cell is to affect the pore pressures in the specimen. The metal ring has the purpose to contribute with no lateral strain on the specimen and this ring can either be fixed or vertically floating (Knappett and Craig, 2012).

The procedure of the test is divided into a sequence of loading steps. Each step with a specific loading applied on top of the cap is 24 hours long. The pressure applied in one step is then doubled in the next step. The start pressure depends on which soil is tested. When the applied stress and the effective vertical stress is equal due to the dissipation of excess pore pressure is the test finished. During the test is the compression of the specimen due to loading stress measured with time and the pore pressure. Characteristics of the soil that can be defined with Oedometer test data are void ratio, compression and swelling behaviour. The stress history of the soil can be defined using the effective stress and pre-consolidation stress obtained. The stress history is then defined by the overconsolidation ratio (OCR) (Knappett and Craig, 2012).

2.6.3 Constant Rate of Strain test

To determine soil characteristics of clay it is common in Sweden to use a Constant Rate of Strain (CRS) test. Similar to an Oedometer test there is a specimen of soil surrounded by a metal ring. The metal ring prevents the specimen from changing shape radially. The deformations obtained and measured should only appear laterally. Pore pressures can be measured at the bottom of the specimen where the surface is undrained. The top of the specimen where the load is applied has a drained surface. When the load is applied to the specimen is the purpose to create a deformation with a constant strain rate. The Swedish standard is to use a strain rate of 0.0025 mm/min. It is possible to apply a back pressure on the specimen to create a fully saturated soil. From the CRS test data of stress, strain, pore pressures with time can be retrieved. The advantages of using CRS instead of Oedometer is the time frame of the test to get completed. With the data from CRS compression and swelling behaviour can be obtained and stress history (Holm, 2016).

2.7 Software

There are several existing software for modelling slope stability problems. In this thesis, two different software are described and used: GeoStudio SLOPE/W and PLAXIS 2D.

2.7.1 GeoStudio SLOPE/W

GeoStudio SLOPE/W is a software for calculating the factor of safety in slopes. The model is based on calculations using limit equilibrium methods. In the software is it possible to choose among several of the different types of limit equilibrium methods. Examples of methods are the Morgenstern-Price, Bishop, Spencer and Janbu. The model analyses force and moment equilibrium and the purpose is to calculate the factor of safety equations for slope stability. With different pore pressures, soil characteristics and loading conditions, the different factor of safety and slip surfaces can be evaluated (Seequent Solutions, n.d.).

In Geostudio SLOPE/W, it is necessary to define five steps for the calculation to work. Firstly, the material is defined regarding characteristics like drained or undrained, unit weight, cohesion and friction angle. The materials are then added to a structure that is defined in step two. In the second step, the geometry is defined using x-y coordinates. When the geometry with materials are defined the next step is to specify which loads that are applied on the slope. The loads can either be point loads or surface loads. The fourth step is to define where the possible entry and exit are on the predicted slip surface. Depending on the accuracy of the entry and exit the results get more detailed. The last step before starting the calculation is to draw or define the pore pressure conditions. Here it is specified that the calculation should base the pore pressure on a piezometric line.

2.7.2 PLAXIS 2D

PLAXIS is a software for finite element analyses of stability, deformations and groundwater flow regarding geotechnical engineering. PLAXIS has different program packages, but this thesis will only consider PLAXIS 2D. This program uses 2D finite element meshes when calculating static elastoplastic deformations, consolidation, steady-state groundwater flow and stability analysis (Bentley (a), 2019).

The software uses a cross-section geometry and soil characteristic defined by the user based on laboratory data, to develop a suitable finite element mesh. In PLAXIS 2D a model in project properties is assigned. The model can either consider plane strain or axisymmetric conditions. With plane strain, it is assumed that the cross-section modelled is uniform considering stress state and loading. The plane strain model takes into account that there are stresses in z-direction but the displacements are assumed to be zero. When the axisymmetric model is assigned the structure is assumed to be circular and have a cross-section that is radially uniform. The loading is radial around the axis of the circle (Bentley (b), 2019).

In the software, the amount of element used needs to be selected. The options are to either have 6-nodes och 15-nodes per triangular element used for creating the cluster and soil layers. A 15-noded model provides for the displacements to be in the fourth-order of interpolation and is the default element to use. In a triangle with 15-nodes will 12 nodes be represented by stress points. The 15-noded model requires more memory and the calculation is slower in comparison with the 6-noded model which is a simplification of the 15-noded option. The 6-noded model provides the displacements to be in the second-order of interpolation. Within a triangle with 6-nodes are three nodes represented by stress points. For standard deformation analysis is the 6-noded model good enough but when more complicated analyses are performed is the result more accurate for the 15-noded option (Bentley (b), 2019).

The geometry is defined using lines and points that create surfaces in 2D. The geometry can also be defined using boreholes with a certain layering obtained in the field. Soil layers in PLAXIS 2D can have both horizontal and vertical directions. Since the software only considers 2D is the model-oriented in x-y-plane (Bentley (b), 2019).

In the calculation process is mesh analysis, flow conditions and staged construction included. In the mesh mode is a finite element mesh created according to the geometry. The mesh is regenerated every time the geometry is updated. In the calculation mode regarding the flow conditions are water levels generated both from the soil conditions and manually created water levels. The last calculation mode which defines the staged construction calculates the project result. In this mode, it is possible to activate and deactivate the structure to create a calculation process. For the results of the model have PLAXIS 2D created an output program where deformations, stresses and strains can be analysed. The results are presented with meshes, contours and graphs (Bentley (b), 2019).

2.7.2.1 Soil test

PLAXIS has a function where soil tests can be simulated on the chosen materials. The input material parameters that are defined by the user using calculations can be tested by performing standard laboratory tests. There is a possibility to for example simulate Triaxial test, Oedometer test and CRS test. The results from the simulated tests in PLAXIS 2D can then be compared with the results from the actual laboratory tests used when evaluating material parameters (Bentley (a), 2019).

2.8 Soil modelling

2.8.1 Creep-SCLAY1S

For soft clays that are either normally consolidated or slightly overconsolidated is Creep-SCLAY1S suitable to use since it is an advanced soft soil model (Gras, Sivasithamparam, Karstunen, Dijkstra, 2017). Soft fine-grained materials like clay have complex nonlinear stress-strain behaviour. The stress-strain behaviour is influenced by time, anisotropy and restructuring in the soil and is therefore in need of an advanced model when analysing the response of the soil (Gras, Sivasithamparam, Karstunen, Dijkstra, 2018). The Creep-SCLAY1S model is based on 14 parameters where 11 are soil parameters (Gras et al., 2017). Most of the parameters can be evaluated from experimental data but some parameters regarding anisotropy and structure are not directly measurable. The non-measurable parameters are evaluated through comparison between the response of the model and the response from non-standard laboratory testing (Gras et al., 2018).

Data for the model are based on Oedometric and Triaxial sample testing and this contributes to the possibility to analyse cross-anisotropic response. The stresses for the triaxial stress space are defined with the mean effective stress (p'), deviatoric stress (q), volumetric and deviatoric strain (ϵ_v and ϵ_q). See equations (2.5)-(2.8) for calculation of these parameters (Sivasithamparam, Karstunen and Bonnier, 2015).

$$p' = \frac{\sigma_1' + 2\sigma_3'}{3} \tag{2.5}$$

$$q = \sigma_1' - \sigma_3' \tag{2.6}$$

$$\epsilon_v = \epsilon_a + 2\epsilon_r \tag{2.7}$$

$$\epsilon_q = \frac{2(\epsilon_a - \epsilon_r)}{3} \tag{2.8}$$

σ_1 and σ_3 are effective stresses in axial respectively radial directions. ϵ_a and ϵ_r are strains in axial respectively radial directions (Sivasithamparam et al., 2015).

The strain can be divided into elastic, plastic and creep strain. In the Creep-SCLAY1S model is a combination with an elastoplasticity theory developed. The natural properties of a soil behave plastic which contributes to creep and therefore it is less accurate to assume only elastic behaviour. In equation (2.9) and (2.10) are the combinations described with the elastic (ϵ^e) and creep (ϵ^c) strain rate for volumetric (ϵ_v) and deviatoric strain (ϵ_q) (Sivasithamparam et al., 2015).

$$\dot{\epsilon_v} = \dot{\epsilon_v^e} + \dot{\epsilon_v^c} \tag{2.9}$$

$$\dot{\epsilon_q} = \dot{\epsilon_q^e} + \dot{\epsilon_q^c} \tag{2.10}$$

The elastic rate of deviatoric and volumetric strain can be calculated using equation (2.11) and (2.12) (Gras et al., 2018).

$$\dot{\epsilon_v^e} = \frac{\dot{p'}}{K} \tag{2.11}$$

$$\dot{\epsilon_q^e} = \frac{\dot{q}}{3G} \tag{2.12}$$

K is the elastic bulk modulus and G is the elastic shear modulus.

The state of the soil can be described using three ellipse formed surfaces in a plot with mean effective stress (p') on the x-axis and deviatoric stress (q) on the y-axis, see Figure 2.5. The surface that limits small and large strains due to creep is described as the normal consolidation surface (NCS). From this ellipse, it is possible to get the effective pre-consolidation pressure in triaxial space (p'_p) which is where the tangent from the ellipse intersects the p'-axis. The second surface that describes the soil state is the current stress surface (CSS). Here is the vertical tangent to the ellipse represented by the equivalent mean stress (p'_{eq}) on the intersection with the p'-axis (Gras et al., 2018). The inclination of the NCS and CSS ellipses are the same and are represented by α. The difference between p'_p and p'_{eq} is correlated to the amount of visco-plastic strain in the soil (Petalas, Karlsson and Karstunen, 2019). The strains that describe the state of CSS within NCS were described in Equation (2.9)-(2.12). The third surface is represented by an imaginary intrinsic compression surface (ICS) which describes the bonding (χ) of the soil. The ICS and NCS surface are correlated by having the same shape. However, the difference in size between ICS and NCS is determined by the value of bonding (Gras et al., 2018). In this graph with the surfaces is the anisotropy in the soil represented by the inclination and the amount of bonding (Petalas et. al., 2019).

The Creep-SCLAY1S considers three different processes of hardening; isotropic, structural and rotational. The first two processes affect the normal consolidation surfaces (NCS) and the intrinsic compression surfaces (ICS) sizes. The rotational hardening process will have an effect on the orientation of all surfaces (NCS, CSS and ICS) (Gras et. al., 2018).

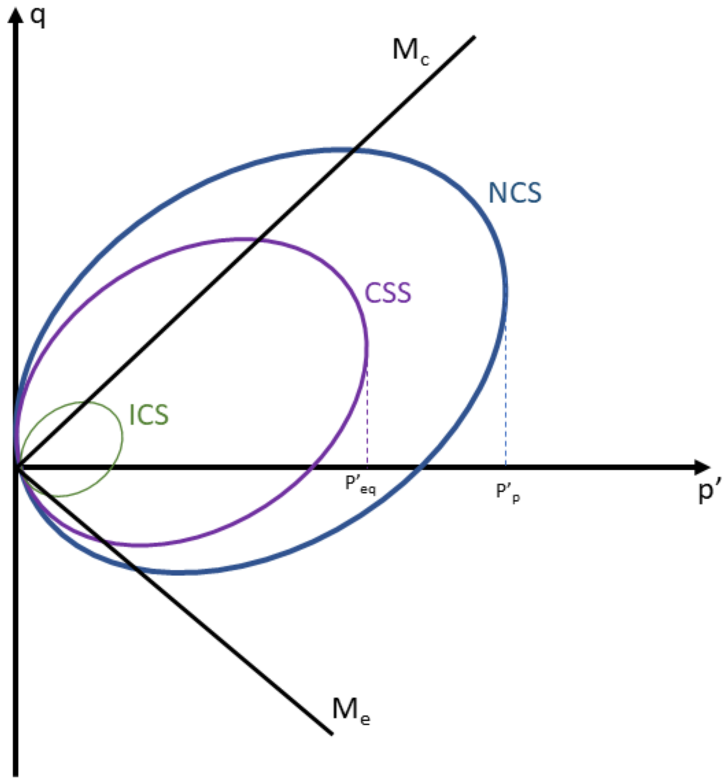

Figure 2.5: *Surfaces that describes the state of a soil.*

2.8.2 Mohr-Coulomb

The Mohr-coulomb model is a simpler model and needs less input data than the Creep-SCLAY1S model. With the Mohr-coulomb model is the failure envelope of the soil described using a plot with shear stress (τ) and effective normal stress (σ'), see Figure 2.6. By plotting the effective principal stresses which are the axial (σ'_1) and radial stress (σ'_3) on the x-axis a Mohr-circle can be created where the distance between (σ'_1) and (σ'_3) is the diameter of the circle. The point of the Mohr-circle that represents an angle of two times the angle the shear appeared (*theta*) in a failure test, is where the failure envelope tangents the circle (Knappett and Craig, 2012).

When failure is reached in the soil it indicates that the Mohr-circle touches the failure envelope. The failure envelope can also be described using equation (2.13) (Knappett and Craig, 2012).

$$\tau_f = c' + \sigma' tan\phi' \tag{2.13}$$

Where c' is the cohesion and ϕ' is the friction angle which represents the shear strength parameters in the soil.

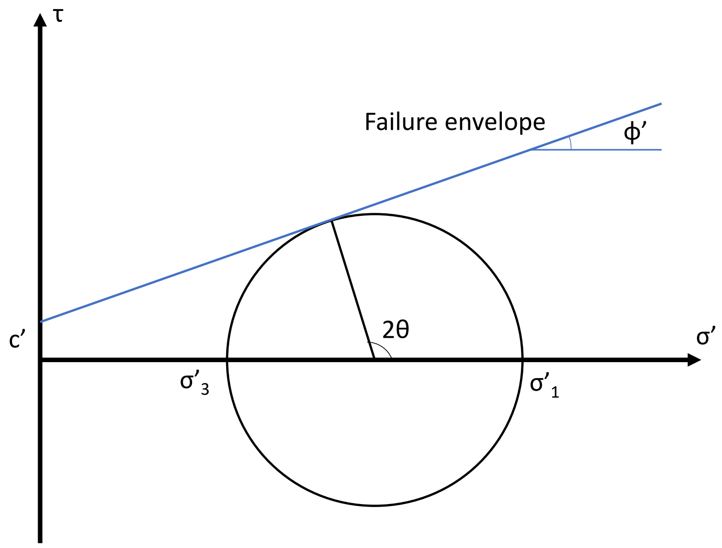

Figure 2.6: *Mohr Coulomb model described using a plot with the Mohr-cricle.*

2.9 Smådala

Smådala is located approximately 8 km south of Trollhättan on the western side of Göta Älv river, see Figure 2.7. The area consists mainly of agricultural land with a few buildings and the road Edsvägen which crosses the area from northeast to southwest (Google Maps, 2020). The geological map provided by SGU (Geological Survey of Sweden) shows that the area mainly consists of glacial clay with some parts with post-glacial silt, see Figure 2.8. Approximately 560 meters from the river towards northeast is the geology characterised by mostly bedrock with areas of clay and till (SGU, 2019). It can be assumed that the geological stratigraphy is following the typical soil layering that can be found in areas around Gothenburg. The layering is assumed to be clay, friction material and bedrock where the magnitude of the soil is between 0 to 40 meters (Bergström and Alaydi, 2020). The ground level for the top of the slope towards the Göta Älv river is located at an average level of +30 meters above sea level. Close to the river, the inclination of the slope is largest and the shoreline has an average level of +9 meters above sea level. The deepest parts of the Göta Älv river is located at a level that varies between -3 and -8 meters above sea level (Turesson, 2020).

Figure 2.7: *Location of Smådala marked with black pin with number one and red rectangle (Eniro, 2020).*

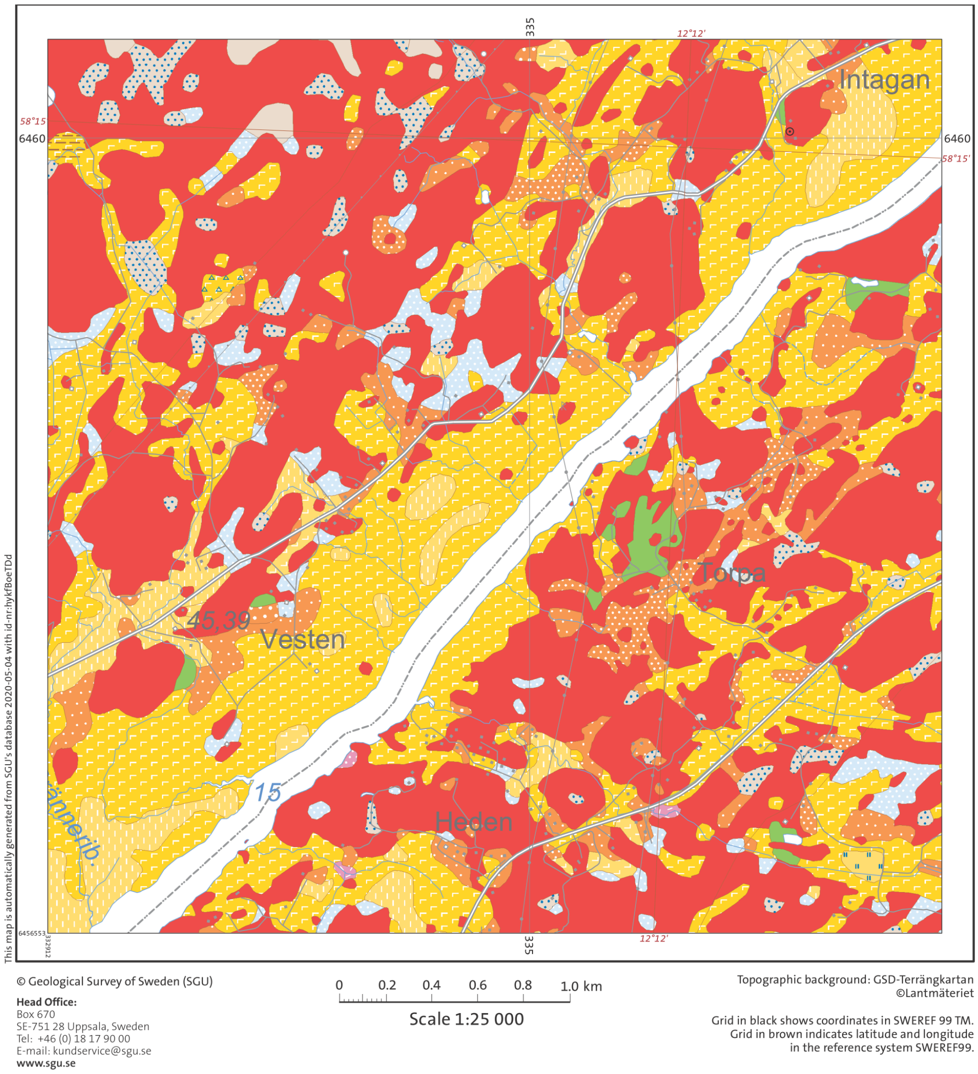

Figure 2.8: *Quarternary map over the area around Smådala. Material description, Red: Bedrock, Yellow: Clay, Blue: Till, Orange: Postglacial sand (SGU (c), n.d.).*

The section of the slope analysed in this Master's thesis is described as slope section V18/910 and is located in the central parts of the investigation area in Smådala, see maps of sections in Figure 3.3 in Chapter 3.2.1. Slope section V18/910 includes investigation points 19WS57 and 19WS58 where field and laboratory data of the soil from these points are provided. In previously performed analyses was the slope divided into three geological subareas. The geological subareas were divided by using results from performed laboratory and field tests. Subarea one is covering the land of the slope and subarea two is covering the shore between the river and the land. Lastly, the area covering subarea three is the part of the slope located in the Göta Älv river. The slope consists mainly of clay on top of bedrock where indications of quick clay can be found. The areas with quick clay are highly sensitive with high resulted values of sensitivity from the laboratory test. On top of the clay a dry crust is found which varies between 1-3 meters. (Bergström and Alaydi, 2020).

In the area of Smådala are wells installed for measure groundwater levels. According to WSP measurements is the groundwater level located at approximately 2.5 meters below ground level. The pore water pressure measurements indicate a pressure that is lower than hydrostatic pressure. Hence this is the situation it is possible to assume hydrostatic conditions in the analysis of this Master's thesis (Bergström and Alaydi, 2020).

3

Method

In this chapter the method of modelling in Geostudio SLOPE/W is described. The method of evaluating input data, performing soil test and modelling in PLAXIS 2D using Creep-SCLAY1S is also described.

3.1 Geostudio SLOPE/W

The first step after the literature study was to perform a calculation of the slope using Geostudio SLOPE/W. For this calculation data was retrieved from WSP:s investigation of the area in Smådala. In that investigation decided WSP to divide the section into three subareas. Area one is from the top of the slope to the edge of the shore, the second area is represented by the shore and the last area is the part covered by the Göta Älv river. The layering of the soil in the slope was decided to consist of three clay layers in subarea one and two, and two layers of clay below the river. On top of subarea one and two, a dry crust of approximately 2.5 meters was considered. The boundaries between the clay layers were located at +15, +5 and -5 meters above sea level. The geometry of the slope section is presented in Figure 3.1. This geometry was used when the slope was analysed with Geostudio SLOPE/W.

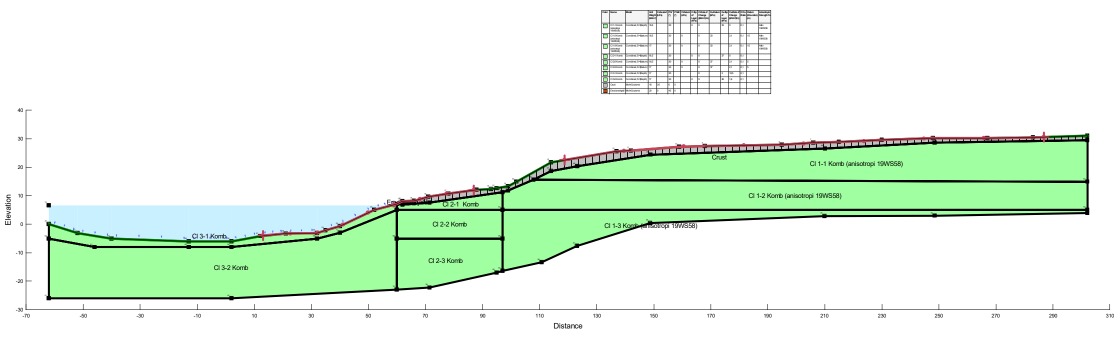

Figure 3.1: *Geometry of the slope section in Geostudio SLOPE/W.*

The material parameters were evaluated using data retrieved from WSP's investigation. A summary of used data for each clay section and the dry crust is presented in Table 3.1. The material parameters presented in Table 3.1 are values considering anisotropy with a combined analysis. Combined analysis implies that both undrained and drained conditions were considered depending on which value that gave the worst-case scenario. The anisotropy, in this case, was considered by using three vertically divided subareas. Since the anisotropy did not agree with Swedish empirical values in the passive zone (zone of extension), the anisotropy was only considered in the active zone (zone of compression), which was subarea one. An analysis using material parameters with undrained behaviour was also simulated and a combined analysis without anisotropy. The modelling of the slope in Geostudio SLOPE/W has the purpose of providing values of factor of safety and a visualisation of the slip surface for further finite element analysis in PLAXIS 2D. The results from the combined analysis with anisotropy was therefore of a bigger interest.

Table 3.1: *Data used for materials in Geostudio SLOPE/W calculation*

Clay	Unit weight [kN/m^3]	Cohesion, c_u [kPa]	c'/c_u	ϕ'
1-1	16.5	33	0.1	30
1-2	16.5	33+2.1z	0.1	30
1-3	17	33+2.1z	0.1	30
2-1	16.5	37	0.1	30
2-2	16.5	37+2.1z	0.1	30
2-3	17	37+2.1z	0.1	30
3-1	17	3+16.5z	0.1	30
3-2	17	36+1.9z	0.1	30

The entry and exit section for the slip surface was defined after the geometry and material parameters were set. In Figure 3.2 the areas are visualised with a red line at the ground surface. The entry section was more uncertain and was therefore defined over a larger area on the upper part of the slope. The exit section was assumed to be somewhere from the end of the steepest part of the slope to the middle of the river. With the entry and exit method were total 9 exit and 9 entry search points created. This indicates that in the entry area is the distance between every search point about 25 meters.

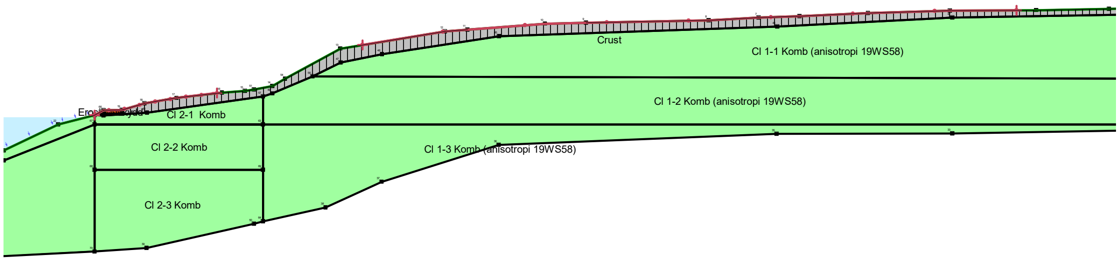

Figure 3.2: *Entry and exit definition of slip surface in Geostudio SLOPE/W.*

The last step before calculating the stability of the slope was to define the pore water pressures in the slope section. A spatial function for pressure head of water was created by defining pressures at certain locations within the slope section. The behaviour of the function considered hydrostatic conditions. In Appendix B.1 are the used values of pore pressures presented. The function of the pore water pressures started at the groundwater level which was estimated to be at a depth of 2.5 meters below ground level. The crust was additionally defined to have cracks.

3.2 Creep-SCLAY1S model

3.2.1 Evaluation of data

The Triaxial, CRS and Oedometer tests were performed for samples from three different locations in the chosen section. The first sample point is located above the steepest part of the slope and is named as point 19WS58. The second sample point is located below the steepest part of the slope and is named point 19WS57. In point 19WS58, four samples at different depths were analysed and in point 19WS57 were three samples at three different depths analysed. The third point, NV00067B, analysed is not located in the slope section V18/910. This point is located in the upper part of section V18/740 which is the section next to V18/910 in northeast direction, see Figure 3.3.

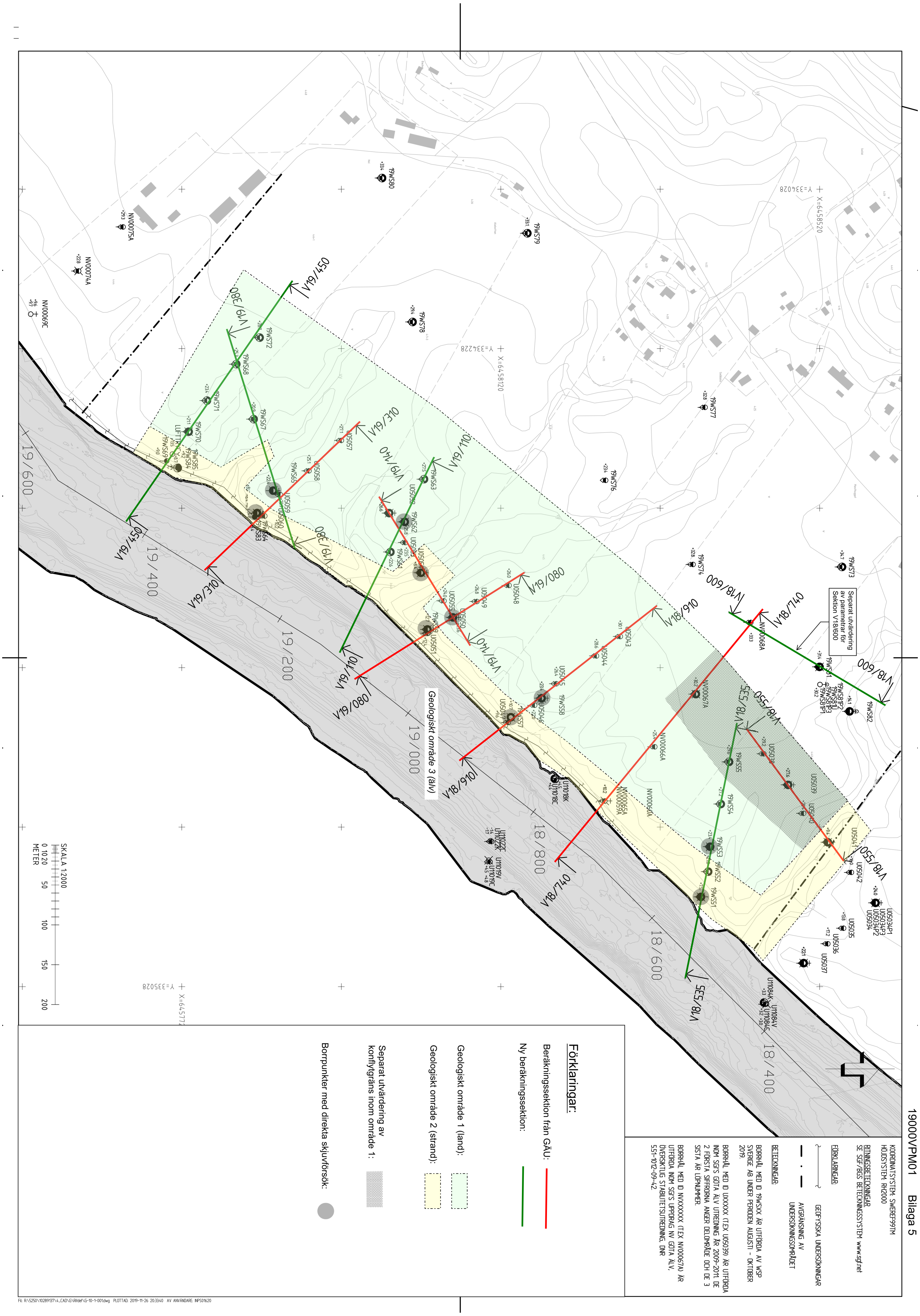

Figure 3.3: *Slope sections created by WSP (Bergström and Alaydi, 2020).*

The results from the CRS tests were analysed with the purpose to determine values for modified compression and swelling index which were necessary parameters for the Creep-SCLAY1S model. The results were analysed by plotting the effective stress with natural log scale against the volumetric strain. From this plot the modified swelling index (κ^*) and the modified compression index (λ^*) could be derived by determining the inclination of different parts of the graph, see Figure 3.4 (Karstunen and Amavasai, 2017). This analysis was performed for both borehole 19WS57, 19WS58 and NV00067B, and for each sample from the different depths.

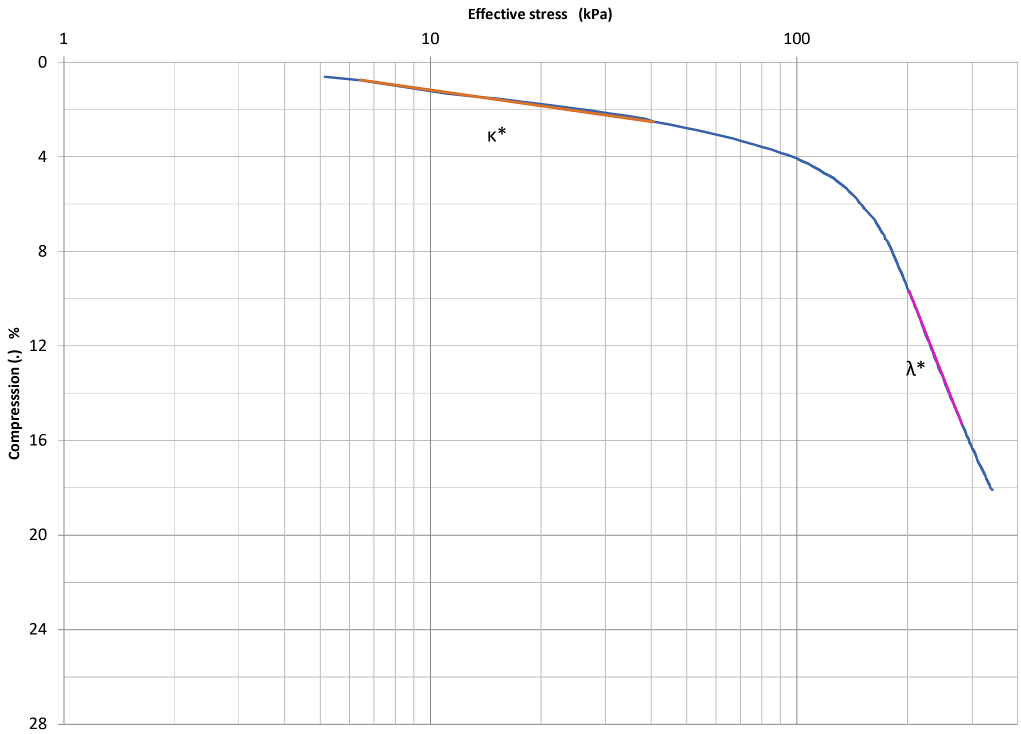

Figure 3.4: *Results from CRS test where effective stress is plotted against volumetric strain concluding the evaluation of modified swelling index (orange) and compression index (purple).*

The lab results from the Oedometer tests were used to define the parameters connected to creep behaviour in the soil. The modified creep index μ^* could be derived by plotting volumetric strain against the time in logarithmic scale. To define μ^* the inclination of the last part of the curve was calculated using a reference time τ equal to one day. For the creep-SCLAY1S it was the intrinsic creep index μ_i^* which was defined as the value of μ^* at the largest load applied on the soil, this was normally from the last loading step (Sivasithamparam, 2012). The plot with the derivation of the creep parameters from Oedometer tests can be found in Appendix B.1.

Additional values of κ^* and λ^* could be derived from the Oedometer tests. By plotting the sum of loading from each loading step on the x-axis and the compression measured on the y-axis it was possible to analyse the modified swelling and compression indices. The values of κ^* and λ^* were derived in the same way as from the CRS results, see Appendix B.2.

The pre-consolidated stress σ'_p could be evaluated using the Oedometer test results. Where the tangent lines that define modified compression and swelling indices are crossing was where the pre-consolidation stress was represented by the value on the x-axis (Karstunen and Amavasai, 2017). The pre-consolidation stress was, however, provided in the result retrieved from the laboratory and therefore was these used for further calculations of OCR. As defined in the consolidation chapter in the theory, is OCR the over consolidation ratio calculated with the pre-consolidated stress divided by the effective stress in the soil. The effective stress for the slope profile was calculated using the defined unit weight from laboratory test and hydrostatic groundwater conditions ($\gamma_w = 10$) from 2.5 meters below the ground surface. The process of calculating the effective stress is described in chapter 2.4.1 Effective stress. In the input of soil parameters in Creep-SCLAY1S in PLAXIS 2D, it was possible to either define OCR or a pre-overburden pressure (POP). The pre-overburden pressure (POP) was calculated using equation (3.16). A plot with the pre-consolidation stress and the calculated effective stress can be found in Appendix B.3.

$$POP = \sigma'_p - \sigma'_0 \tag{3.1}$$

Both OCR and POP were calculated when deriving parameters for the slope. For the input data in Creep-SCLAY1S were both methods with either using OCR or POP tested. The option was to either set a value of POP and then was OCR equal to one or value for OCR was defined and POP was set to zero. If the calculation of OCR and POP was right should there not appear any differences in results depending on which parameter that was defined in the input data.

When analysing the laboratory results from the Triaxial tests, considering compression, standard parameters and parameters related to anisotropy could be derived. Firstly, the critical state line in compression (M_c) was evaluated through plotting mean effective stress and deviatoric stress. The M_c-value was then represented by the inclination of a line from point (0.0) to the plotted lab results (Karstunen and Amavasai, 2017). The principle of evaluation of M_c is visualised in a plot from point 19WS58 and depth 18 meters which can be seen in Figure 3.5. All other M_c from different points and depths were evaluated the same way.

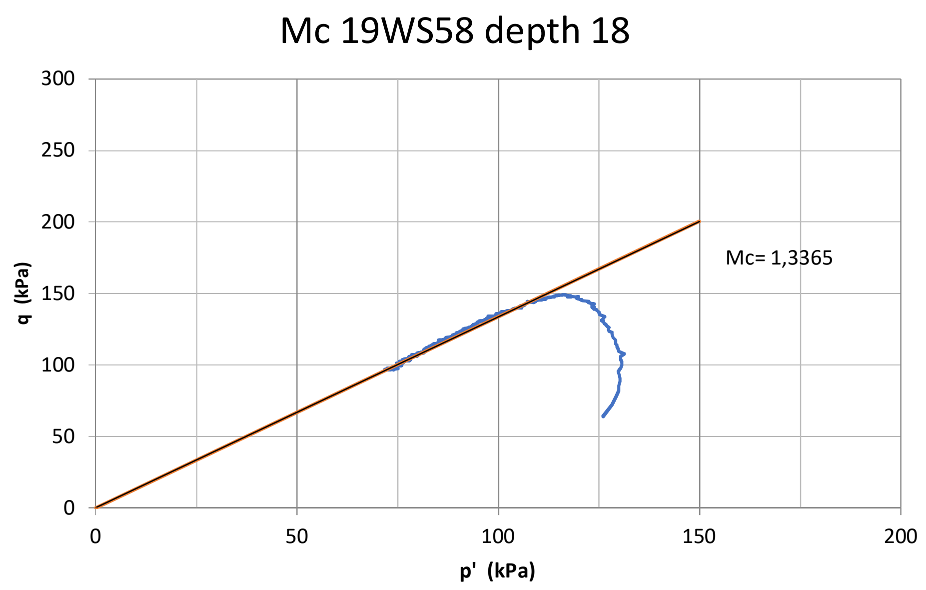

Figure 3.5: *Plot from Triaxial test in compression with evaluation of M_c (19WS58 depth 18 meters).*

The M_c-value could then be used to calculate further parameters related to anisotropy and destructuration parameters for the soil. Firstly, the stress ratio η_{K0} for normal consolidation was calculated using equation (3.2) (Karstunen and Amavasai, 2017).

$$\eta_{K0} = \frac{3M_c}{6 - M_c} \tag{3.2}$$

Next step was to calculate the state variable for the initial anisotropy, α_0. Since the initial anisotropy was assumed to be described with cross anisotropy, the parameter evaluated was described as α_{K0}. This was done using equation (3.3) which consists both the critical state line M_c and the stress ratio η_{K0} (Wheeler, Näätänen, Karstunen and Lojander, 2003).

$$\alpha_{K0} = \eta_{K0} - \frac{M_c^2 - \eta_{K0}^2}{3} \tag{3.3}$$

The evolution of the anisotropy in the soil was described with the parameters ω and ω_d. The value for ω_d could be calculated using equation (3.4) and the value for ω could be estimated using equation (3.5). The final value for ω was later evaluated using model-simulated Triaxial test (Karstunen and Amavasai, 2017).

$$\omega_d = \frac{3(4M_c^2 - 4\eta_{K0}^2 - 3\eta_{K0})}{8(\eta_{K0}^2 + 2\eta_{K0} - M_c^2)} \tag{3.4}$$

$$\omega \approx \frac{1}{(\lambda_i^* - \kappa^*)} \ln\left(\frac{10M_c^2 + 2\alpha_{K0}\omega_d}{M_c^2 + 2\alpha_{K0}\omega_d}\right) \tag{3.5}$$

An interval for the degree of destructuration ξ could be estimated using the parameter for the evolution of anisotropy, see equation (3.6). This interval was both based on ω and ω_d where two different degrees of destructuration ξ and ξ_d were estimated (Gras et al., 2018). This was only an estimation, the real values of ξ needed to be determined through soil test simulations. However, the values calculated with equation (3.6) gave a first hint of what value to start the model simulation with (Sivasithamparam, 2012).

$$\frac{1.5}{\omega} \leq \xi \leq \frac{4.2}{\omega} \tag{3.6}$$

In other literature was the destructuration parameters defined as a and b where a=ξ and b=ξ_d. With the evaluated parameters from both CRS and Triaxial laboratory results could a and b be determined. For the b-value, which is the relative rate of destructuration, was the suggestion by Karstunen and Amavasai (2017) to choose a value between 0.2 < b < 0.4 based on experience with Scandinavian clay. An interval for the a-value, which is the absolute rate of destructuration, was calculated using equations in Equation (3.7). For the calculation for the interval of a, a b-value of 0.4 was chosen. Normally the a-value is somewhere between 8-12 (Karstunen and Amavasai, 2017).

$$\frac{ln2}{[ln(2+2\chi_0) - ln(1+\frac{\chi_0}{2})](1+b)(\lambda_i^* - \kappa^*)} \leq a \leq \frac{(1+\chi_0)}{\chi_0(\lambda_i^* - \kappa^*)[1+2b\frac{\alpha_{K0}}{M_c^2}]} \tag{3.7}$$

By using the critical state line M_c the friction angle representing critical state could be evaluated with equation (3.8) (Karstunen and Amavasai, 2017).

$$sin\phi_c' = \frac{3M_c}{6+M_c} \tag{3.8}$$

With the critical friction angle and Jaky's simplified formula it was possible to calculate the stress history parameter K_0 in the normally consolidated state, see equation (3.9) (Karstunen and Amavasai, 2017).

$$K_0 = 1 - sin\phi'_c \tag{3.9}$$

Similar analyses were performed for the Triaxial tests in extension. The laboratory results were plotted with mean effective stress on the x-axis and deviatoric stress on the y-axis. By calculating the inclination of a created line between point (0.0) and the graph the critical state line in extension (M_e) could be determined (Karstunen and Amavasai, 2017). Plot and evaluation of M_e from depth 18 meters for 19WS57 is visualised in Figure 3.6. The M_e-value for the other points and depths were evaluated using the same principle.

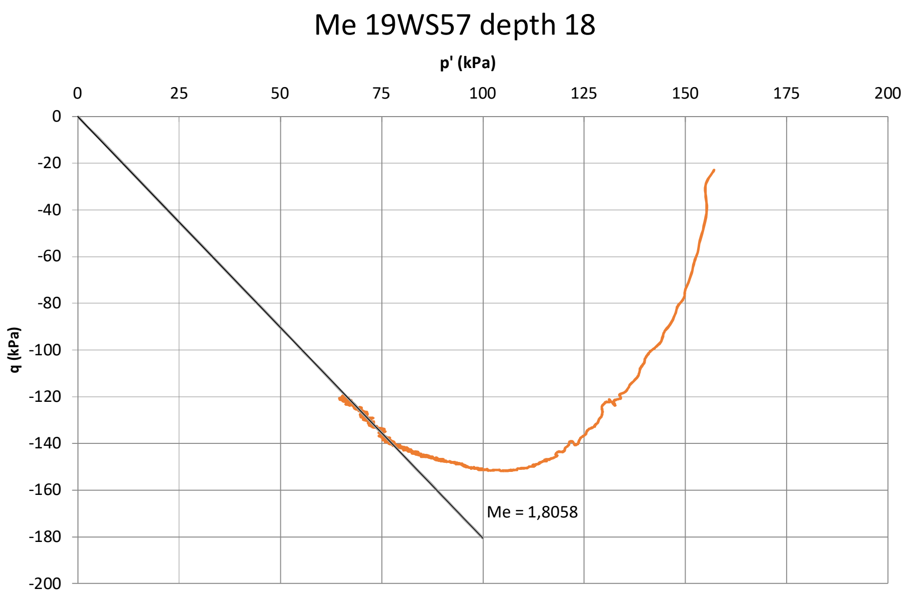

Figure 3.6: *Plot from Triaxial test in extension with evaluation of M_e (19WS57 depth 18 meters).*

With the M_e-value could the friction angle for the critical state in extension be calculated using equation (3.10) (Karstunen and Amavasai, 2017).

$$sin\phi'_c = \frac{3M_e}{6 - M_e} \tag{3.10}$$

Additional to the Triaxial, CRS and Oedometer test results, index test results of the soil samples were retrieved for both 19WS57, 19W58 and NV00067B. In this laboratory results, the sensitivity and the unit weight of the soil at different depths could be used for further evaluations. The sensitivity S_t was used to define the initial degree of bonding χ_0 in the soil, see equation (3.11) (Karstunen and Amavasai, 2017).

$$\chi_0 = S_t - 1 \tag{3.11}$$

The sensitivity of a soil is normally tested through a fall cone test. This way of evaluating bonding may however not be suitable if the sensitivity is high (Karstunen and Amavasai, 2017). In Smådala the presence of quick clay is high and therefore is the sensitivity very high.

When evaluating the geometry and the different soil layers in the slope an analysis of the difference in unit weight over the section was performed. To see possible layering the unit weight was plotted against level for points 19WS57, 19WS58 and NV00067B, see figure 3.7. It could be seen from the field tests that a dry crust exists and is varying between 1-3 meters on top of the clay layers. The previously described parameters were plotted with depth to get a view of possible deviations in the soil layering. A summary of all parameters for the decided layering is presented in Table 3.2. It was decided that there are different clay layers with different characteristics. The top layer was decided to be located from the top to +15 meters a.s.l., the second layer was from level +15 to +5, the third was from level +5 to -5 and the fourth and last layer was from level -5 and to the bedrock.

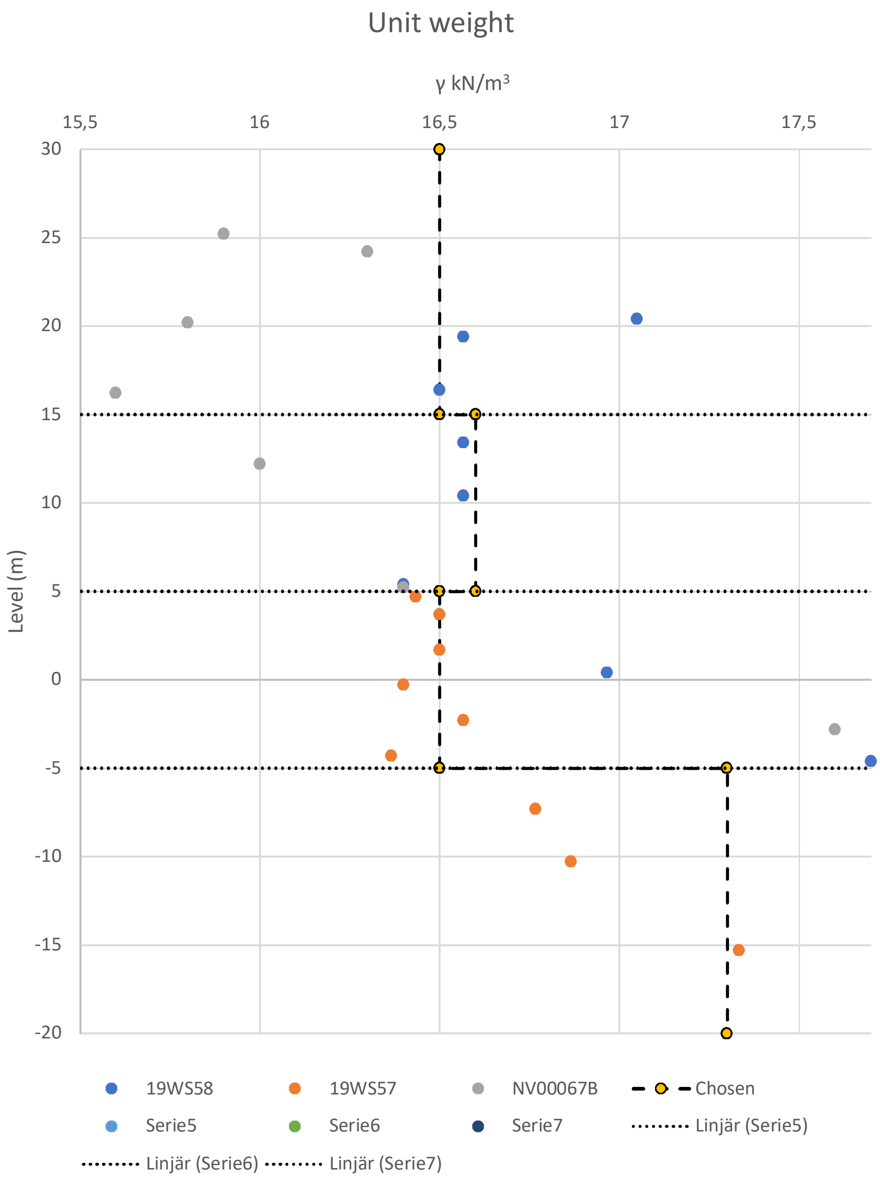

Figure 3.7: *Evaluation of unit weight for the clay layers.*

When choosing the unit weight for clay layer 1 and 3 a comparison between several parameters were needed due to the large difference in unit weight between the data from different points. Since the result of water content and pre-consolidation pressure were similar in the two points an assumption was made that the chosen parameter should be based on the borehole with the most data from these depths for clay layer 3. A unit weight was therefore chosen from the results from 19WS57. This pattern could be seen when evaluating the other parameters and in all cases most of the data were received from 19WS57 and therefore were the other parameters also based on this point. For clay layer 1 was the unit weight chosen to be based on the points from 19WS58 since this point was located in the section and NV00067B was located further away.

Additional to the calculated and derived material parameters were three parameters assumed based on previously performed studies and standard values. The first parameter was τ which is the reference time in days. This parameter was chosen to be one day since that was normally chosen in other Creep-SCLAY1S analyses. The second parameter that was assumed based on previously performed analyses was the Poisson's ratio. This parameter was chosen to be 0.2 (Karstunen and Amavasai, 2017). Parameters considering flow, k_x and k_y, were chosen to be 10^{-5} for all layers. The last parameter not calculated was the initial void ratio, which in some cases could be provided in the laboratory test result. Since, this was not the case the value was chosen to be 1.8 based on previous data of clay in Gothenburg (Sellin, Karlsson and Karstunen, 2021). A summary of all chosen parameters from laboratory results and calculations are presented in Table 3.2.

The evaluated parameters were lastly compared with previously obtained values for Gothenburg clay by Petalas et. al (2019) before starting the Creep-SCLAY1S modelling. The values by Petalas et. al. can be seen in Table 3.3.

Table 3.2: *Chosen parameters for modelling the slope in PLAXIS 2D with Creep-SCLAY1S model.*

General	**Layer 1**	**Layer 2**	**Layer 3**	**Layer 4**
Top level	35	15	5	-5
Bottom level	15	5	-5	bedrock
γ	16.5	16.6	16.5	17.3
Parameters				
κ^*	0.016	0.013	0.017	0.014
λ_i^*	0.07	0.073	0.07	0.077
M_c	1.4	1.4	1.3	1.5
M_e	1.2	1.4	1.4	1.8
ν'	0.2	0.2	0.2	0.2
ω	36	32	36	31
ω_d	1	0.86	1	1
ξ	8.4	8.4	8.2	8.8
ξ_d	0.4	0.4	0.4	0.4
τ	1	1	1	1
μ_i^*	0.0044	0.0042	0.0039	0.0033
ϕ_c'	33	33	37	37
Initial parameters				
OCR	1	1	1	1
POP	80	116	141	185
K_0	0.4	0.47	0.43	0.4
α_0	0.58	0.5	0.54	0.58
χ_0	126	500	400	32

Table 3.3: *Previous obtained characteristics of Gothenburg clay by Petalas et. al., (2019).*

Parameter	Value
λ^*	0.29
λ_i^*	0.08
κ^*	0.01
ν'	0.2
M_c	1.4
M_e	1.1
ω	300
ω_d	0.95
α_0	0.54
χ_0	8
ξ	8
ξ_d	0.5

3.2.2 Soil test

Before starting to define the phases of the calculation a soil test in PLAXIS 2D was performed to analyse the accuracy of the calculated parameters and to determine the quality of the laboratory tests. The tests simulated in PLAXIS 2D were Triaxial, Oedometer and CRS tests. Samples tested in the laboratory from point 19WS57, 19WS58 and NV00067B were used for comparison. For each clay layer, a certain sample from a certain depth was considered for the comparison to the simulated data from PLAXIS 2D. For clay layer 1 laboratory results from NV00067B and 19WS58 were mostly used and for clay layer 2 results from 19WS58 were used. For clay layer 3, results from both 19WS57 and 19WS58 could be used depending on which test performed and the estimated quality of the laboratory tests and samples. Clay layer 4 was represented by results from 19WS57.

Firstly, Triaxial test simulation was performed to analyse the accuracy of M_c and M_e. The initial value needed for the simulation was the K0-value which was represented by the ratio between the initial axial and radial stress used in the real Triaxial test performed in the laboratory. By defining a K0-value the test considers non-isotropic conditions. Further, the test was set to undrained and an initial cell pressure retrieved from the real laboratory test was used as input. When evaluating M_c the test direction was defined as compression and when evaluating M_e the test direction was set to extension. From the simulated Triaxial test in PLAXIS 2D data of the deviatoric stress (q) and mean effective stress (p') could be derived. These values were then plotted against each other in the same way as the data from the real laboratory tests for comparison. Before changing M_c or M_e to a good fitting curve the POP needed a change to get a reasonable curve for evaluation.

When simulating the Oedometer test two different methods were used in PLAXIS 2D. Firstly, the Oedometer test function was used where the phases of loading that were used in the real laboratory test were defined. For all Oedometer laboratory tests performed for samples from 19WS57 and 19WS58, a total of 9 phases over 9 days were simulated. In each phase either loading or unloading of stress (kN/m^2) was defined. The other method used for simulating the Oedometer test was by using the general function in Plaxis 2D. Similar to the Oedometer, function 9 phases with either loading or unloading were defined. The difference was that in the general method it was possible to define the initial stresses or strains. This contributed to the possibility of a better fit of the simulated curve to the curve from the real laboratory test. Both methods were used since the simulated curve from the Oedometer function in the soil test was dislocated in comparison with the real laboratory test. From the simulated test, stress, strain and time data were derived. The most interesting curve to plot and compare was the behaviour of stress and strain. The main purpose of simulating the Oedometer test was to evaluate if the calculated kappa (κ^*) and lambda (λ^*) from the real laboratory test agreed. For all clay layers, similar adjustments were needed to match the soil test curve with the laboratory curve. Both κ^* which was the inclination of the first part of the curve and λ^* which was the later inclination of the curve needed minor adjustments for all layers. The main adjustments that were needed for the curves to fit each other was a change in POP but also another initial start stress than the real laboratory test. The adjustments of POP was, however, not of the same interest as the adjustments of κ^* and λ^* since the POP differs among the Triaxial, Oedometer and CRS tests.

The simulation of the CRS test was in the same way as the Oedometer simulated using two different methods in PLAXIS 2D due to the same purpose. Firstly, the function in the soil test developed for CRS was used where only duration and a strain needed to be defined. The chosen strain in this simulation depended on the total strain developed for each real CRS test performed in the laboratory. Secondly, the general function in soil test was used where the same total strain was defined but with other initial values to start the simulation with. From the CRS soil test could κ^* and λ^* be modified. Since the evaluated values of κ^* and λ^* between the Oedometer test and the CRS test differed in the laboratory tests were also the values different in the soil test. Fitting of the curve was possible in the soil test but for further calculations were κ^* and λ^* based on the Oedometer test.

One thing that all simulated tests had in common was the adjustments of POP, however, for Oedometer and CRS tests, an increase in POP was needed and for the Triaxial test, a decrease was needed. The final chosen POP will be based on calculations and stresses from in situ tests and not the adjusted values in the soil tests.

3.2.3 Modelling

The first step of the modelling was to create the material and the geometry of the slope section. There were four materials created representing the four clay layers and a material for the dry crust. The materials were created by using the material parameters derived in the previous chapter. By using the width and height of the slope as in the analysis performed in Geostudio SLOPE/W could a rectangular start geometry be created. To know where the erosion should stop the points of today's slope profile were marked using coordinates from the slope modelled in Geostudio SLOPE/W where the material was provided by WSP.

3.2.3.1 Phases

When constructing the calculation method for the slope a certain amount of phases with different characteristics were defined. For this slope, a total of 14 phases were constructed including the initial phase, steps for erosion, a step for the creation of the dry crust and lastly a safety phase to analyse the failure mechanism. The calculation, loading and pore pressure types for each phase are presented in Table 3.4. The ten steps that define how the soil slowly erodes to current slope topography has a total erosion of 4 meters in 100 years per phase. The total process of erosion is in reality about 10000 years or more but since the model will take a long time to calculate, a total time of 4000 years was considered. The differences were assumed to be minor and only due to creep.

Table 3.4: *Phases and the characteristics of each phase used for calculation in Creep-SCLAY1S*

Phase	Calculation type	Loading type	Pore pressure type	Time [days]
Initial phase	K0-procedure	Staged construction	Steady state groundwater flow	-
Null-step	Consolidation	Staged construction	Steady state groundwater flow	3650
Erosion 1	Consolidation	Staged construction	Steady state groundwater flow	36500
Erosion 2	Consolidation	Staged construction	Steady state groundwater flow	36500
Erosion 3	Consolidation	Staged construction	Steady state groundwater flow	36500
Erosion 4	Consolidation	Staged construction	Steady state groundwater flow	36500
Erosion 5	Consolidation	Staged construction	Steady state groundwater flow	36500
Erosion 6	Consolidation	Staged construction	Steady state groundwater flow	36500
Erosion 7	Consolidation	Staged construction	Steady state groundwater flow	36500
Erosion 8	Consolidation	Staged construction	Steady state groundwater flow	36500
Erosion 9	Consolidation	Staged construction	Steady state groundwater flow	36500
Erosion 10	Consolidation	Staged construction	Steady state groundwater flow	36500
Consolidation	Consolidation	Minimum excess pore pressure	Pressures from previous phase	-
Safety phase	Consolidation	Staged construction	Pressures from previous phase	1

K0-procedure is a calculation method used to define the initial stresses of the initial phase. This method was available to consider the stress history of the soil. When using the K_0-procedure was PLAXIS 2D generating the vertical stresses and the horizontal stresses were developed with the specified K_0-value. The vertical stresses and the self-weight of the soil were supposed to be in equilibrium. This method was therefore most suitable when the modelling begins with a horizontal surface which was the case of the slope modelled (Bentley (b), 2019).

The calculation type could either be plastic, consolidation or safety. With the plastic is the model considering either drained or undrained conditions but with infinite consolidation. The safety calculation is a PLAXIS 2D function to calculate the factor of safety with reduction of strength. The last calculation type which was used for the slope calculation is consolidation which is a time-dependent analysis. The model considers excess pore pressure and deformations over a certain time interval and allows elastic-plastic consolidation. This type of calculation is most suitable for problems with clay soils (Bentley (b), 2019).

In calculation type consolidation are three different loading types available, staged construction, minimum excess pore pressure and degree of consolidation. Staged construction implies that the model changes the loading and consolidation simultaneously due to change in stress, strength, stiffness and weight of the element. Necessary for this loading type was to specify a time interval of the consolidation in which the loading was increased linearly. The second loading type which was used in this model was a minimum excess pore pressure. In this loading type, the consolidation is applied to the elements until a specified value of excess pore pressure is reached. There is no definition of time in this loading type. The third loading type which was not used in this model is when the loading is applied to the elements until a certain degree of consolidation. Similar to the loading type with excess pore pressure is no time interval needed (Bentley (b), 2019).

The boundary conditions defined in the calculation phases were the same through all 14 phases. Considering deformations were the boundary conditions defined as normally fixed at the right and left boundary (Xmin and Xmax), fully fixed at the lower boundary (Ymin) and free at the upper boundary (Ymax).

3.2.3.2 Flow conditions

The water levels and pore water pressures for the slope were modelled using the function defined as flow conditions provided by PLAXIS 2D. For every calculation phase created in the staged construction function in PLAXIS 2D was a certain flow condition defined. When the erosion of the material took place was also a lowering of the groundwater level happening. According to previous studies is the groundwater level located below the dry crust in today's conditions. However, for the modelling, it was assumed that the water level was located at the ground surface during the erosion processes. The water level was defined by creating a water head at the left and right boundary of the slope section.

The initial phase and null-step phase started with a left and right boundary head of 35 meters above sea level. Successively as the soil eroded 4 meters each phase the water level was lowered 4 meters. The right boundary which was the top of the slope only eroded to a level of 31 meters which contributed to that the water level head for the right boundary stayed at 31 meters through erosion phase 1-9. Meanwhile was the lowering of the water level 4 meters for each erosion phase at the left boundary. When the left boundary reached the erosion 7 phase where the water level of today's Göta Älv river is located was the left boundary head defined as 6.6 meters. The left boundary head stayed 6.6 meters for the following phases. When the material eroded in erosion 7-10 was the area of eroded soil replaced with water using the selection explorer. In erosion 10 phase had the erosion reached the bottom of today's river and conditions, therefore was the right boundary head lowered to

28 meters in this phase. In the following consolidation phase and safety phase were the boundary heads equal to the defined heads in erosion 10 phase.

3.2.3.3 Mesh analysis

In the mesh analysis could different meshes be generated for the purpose of specifying the number of finite elements. The purpose of the mesh analysis was to get a comparison and behaviour of the slip surface due to different meshes and different areas where the mesh was more refined than other areas of the slope section. To begin with, was a coarse mesh chosen to minimize the calculation time of the model and get a preliminary view of the results. The mesh was later refined to see if the mesh size made any difference. A certain area of the slope was more refined than the edges of the slope to get a more detailed slip surface but still minimize the calculation time for the model.

3.2.3.4 Factor of safety

The factor of safety is an indication of failure and depends on slope stability. When evaluating the failure mechanism in Creep-SCLAY1S a safety phase was created after the erosion steps and the consolidation. This phase aimed to force the slope to failure so that a result of failure mechanisms and a value of the factor of safety could be obtained. In the Creep-SCLAY1S model was the failure created through an increase in the gravity of the model. Normally a target gravity of one is pre-defined in the model but to create failure a value larger than one needed to be selected. When selecting this value it was recommended to have a pre-knowledge about the possible value of the factor of safety. To get an idea of the factor of safety, GeoStudio SLOPE/W was used for a first calculation of the slope stability. In PLAXIS 2D the factor of safety is defined using equation (3.12) (Sellin, Karlsson and Karstunen, 2021).

$$FS = \sum M_{weight} \times \sum M_{stage} \tag{3.12}$$

When the gravity was applied to the model in the safety phase it contributes to that the pore pressures in steady-state conditions reach the final value immediately. The increased value of $\sum M_{weight}$ affected the soil weight and the excess pore pressures so that the slope could collapse. When the slope reached the failure state the value of $\sum M_{stage}$ stop increasing and stayed constant for the rest of the calculation phase (Sellin, Karlsson and Karstunen, 2021). In that way could the factor of safety be estimated with the defined $\sum M_{weight}$ and the retrieved $\sum M_{stage}$. Additionally to the definition of $\sum M_{weight}$ was a calculation time set to this phase. To develop the factor of safety for the failure in the slope several combinations of $\sum M_{weight}$ and time frame were tested.

3.2.3.5 Sensitivity analysis

After the calculation of the slope stability with the input data presented in 3.2 a couple of modifications were needed to optimise the input data and to perform a sensitivity analysis. After the result was reasonable based on expectations were further modification tested like change in the time frame, M_c, M_e and sensitivity to see how this affected the result.

The first calculation included a dry crust located on top of the clay. When the phase with the dry crust was activated, the failure in the safety phase was developed in the crust and not in the clay. Therefore was this soil layer neglected in further calculations to get the failure surface in the clay layers.

Firstly, was the POP changed since this was the parameter that differed the most in the soil tests. The soil data used for the model were based on conditions measured today. When modelling over a long time may the conditions be different at the start than what can be measured today. Therefore was a check of the OCR and POP calculated and used by PLAXIS 2D necessary to evaluate the accuracy of the chosen material parameters. From the calculated results it was possible to retrieve values for OCR at different locations in the soil at different times. The results of OCR retrieved in the output of the model was not the same OCR as the input data for the soils. By using equation (3.13) - (3.16) it was possible to calculate the POP represented by the output OCR (Bentley (b), 2019).

$$p_{eq} = p' + \frac{q^2}{M^2(p' + c * cot\phi)} \tag{3.13}$$

For soft soils was the cohesion assumed to be zero for this equation. The equation used was then represented by equation (3.14).

$$p_{eq} = p' + \frac{q^2}{M^2 p'} \tag{3.14}$$

p' is the mean effective stress and q is the deviatoric stress both retrieved from the output in PLAXIS 2D. The M-value was the same as M_c defined for each layer in the input data used for the calculation. With p_{eq} (equivalent isotropic stress) and the OCR from the output in PLAXIS 2D was the isotropic pre-consolidation stress (p_p) calculated using equation (3.15).

$$OCR = \frac{p_p}{p_{eq}} \tag{3.15}$$

Since, the pre-overburden pressure POP was the value used in the input of the model was this value calculated with equation (3.16). The calculated value of POP was then compared with input value for POP in a plot where POP was plotted against level.

$$POP = p_p - p_{eq} \tag{3.16}$$

This back-calculation was only an estimation of the triaxial equivalent of OCR and POP. But with this, it was possible to see the behaviour of POP between different calculations with different input for POP. In general, the evaluated POP from the laboratory test were very high and needed to be lowered if the POP should represent values before erosion. The values for pre-consolidation stresses varied between CRS and Oedometer. The provided pre-consolidation stresses from the laboratory data were probably not exactly correct due to disturbance of tests. The test qualities from point 19WS57 and 19WS58 were classified as bad/okay in the test report provided by WSP. Therefore was the POP lowered in the following calculations to create more realistic conditions.

After the lowering of POP was the impact of M_c and M_e tested. The M_e value for clay layer 4 was chosen to be lower since the value of 1.8 is not possible. A value of 1.8 indicated that the friction angle was larger than 90 degrees. From the soil test was the model assumed to consider the value of 1.5. For clay layer 1 was the calculated value 1.4 but after several tests was this not working and therefore was the value lowered until the model worked. For comparison of results was a calculation tested by using standard values for Gothenburg clay retrieved from previously performed analyses, presented in Table3.3. Additionally, the difference in results between using a value for M_e derived in the laboratory test and evaluated values in the soil test were thereafter tested.

With lowered POP and the M_c- and M_e-value from the soil test with an exception for clay layer 1 was the sensitivity aspect of the clay tested. The values from the laboratory test gave a very high value of sensitivity which was directly connected to the amount of quick clay in the area. The behaviour of the sensitivity in the model was represented by the value of bonding, χ_0. For comparison of results was this value lowered to values below 50 since previous analyses indicate that the model only works for values between 5-100 (Gras et al., 2017).

Finally, the change in time for each phase was tested to see if the result got affected. This was done on the result with lowered POP and the M_c- and M_e-value from the soil test which was assumed to give the most accurate result.

When plotting different results five points were used. The location of these points are presented in 3.8.

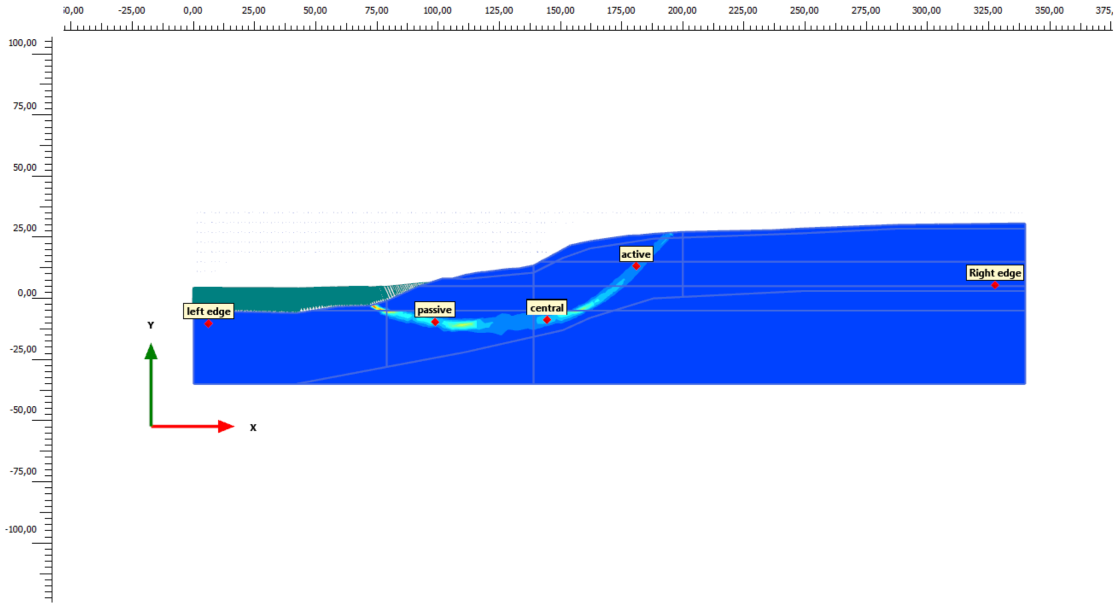

Figure 3.8: *Location of points for analysis of the final result.*

4

Results

In this chapter the results from Geostudio SLOPE/W and PLAXIS 2D are presented. The results from PLAXIS 2D are divided into results from soil test performed, the sensitivity analysis and the final result.

4.1 Geostudio SLOPE/W

The results of the slip surface and factor of safety are presented in Figure 4.1 for the combined analysis with considerations for anisotropy. A larger view of the results can be found in Appendix C.1 with the results from the undrained and combined without anisotropy calculations, Appendix C.2 and C.4. In the combined case with anisotropy is the factor of safety calculated to be 1.18. The critical slip surface is visualised with the white line in the red area in Figure 4.1. The results of the pore pressure distribution along the slip surface are presented in Appendix C.5-C.7.

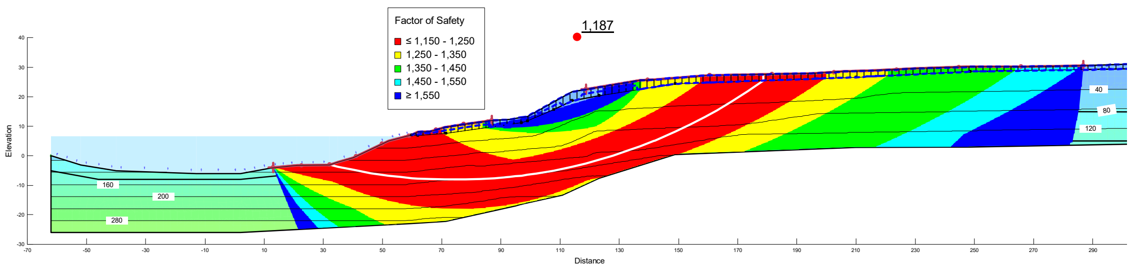

Figure 4.1: *Results from GeoStudio SLOPE/W with combined analysis and anisotropy.*

A summary of the factor of safety for the three different calculations are presented in Table 4.1.

Table 4.1: *Factor of safety from calculations in Geostudio SLOPE/W.*

Calculation type	Factor of safety
Undrained	1.17
Combined without anisotropy	1.15
Combined with anisotropy	1.18

All results give a factor of safety larger than one. The difference in results between the calculations indicates that the slope is more stable when more characteristics related to anisotropy are considered. The combined analysis without anisotropy gives the lowest factor of safety and is therefore normally considered as the valid value for the analysis to be on the safe side and represent the worst-case scenario. However, as mentioned in the method the combined analysis with anisotropy (FS=1.18) is of interest for comparison with the PLAXIS 2D results.

4.2 Soil test PLAXIS 2D

The fitting of the curves from the soil test performed in PLAXIS 2D for Triaxial, Oedometer and CRS tests with retrieved laboratory test data are presented in the following chapters.

4.2.1 Triaxial test

The results from the soil test in PLAXIS 2D of the Triaxial tests in compression are presented in Figure 4.2 and 4.3. The results visualise both plots of the simulated curve from soil test and the real laboratory test result curve. For the curve from the soil test were firstly different POP tested to retrieve a curve with similar stresses as the laboratory curve, see Figure 4.2. Thereafter was the most suitable POP used and different M_c-values were used to fit the inclinations of the curves, see Figure 4.3. This procedure was done for all clay layers and the results of the fitting of curves considering M_c for clay layer 2-4 can be found in Appendix D.1-D.3.

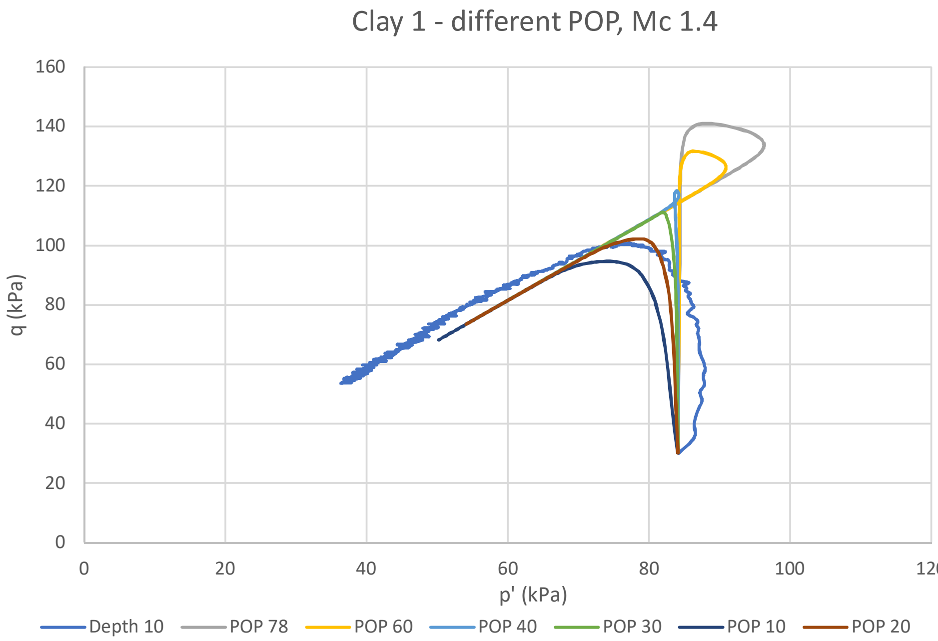

Figure 4.2: *Data from soil test in PLAXIS 2D in comparison with laboratory results of Triaxial test with different POP for Clay 1.*

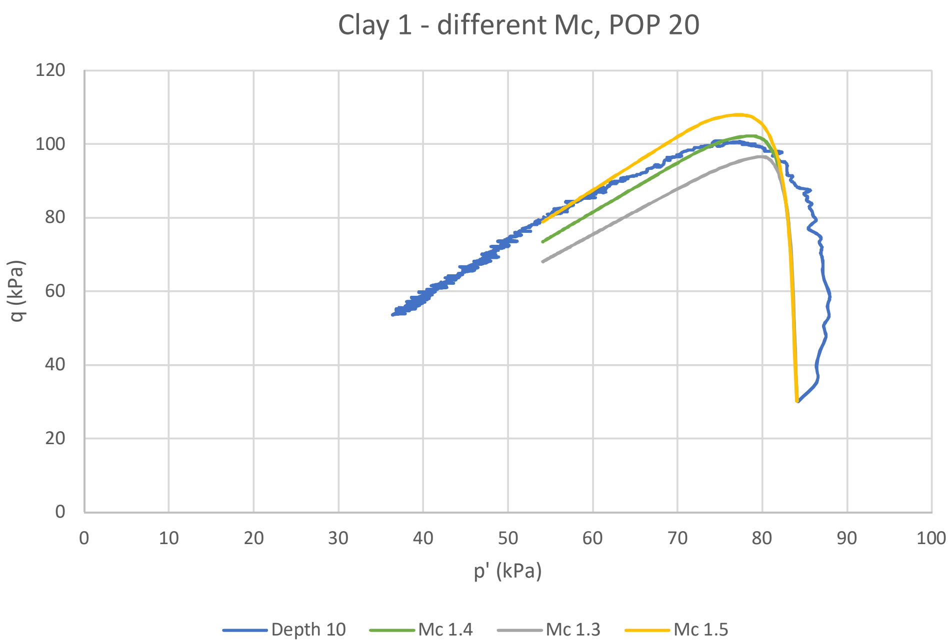

Figure 4.3: *Data from soil test in PLAXIS 2D in comparison with laboratory results of Triaxial test with different M_c for Clay 1.*

The values of M_c from the soil test are similar to the results from the derived values. The change in POP is due to the difference in the stress history of the soil. The evaluated POP represents more overconsolidated clay layers than when using the POP retrieved in the soil test. The input value of POP is also based on the Oedometer test and not the Triaxial test. However, have the clay layers still overconsolidated characteristics with the low POP used in the soil test.

The results from soil test of the Triaxial test in extension are presented in Figure 4.2 and 4.3 for clay 1. The results presented are the same as for M_c with fitting the curve by first changing POP and then fit the inclination by changing M_e. The retrieved results for clay layer 2-4 are found in Appendix D.1-D.3.

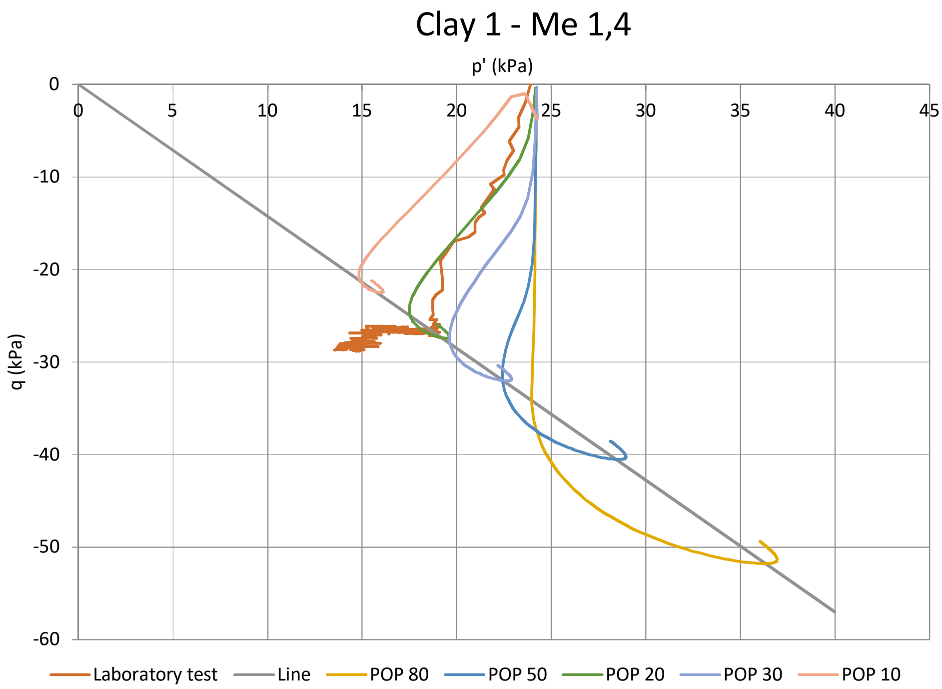

Figure 4.4: *Data from soil test in PLAXIS 2D in extension comparison with laboratory results of Triaxial test with different POP for Clay 1.*

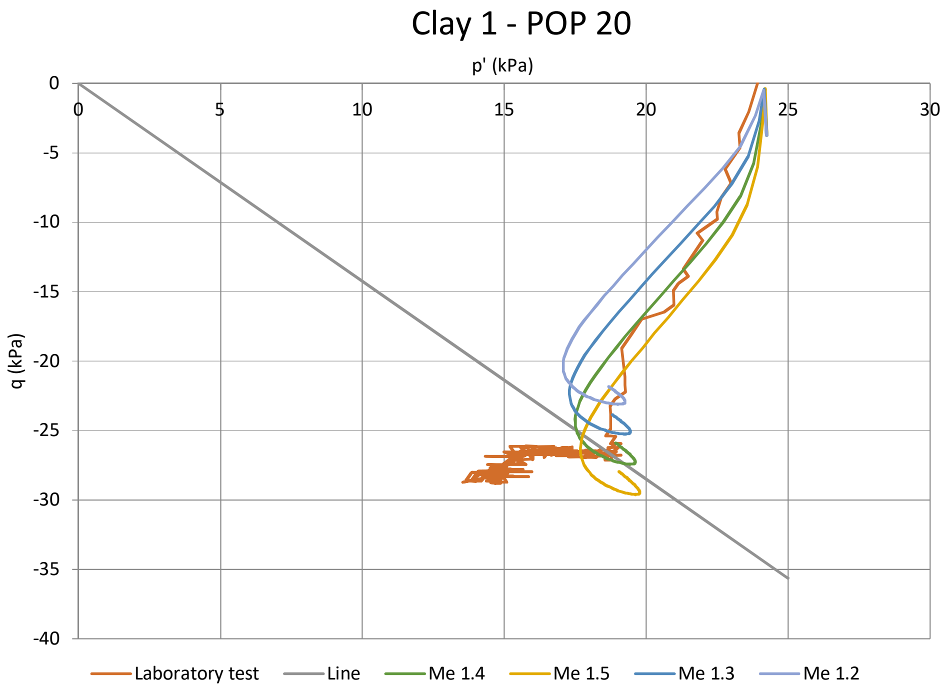

Figure 4.5: *Data from soil test in PLAXIS 2D in extension and laboratory results of Triaxial test with different M_e for Clay 1.*

A lowering of POP gives a more reasonable fit to the laboratory test curve. The retrieved POP of the best-fitted curve is similar as the POP for the M_c (POP=20) but in some cases even lower. The graph from the laboratory test and the soil test does not have the same shape but in this case are the stress levels and the evaluation of M_e of interest. As can be seen in Figure 4.4 is the evaluated value for Clay 1 (M_e=1.4) the best fitting when comparing inclinations. However, a pattern could be seen for clay layers 2-4 when evaluating M_e. In all three layers a maximum M_e is evaluated, any increase in M_e after this does not give any change in the curve formation. The maximum of M_e could directly be connected to the used M_c-value for each layer. If the M_e is larger than M_c would there not result in any difference in the model. Therefore, if the M_e value is 1.8 and M_c is 1.4 would the model still calculate M_e=1.4. A value of M_e larger than 1.5 would also indicate a critical friction angle larger than 90 degrees which would be unreasonable.

A summary of the values of M_c and M_e from the soil test can be seen in Table 4.2.

Table 4.2: *Values of M_c and M_e from soil test.*

	Clay 1	Clay 2	Clay 3	Clay 4
M_c	1.4	1.4	1.3	1.5
M_e	1.4	1.3	1.3	1.5

4.2.2 Oedometer test

The results of the comparison between the Oedometer soil test, general soil test and the laboratory test are presented in Figure 4.6 for Clay 1. The results for clay layer 2-4 are presented in Appendix D.4-D.6.

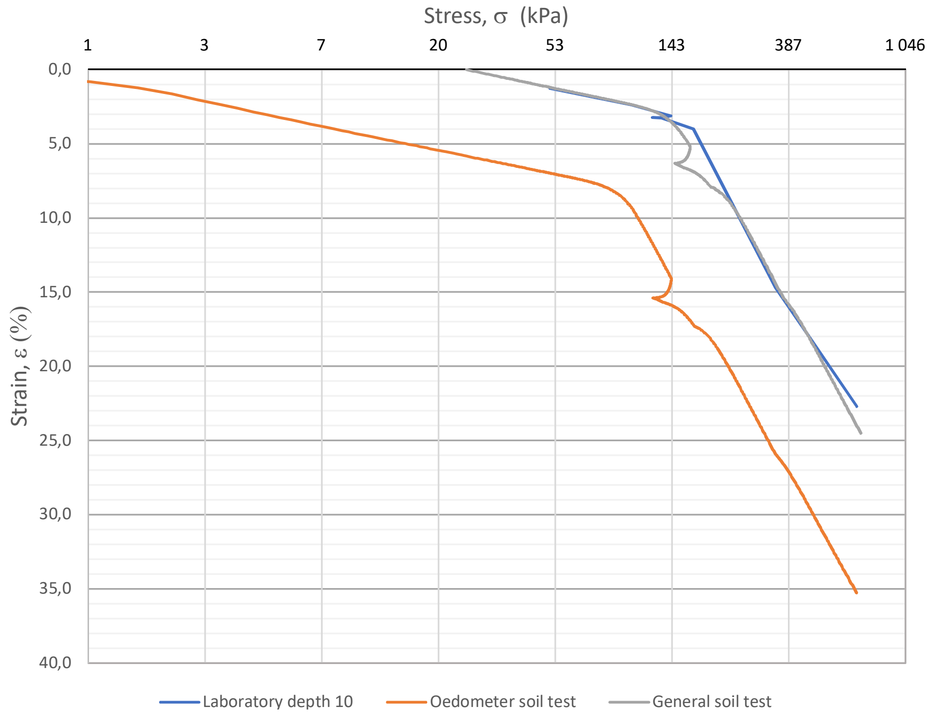

Figure 4.6: *Data from soil test in PLAXIS 2D using both Oedometer function and general function in comparison with laboratory results of Oedometer test for Clay 1.*

The fitting of the curves resulted in changes of values for κ^* and λ^*. In the input data to Creep-SCLAY1S it is λ_i^* that affects the λ^*-value in the plotted graph. A summary of retrieved results for each clay layer are presented in Table 4.3.

Table 4.3: *Values of κ^*, λ^* and λ_i^* from Oedometer soil test.*

	Clay 1	Clay 2	Clay 3	Clay 4
κ^*	0.016	0.013	0.017	0.014
λ^*	0.17	0.19	0.22	0.19
λ_i^*	0.07	0.073	0.07	0.077

4.2.3 CRS test

The results from the soil test where the CRS test, general test and laboratory tests are compared are presented in Figure 4.7. Results for clay layer 2-4 are presented in Appendix D.7-D.9.

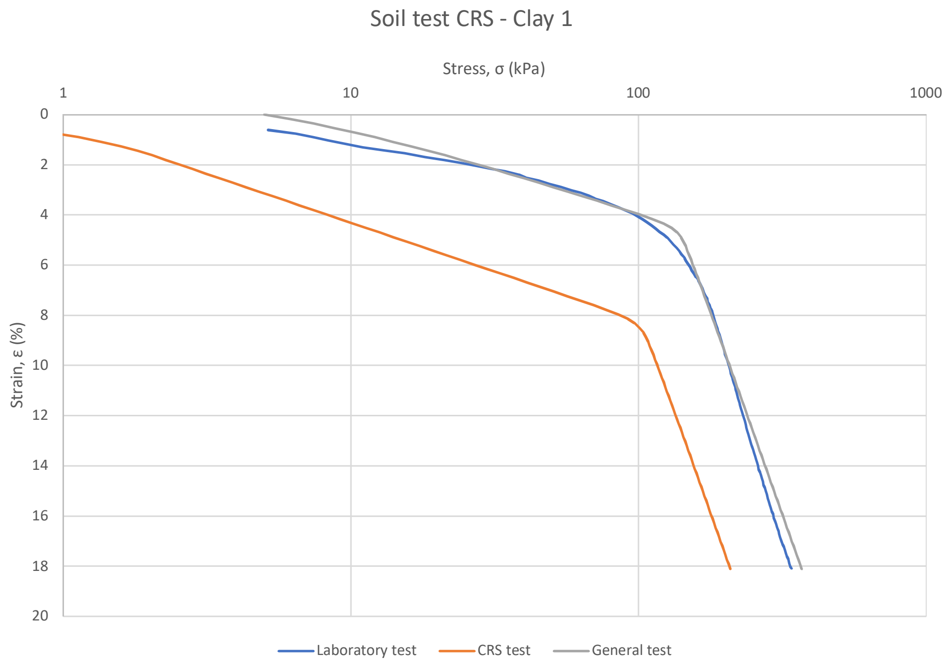

Figure 4.7: *Data from soil test in PLAXIS 2D using both CRS function and general function in comparison with laboratory results of CRS test for Clay 1.*

A summary of retrieved values of κ^*, λ^* and λ_i^* are presented in Table 4.4. This result fits the laboratory results from the CRS test but has a deviation from the same parameters evaluated in the Oedometer soil test.

Table 4.4: *Values of κ^*, λ^* and λ_i^* from CRS soil test.*

	Clay 1	Clay 2	Clay 3	Clay 4
κ^*	0.010	0.010	0.017	0.012
λ^*	0.17	0.46	0.31	0.29
λ_i^*	0.07	0.073	0.08	0.077

4.3 Calculations PLAXIS 2D

By using the input data evaluated from the laboratory tests and the soil tests could a first result be calculated. The slip surface retrieved from the first calculation is presented in Figure 4.8. The slip surface is visualised by using the incremental deviatoric strain in the soil which presents where the soil fails. This calculation gives a factor of safety of 3.16 with M_{stage}=4. Results presenting horizontal and vertical displacements after erosion, pore pressure distribution and amount of bonding after erosion can be found in Appendix E.1-E.4.

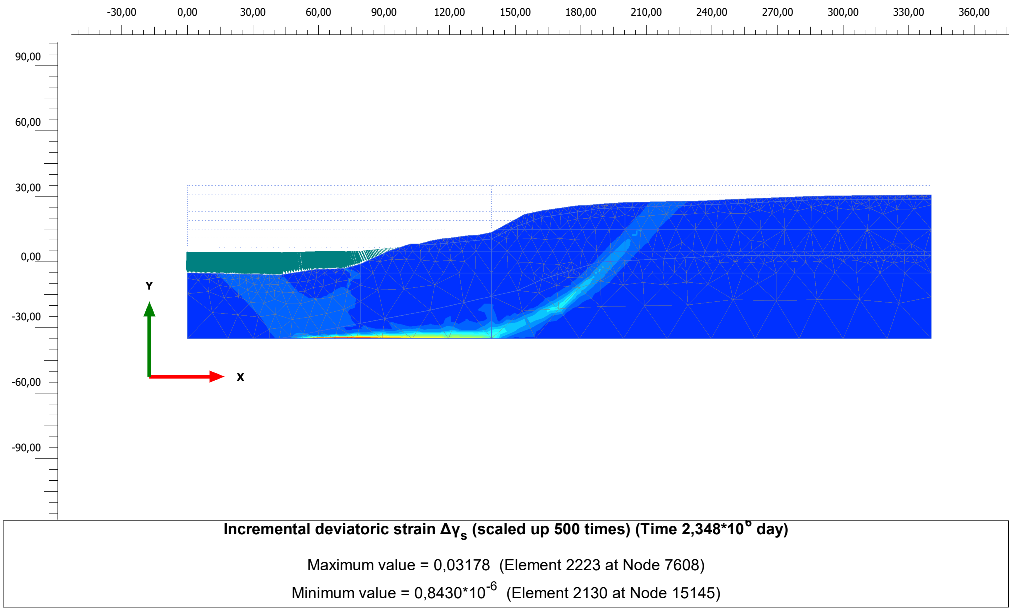

Figure 4.8: *Contour of incremental deviatoric strain for the first calculation completely based on evaluated data.*

The shape of the slip surface in this calculation could be due to anisotropy which contributes to a non-circular surface. Since the slip surface is passing through the entire model modifications are needed. Modifications needed may be to refine the mesh or modify strength characteristics. The deep slip surface is probably due to strength changes in the soil when the erosion takes place. Hence, the input data are representing values after erosion are other stress history parameters needed for the soil before erosion.

4.3.1 Sensitivity analysis

The results from the sensitivity analysis is presented in following chapters.

4.3.1.1 Modification OCR and POP

The results retrieved by using the evaluated data from laboratory tests were not expected. A calculation with decreased POP was therefore tested as described in chapter 3.2.3.4. The contour with incremental deviatoric strain from this calculation is presented in Figure 4.9. This Figure visualises the slip surface of the failure in the slope when the POP is decreased to 30 kPa in each layer. Several calculations were tested and a POP of 20-50 kPa in all layer gives a similar slip surface but with different incremental strain value. This calculation gives a factor of safety of 3.0 with M_{stage}=4.

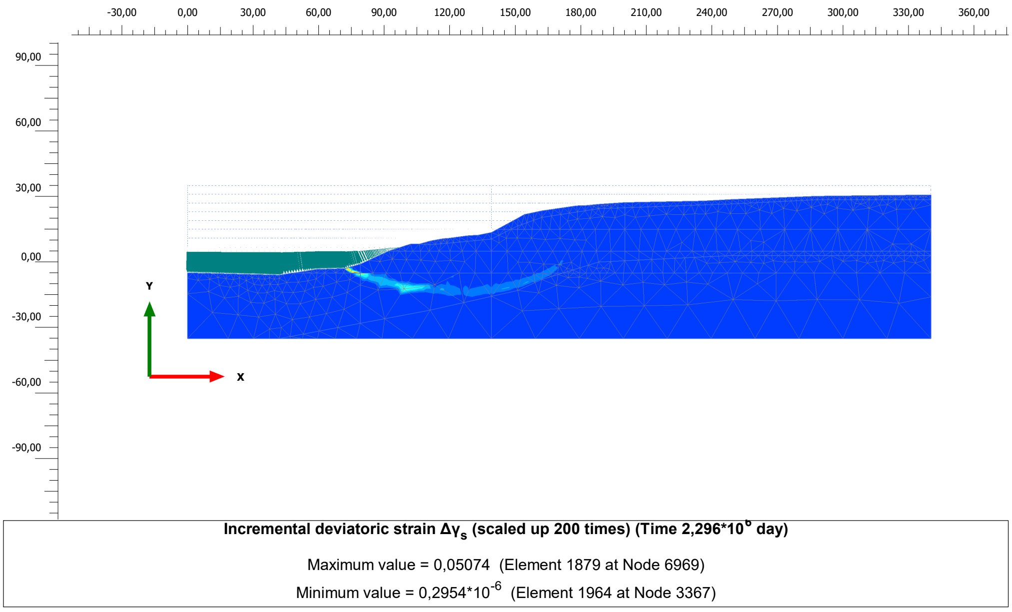

Figure 4.9: *Contour of incremental deviatoric strain for the case with lowered POP.*

In comparison with the first calculation based on laboratory data, this slip surface is more reasonable since there is no unexpected change in direction. The slip surface is almost circular and quite similar to the slip surface retrieved in the calculations performed in Geostudio SLOPE/W (see Figure 4.1).

4.3.1.2 Impact of M_c and M_e

The results from changes in M_c and M_e are of interest since the parameters are based on how the soil behaves in compression and extension in both vertical and horizontal direction. The slip surface of the calculation with M_e values based on a previous analysis in the Gothenburg area is presented in Figure 4.10. The chosen values of M_e is from clay layer 1-4: 1.0, 1.1, 1.1, 1.3. This calculation gives a factor of safety of 2.6 with M_{stage}=4.

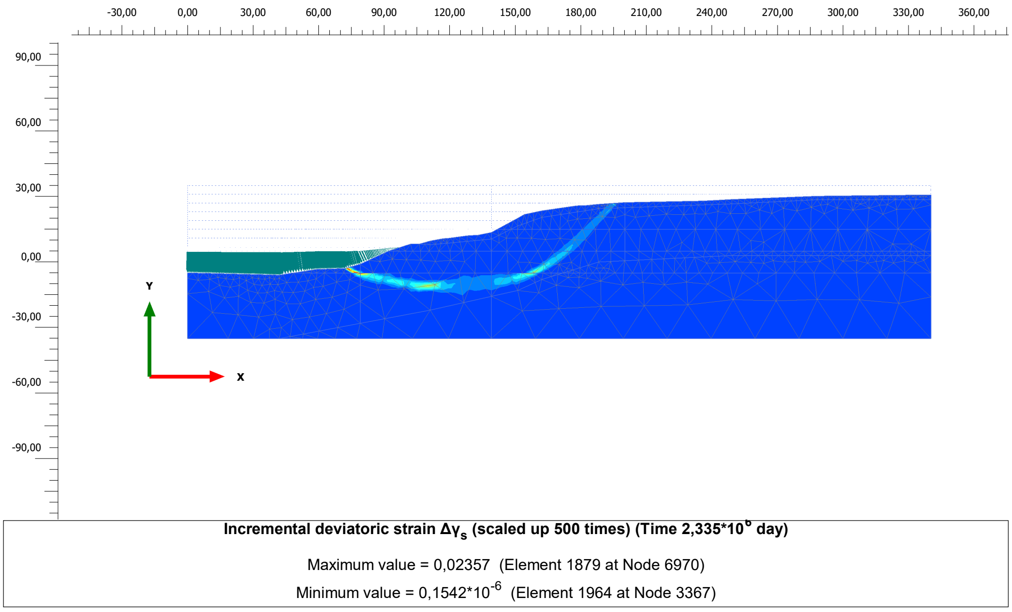

Figure 4.10: *Contour of incremental deviatoric strain for the case with lowered M_e.*

The result of the slip surface from using the M_e-values retrieved in the soil test is presented in Figure 4.11. In the original calculation were values used from the laboratory test. For the model to work was M_e set to 1.2 in clay layer 1. This calculation gives a factor of safety of 2.96 with M_{stage}=4.

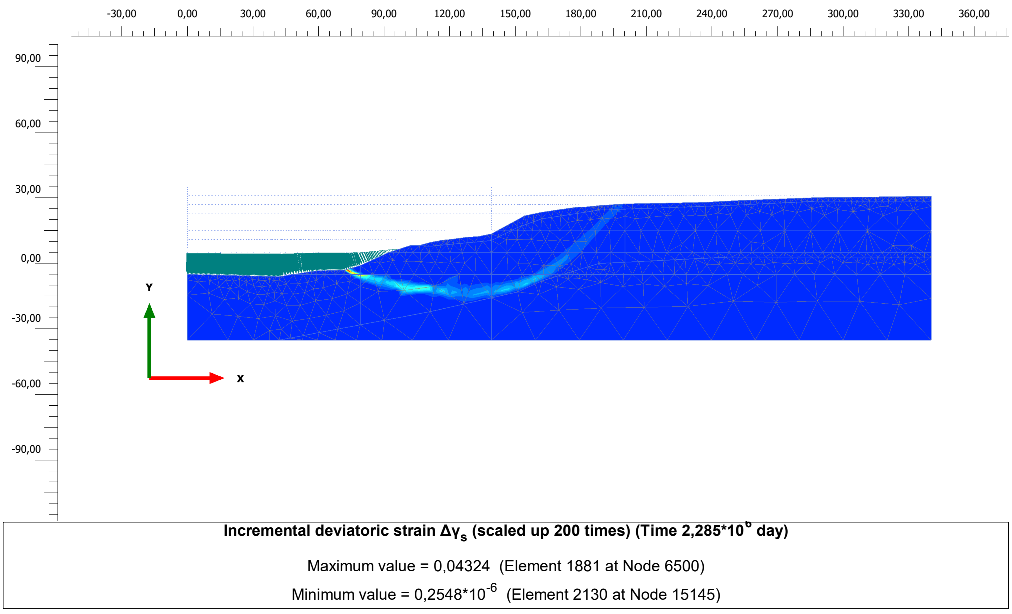

Figure 4.11: *Contour of incremental deviatoric strain for the case with M_e from soil test instead of laboratory test.*

These results show that minor differences appear when lowering the M_e to values not higher than M_c. This indicates that the assumption that the model has maximum values for M_e is true. When 1.8 is defined for clay layer 4 the model is most probably using 1.5 instead. However, it can be seen that the slip surface reaches through layer 1 and 2 in the case of M_e from the soil test. This can directly be connected to that in layer 1 and 2 are the values of M_e lowered to values below M_c defined for each layer. The slip surface is changed in these layers since the characteristics are changed. In the case with M_e-values around 1.1, like previous Gothenburg characteristics, the slip surface is more distinct in layer 1 and 2. The shape is less circular than with the soil test values which could be due to more anisotropy effect when the difference between compression and extension failure characteristics are bigger.

4.3.1.3 Lowering sensitivity of soil

The lowering of the sensitivity and the amount of bounding in the soil mainly affects the magnitude of the deformations. The result of the total deformation is calculated to be 4 meters, the same as the deformation with modified POP and M_e from soil test. This calculation gives a factor of safety of 2.96 with M_{stage}=4. A contour of the total displacement and the slip surface with lowered sensitivity can be found in Appendix E.5. The slip surface and area of maximum deformations during failure are similar to the calculation with modified POP and M_e from soil test.

The result from this calculation indicates that the lowering of sensitivity to 50 contributes to minor changes. The slip surface is the same and the small difference in the result indicates that the model probably uses a maximum value of 100 and not values of 500 in bonding like defined in the first calculation from laboratory results. The soil deformations in failure could therefore be larger in reality since the model does not consider such high sensitivity as measured when quick clay appears. A comparison of the amount of bonding in the layers between the original calculation and this calculation with lowered sensitivity can be seen in Figure 4.12.

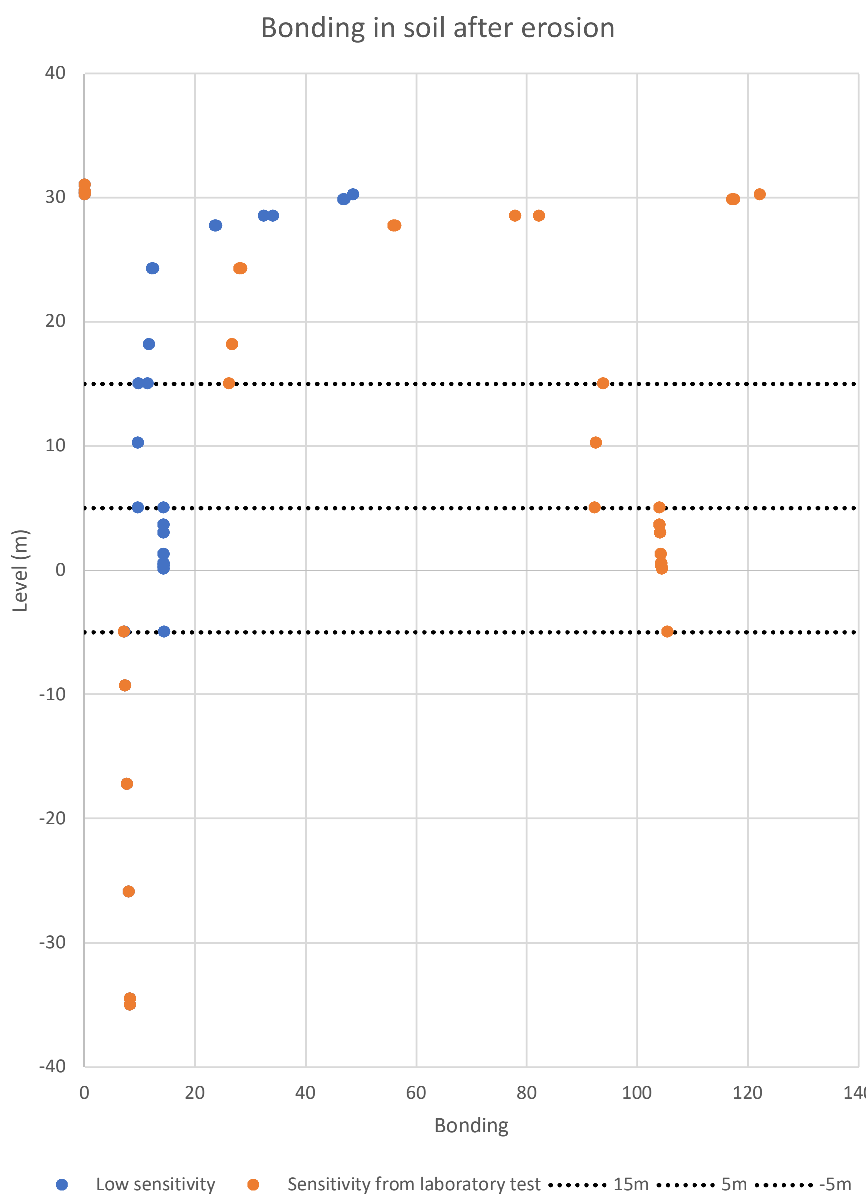

Figure 4.12: *Comparison of bonding with level in the soil in the upper part of the slope using different input values.*

The quick clay with high sensitivity is mostly represented in clay layer 2 and 3. In these layers are the values of bonding different between the two calculations with high and low sensitivity. For the calculation with input values of 400-500 in layer 2 and 3 is the result of the output bonding which the model uses right above 100. The bonding for the calculation with 50 as input value is, however, lowered to about 10-20 in bonding in the output result. This indicates that the model reduces the bonding approximately 1/5 of the original input value through the erosion process.

4.3.1.4 Time analysis

For all previous calculations were the time for each erosion phase set to 100 years. To analyse if the time affects the result a phase time of 1000 years was tested. The results are presented in Figure 4.13 where displacements with time are compared with the result from the calculation with modified POP and M_e from soil test. The result of the slip surface can be found in Appendix E.6.

Figure 4.13: *Displacements at the right edge of the slope with the comparison between phase time 1000 and 100 years. Left graph: Vertical displacements, Right graph: Horizontal displacements.*

These results show that with a longer erosion process are the displacements decreased. This is due to the stresses that appear in the structure during the erosion. If the erosion process is slower the build-up of effective stresses due to the lowering of the groundwater level are lower. This makes the process more stable which then could explain the lower displacements with a time of 1000 years for each erosion phase. However, the time frame does not affect the location of the slip surface and the faster erosion contributes to a worse scenario.

4.3.2 Mesh analysis

Three different meshes were tested for the mesh analysis: medium with refinement, very fine with 3 refinements and very fine with 6 refinements. These are predefined mesh sizes provided by PLAXIS 2D. The result of the analysis indicates that with an increase in mesh density is the location and failure mechanism of the slip surface not affected. However, with an increase in mesh density is the distinctness and thickness of the slip surface decreasing. The final mesh used for the calculation of the slope stability is a very fine mesh with 3 times refinement in the area between the river and the top of the steeper part of the slope. The very fine mesh can be seen in Figure 4.14 and the medium mesh can be found in Appendix E.7. The factor of safety is slightly increased with increased mesh density.

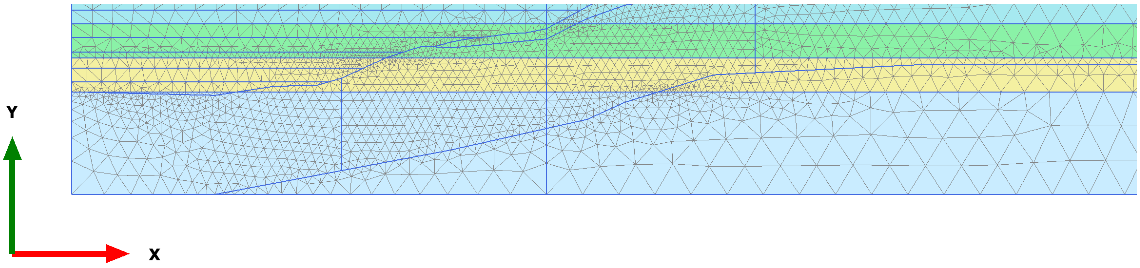

Figure 4.14: *Mesh density for very fine mesh with refinement in the central part of the slope.*

4.4 Final result PLAXIS 2D

The results with most reliable modifications are to calculate the slope stability using the laboratory test with modification of the POP and using all values from the soil tests. The final slip surface with a refined very fine mesh is presented in Figure 4.15. For analysis of the final results, five different points are used when graphs are produced. The location of these points are presented in the method with Figure 3.8.

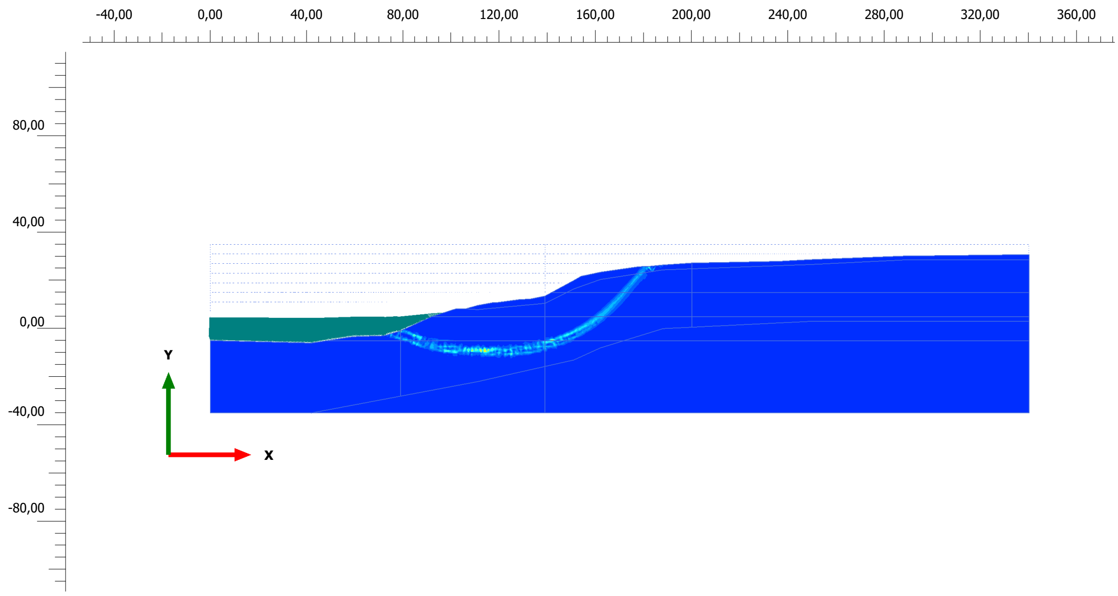

Figure 4.15: *Contour of incremental deviatoric strain for the final result.*

4.4.1 Deformations

Deformations during the erosion process and the consolidation in both vertical and horizontal direction for different locations in the slope are presented in Figure 4.16 and 4.17. The erosion process is during the first 1000 years which is approximately the first 400 000 days in Figure 4.16 and 4.17.

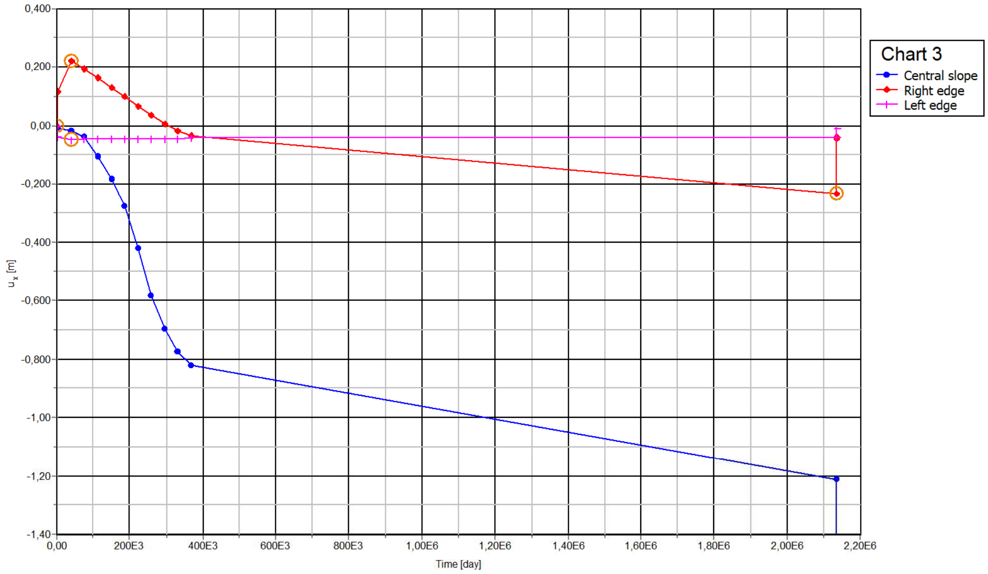

Figure 4.16: *Horizontal deformations with time (days) for points located under the river, in the central slope and in the right edge of the slope section.*

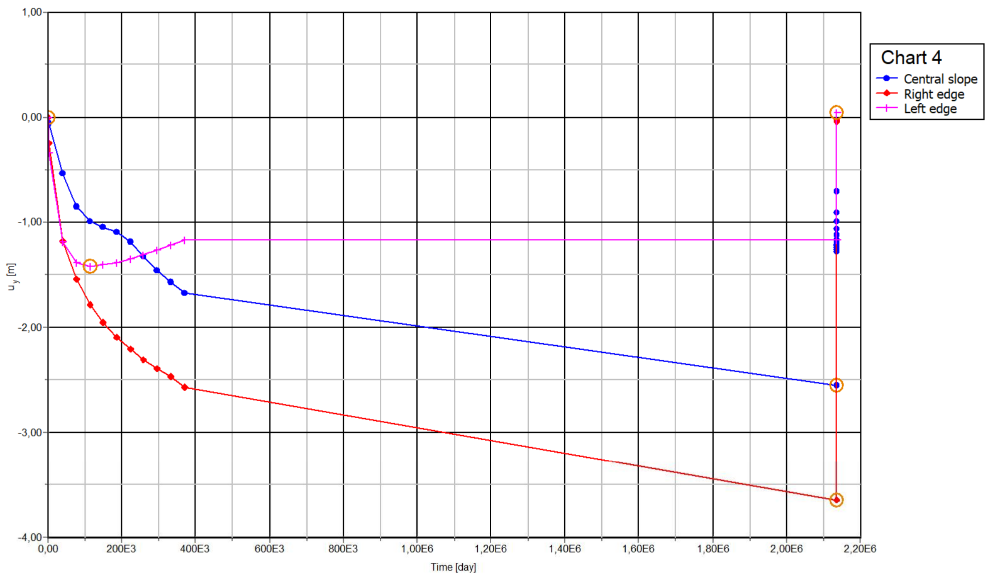

Figure 4.17: *Vertical deformations with time for points located below the river, in the central slope and in the right edge of the slope section.*

In Appendix E.8 and E.9 are the contours for the vertical and horizontal displacements presented after erosion and consolidation. The maximum value of deformation appears at other locations than the graphs visualises in Figure 4.16 and 4.17. The maximum horizontal displacement due to erosion is calculated to med 2.2 meters and the maximum vertical displacements are 9.8 meters. After the last consolidation step is the displacements set to zero. The result of deformation during failure is then calculated to be 8.3 meters in the horizontal direction. The vertical deformations during failure appear with downward displacement of 5 meters and a heave of 3.1 meters. The contour for the vertical displacement during failure can be found in Appendix E.10.

4.4.2 Pore water pressures

Pore pressures measured in the field for point 19WS58 in comparison with the pore pressures the model uses after erosion is presented in Figure 4.18. The orange line in the graph is presented by a hydrostatic condition of the pore pressure from the measured groundwater level. From the model, it is seen that the calculation uses hydrostatic pore pressure distribution. The value of the pore pressure depends on where the groundwater level is located. In the model, the level is located lower than in reality. The location of the phreatic line in the model is presented in Appendix E.11.

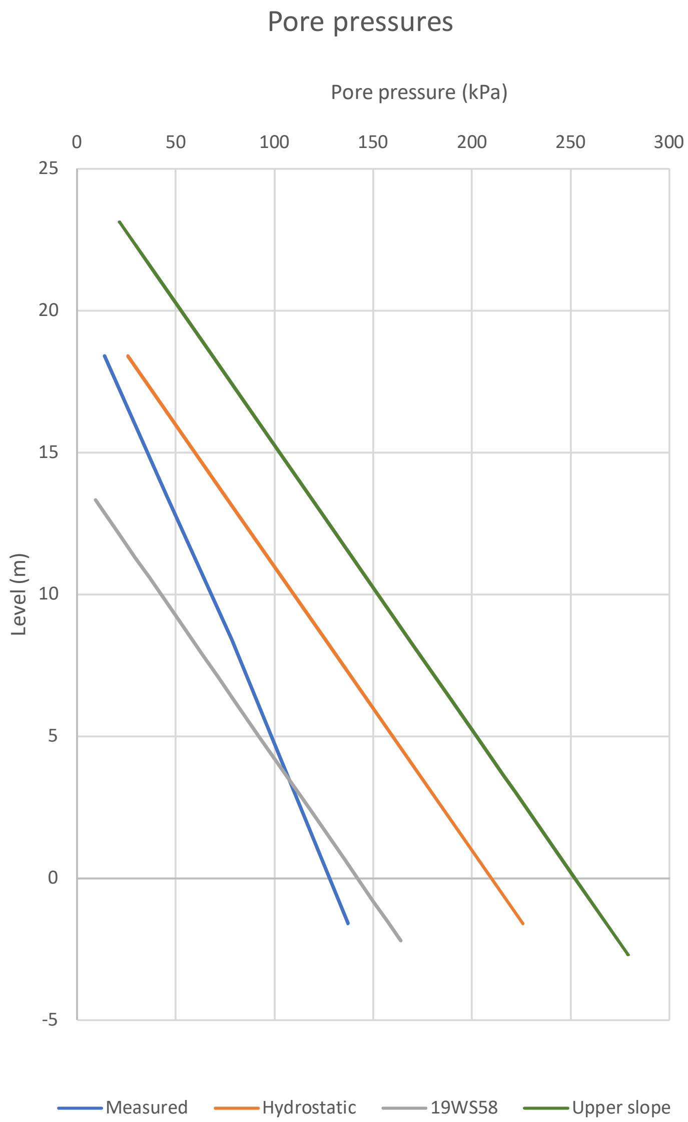

Figure 4.18: *Measured and modelled pore pressures in the slope. Blue: measured in 19WS58, Grey: Calculated in 19WS58, Green: Calculated for right edge of the slope, Orange: Hydrostatic line from 2.5 meters below ground level.*

Excess pore pressure during the erosion process is presented in Appendix E.12. The excess pore pressure is build up during the first loading stage before the erosion takes place. During the erosion is the excess pore pressure slowly decreased towards zero as the soil erodes and the groundwater head is lowered.

4.4.3 Soil characteristics

The stress path for the soil during the erosion process is presented using plots with deviatoric stress and mean effective stress, see Figure 4.19. This is plotted next to the strain-stress behaviour for the erosion process. In Figure 4.19 are values from 5 different locations compared. The graphs can be divided into two groups that imply different behaviour. The left edge and the passive graphs are based on points located in the slope where most erosion takes place. The behaviour here is that the increase of rotational stress does not affect the axial strain largely since the horizontal stresses get larger than the vertical. The right edge, active and central slope graphs are based on points located in the part of the slope which is not exposed for a large amount of erosion. Here the behaviour is more connected to the state of soil surface described in the theory about Creep-SCLAY1S. There is a difference in the state of stresses in the different points which represents the different graphs but a stress path can be seen. The differences in the stress state of the different points could be due to the amount of bonding. The amount of bonding for the five different locations with time and the contour of bonding after erosion can be found in Figure 4.20 and 4.21. These results indicate that there is a larger amount of bonding for the points central slope, active and right edge. The high amount of bonding and sensitive soil is in clay lager 2 and 3. The strain-stress behaviour for these three cases are similar but with different size of strain. The difference in strain can be correlated to the stress state but also the amount of creep that appears.

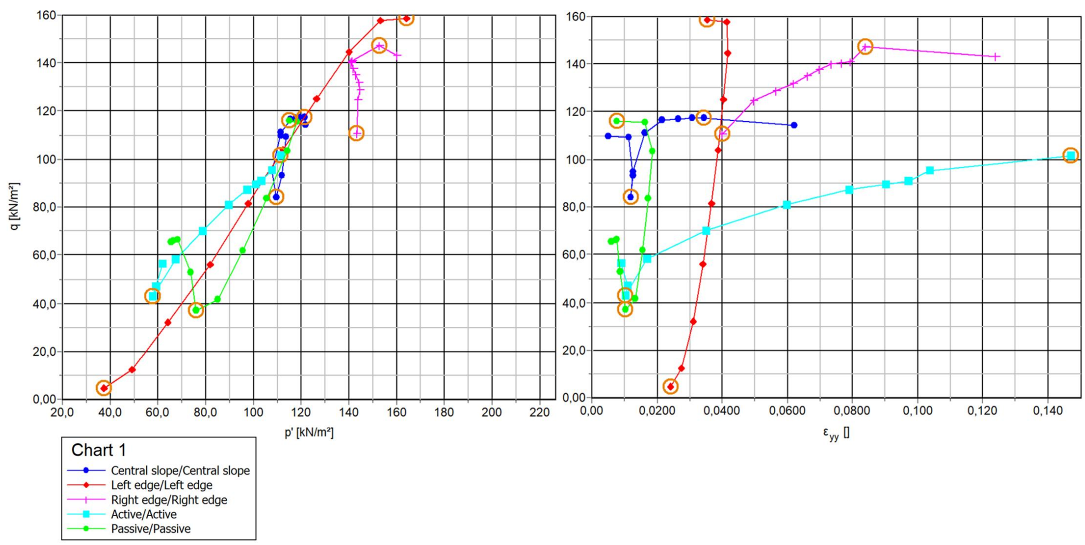

Figure 4.19: *Stress path (left graph) and stress strain curve (right curve) for five points in the slope during the erosion process.*

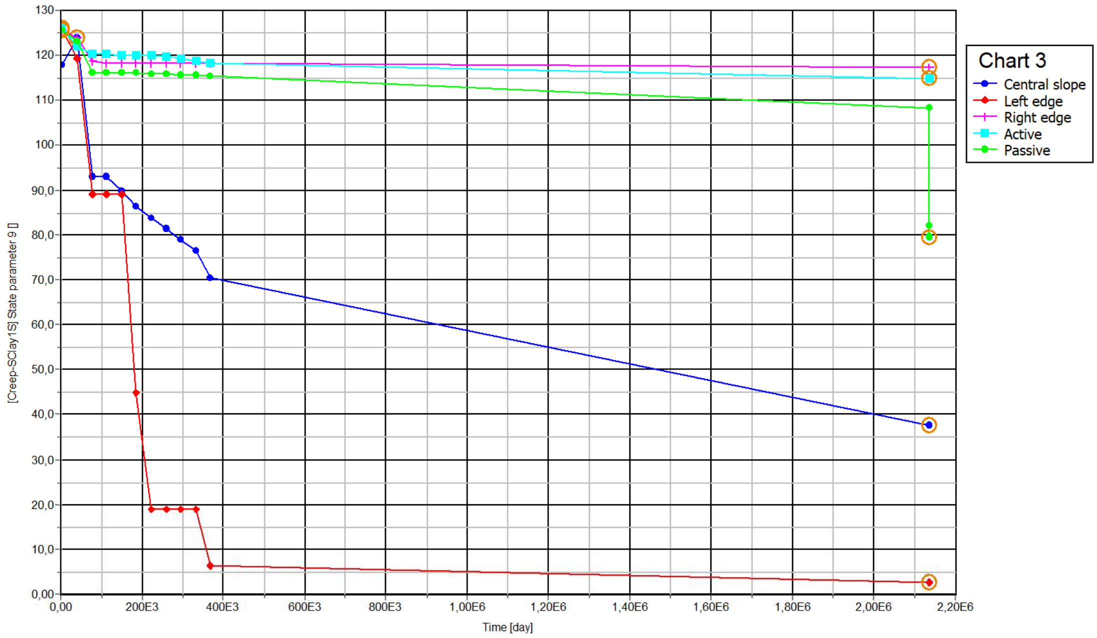

Figure 4.20: *Bonding with time at five different locations in the slope of the final result.*

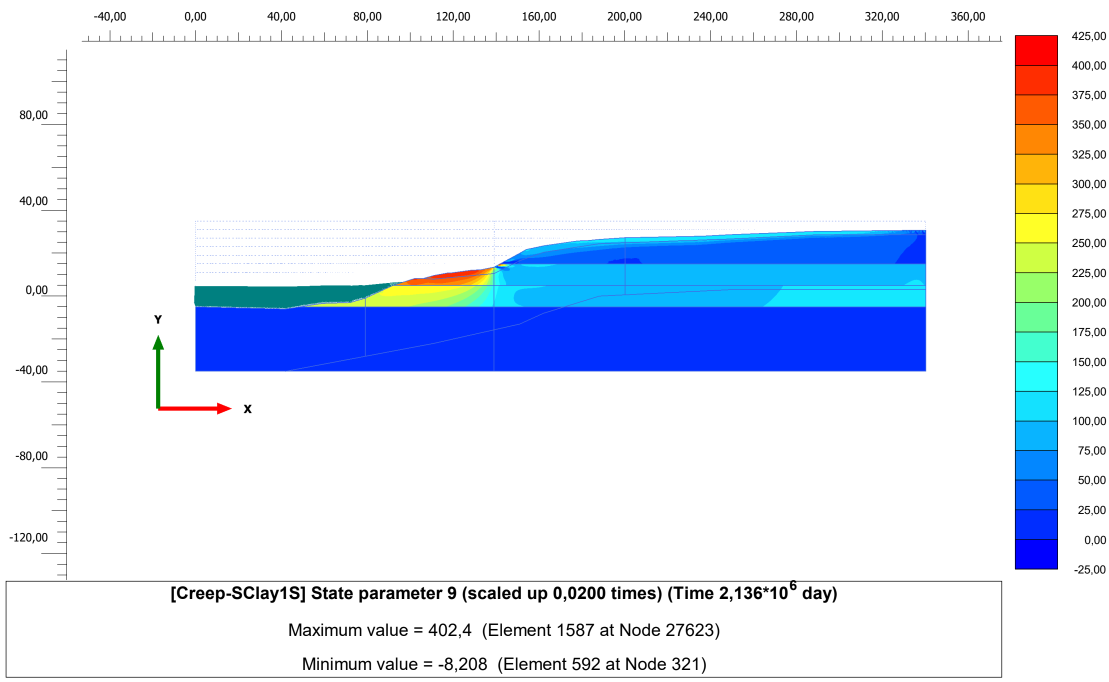

Figure 4.21: *Contour of the final bonding after erosion of the final result.*

In Figure 4.22 is the stress path in the failure presented. The points in the left and right edge are not affected by the failure. The central slope, passive and active point which are located in the slip surface form a stress path which indicates the formation of a possible failure line for the slopes failure mechanism.

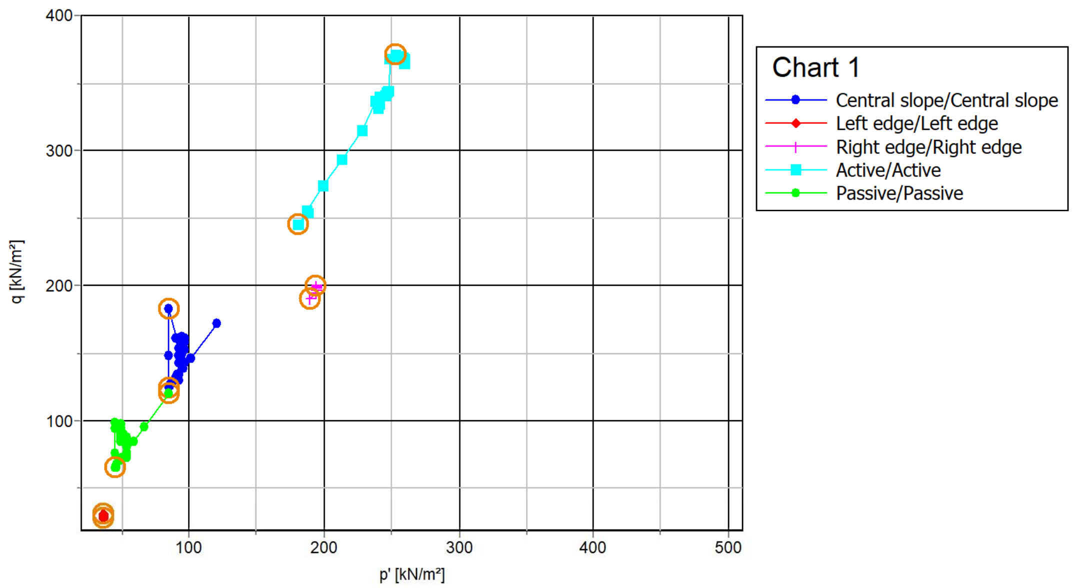

Figure 4.22: *The stress path during failure for five points in the slope.*

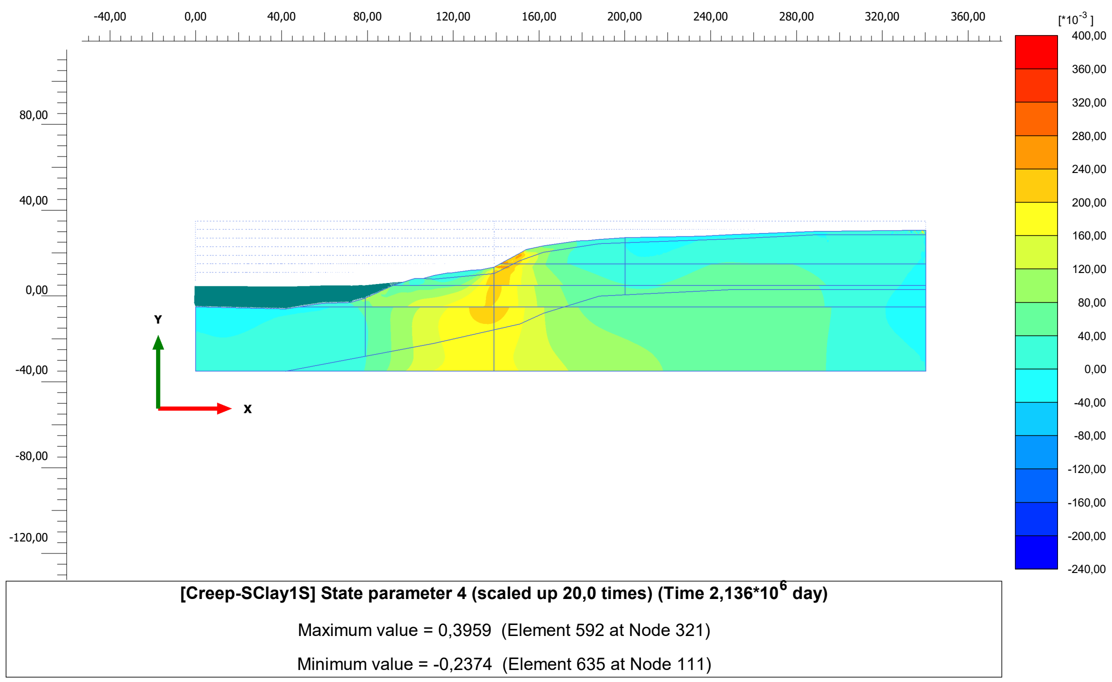

Figure 4.23: *Contour of rotation of yield surface in xy-direction.*

The rotation of fabric in x-y-plane after erosion is presented in Figure 4.23. This result gives a view of where in the slope section the mobilised strength is affected. The largest rotation appears approximately at the lowest point of the slip surface. Hence this is the case it is assumed that it is the area of the soil where the NCS-surface (describe in theory) has the largest rotation.

Results of the difference in change of OCR during the erosion process for a point located below the river and a point at the right edge of the slope are presented in Appendix E.13. Notice that this is the OCR retrieved from PLAXIS 2D which is not the laboratory value for OCR. These results indicate that the input data are largely changes in the areas where most of the erosion appears, meanwhile, is less changed in the area with a low amount of erosion.

4.4.4 Factor of safety

The results of the factor of safety vary largely depending on the input in the safety phase. The variation of the factor of safety due to M_{weight} but with the time of 1 day for the phase is presented in Figure 4.24. The variation of the factor of safety depending on the time of gravity increase in the safety phase is presented in Figure 4.25.

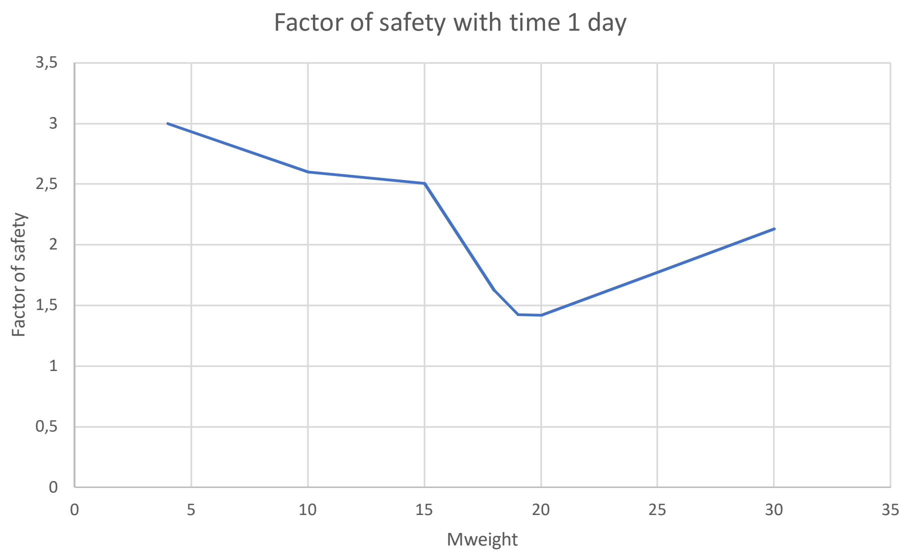

Figure 4.24: *Variation of factor of safety with different M_{weight}.*

Figure 4.25: *Variation of factor of safety with different M_{weight} and time.*

With an increase of M_{weight} is the factor of safety decreased. It is reasonable for the structure to be more unstable when the weight of the soil is increased. However, the increase of M_{weight} is only possible until a certain value before other failure appears than the previously presented slip surfaces. The lowest value of the factor of safety with a safety phase of 1 day is calculated to FS=1.42. If the time is increased it is possible to retrieve lower values of the factor of safety with a lower value of M_{weight}, as seen in Figure 4.25. The lowest value of the factor of safety retrieved from that analysis is FS=1.36 when the time of the phase is set to 100 years and M_{weight} either 10 och 20.

5

Discussion

The discussion chapter is divided into two parts. The first part is comparing the used models and the second part is discussing possible uncertainties in the Creep-SCLAY1S model.

5.1 Comparison modelling methods

A first step in comparing the calculation methods regarding Geostudio SLOPE/W and Creep-CLAY1S in PLAXIS 2D is to compare the result of the slip surfaces. The difference between the slip surfaces is both in shape and location. The largest difference is in the entry location of the slip surface between the models. The entries of the slip surfaces from Geostudio SLOPE/W, depending on calculation type, are varying between 190-215 meters from the left boundary defined in the PLAXIS 2D model and the entry of the slip surface in PLAXIS 2D is located at 181 meters from the same boundary. The difference in the exit of the slip surface is, however, significantly smaller but still 7 meters where the slip surface from Geostudio SLOPE/W exits further into the river. This could be due to the considerations of anisotropy. Hence, the calculation in Geostudio SLOPE/W only considers anisotropy by dividing the slope section into zones may the effects of anisotropy in smaller areas be excluded.

The calculation in Geostudio SLOPE/W is also based on a limit equilibrium where the slip surface always is assumed to be circular. From the comparison between the two models can it be seen that the slip surface is curved but the radius is not constant through the entire slip in the calculations from PLAXIS 2D. The anisotropy effect is that the slip surface is much steeper in the zone of compression (active zone) but then similar to the limit equilibrium calculation in the zone of extension (passive zone). This makes the slip surface from PLAXIS 2D more narrow when considering the horizontal width. The slip surface is still vertically reaching to the same depth as the slip surface from Geostudio SLOPE/W. The differences in slip surfaces could also be due to the initial conditions used as input. In PLAXIS 2D the materials are defined to be calculated with undrained conditions meanwhile in Geostudio SLOPE/W are the conditions a combination of drained and undrained. The shape of the slip surfaces is more similar when comparing the undrained calculation in

Geostudio SLOPE/W with PLAXIS 2D than the combined calculation.

The differences in the results between the models could also be due to the differences in modelling the pore pressure distribution. The pore pressures for Geostudio SLOPE/W are created through a water level of 2.5 meters below ground level and thereafter hydrostatic conditions with depth. The model in PLAXIS 2D indicates a hydrostatic condition after the erosion process but with the use of defining head at the boundaries the water level is located lower in some areas of the slope than in Geostudio SLOPE/W. This contributes to lower pore pressures in PLAXIS 2D and also other stress conditions. The difference in pore pressure is, however, not significantly high (see Figure 4.18 and therefore it is assumed that the lower level of groundwater in PLAXIS 2D is not the reason for differences between the models.

The calculations from PLAXIS 2D indicates that the factor of safety is higher than what the calculation from Geostudio SLOPE/W indicates. The factor of safety in Geostudio SLOPE/W varies between 1.15-1.18 meanwhile the variation from PLAXIS 2D is 1.36-3.0. The expectations were that the factor of safety for PLAXIS 2D should be higher since less simplifications are made in the model. However, there is high uncertainty in the retrieval of the factor of safety in PLAXIS 2D. There is a high variation in result depending on the gravity applied and during what time frame. For the case where FS=1.36 was quite unreasonable high gravity loading applied to the model. When a large amount of gravity is applied it is reasonable for the slope to fail. The factor of safety from Geostudio SLOPE/W is more conservative since it is based on simplifications often related to the worst-case scenario. When evaluating the factor of safety, the worst-case scenario is good to consider to be on the safe side. However, a higher factor of safety could contribute to a different strategy when evaluating further reinforcements if that is the purpose of a project. If the Creep-SCLAY1S model in PLAXIS 2D develops a more certain way of calculating the factor of safety this may contribute to a more accurate number not only considering the worst-case scenario.

5.2 Uncertainties in PLAXIS 2D calculation

There are input parameters and results retrieved that are not as expected. The first uncertainties are the values of M_e which are high. In the final results are values used between 1.2-1.5 which would represent critical friction angles of 48-90 degrees. For the actual values retrieved in the laboratory the friction angle is not even possible to calculate. This fact contributes to that the value of M_e gets uncertain. However, the analysis performed with the lowering of the M_e-value shows that there is no significant change in slip surface due to change in M_e. The lowering of M_e should probably have been larger, for example to values below one which would represent critical friction angles for the soil around 30 degrees. Numbers around 30 degrees are more reasonable for clays. The value of M_e affects the failure in extension and is therefore an important parameter for the failure mechanism when considering anisotropy. If further lowering of M_e would have been analysed the result of the slip surface could have changed in shape.

Another input parameter that is an interesting subject in the modelling of slope stability is the high value of sensitivity in the area of Smådala. This value is assumed to be too high for the model to consider. In reality, high sensitivity is an indication of quick clay which behaviour is hard to anticipate. Since the model is limited to a certain amount of sensitivity consideration may the failure mechanism be different than the result indicates. The sensitivity behaviour can locally have very different characteristics even in the slope section modelled. The difficulty of modelling high sensitivity is, however, the case for both modelling in PLAXIS 2D with Creep-SCLAY1S and Geostudio SLOPE/W since the natural behaviour is uncertain.

There have been difficulties with modelling the erosion process the right way since the input parameters used are based on today's conditions which are after erosion. The problem with the change of the characteristics in the slope to something not representing today's values could be seen. For example, the value for OCR presented in the result is significantly higher below the river where most of the erosion process takes place, meanwhile, the OCR is quite constant at the edge of the slope. For further analysis, it would be preferable to evaluate input parameters that can be developed to values before erosion. During the erosion process, could also the behaviour of large displacements be recognised. The horizontal and vertical displacements are unreasonable large and could be further investigated. However, the reason for such high displacements during the erosion process could be due to boundary conditions. The large horizontal displacements appear at the right boundary of the model and during the erosion is this defined as open for groundwater flow. A closed boundary could decrease displacements. The displacements are, however, set to zero before the failure stage and should not affect the failure mechanism resulted.

6

Conclusion and recommendations

There are different ways of modelling slope stability with considerations for anisotropy. In Geostudio SLOPE/W, which is based on limit equilibrium method, the anisotropy is not considered as a function in the calculation. However, the effects of anisotropy were considered by dividing the slope section into different vertical zones with a change in characteristics. The geometry with vertically divided sections of a soil is not something that appears in reality. Therefore, the method with zones in Geostudio SLOPE/W is considered to be a simplified way of considering anisotropy. In Creep-SCLAY1S in PLAXIS 2D is anisotropy considered in the calculation. This is done by using input data such as stress-path (M-values) both in compression and extension for the soil. By using these values, a stress ratio correspondent to normally consolidated situation can be evaluated, and thus the state variable for anisotropy (α_0). The evolution of anisotropy (ω) in the soil can also be estimated using the stress conditions. With these parameters, the horizontal soil layers are considering anisotropy without dividing the layers vertically.

Problems before this analysis were to consider anisotropy in the zone of extension (passive zone in Swedish terms). By using Creep-SCLAY1S it is possible to consider anisotropy in all locations in the slope section concerning compression or extension behaviour. The finite element mesh allows calculating the different state of the soil in each stress point. This can create a more detailed stress/strain/deformation information at different locations.

The factor of safety is affected by the considerations for anisotropy. The results indicate that the factor of safety is higher when considering anisotropy in Creep-SCLAY1S than in Geostudio SLOPE/W. The calculation of the factor of safety in Creep-SCLAY1S may, however, be uncertain so further conclusions are difficult to determine. An assumption that can be made is that the factor of safety should be higher for the case with appropriate consideration for anisotropy since the characteristics of the soil are not as simplified as for the calculation in Geostudio SLOPE/W.

The use of laboratory data for input data to slope stability problems was needed. For evaluation of compression and swelling index for the soil both CRS and Oedometer tests were available. The evaluated parameters did vary between the different tests, and in the final input to the model used only the swelling and compression index from Oedometer tests. Additionally, more information about creep ratesand the preconsolidation pressure could be evaluated from the Oedometer test. Consequently, that the result from the CRS was largely unused in the end. The test result from the Triaxial test in extension were all much higher than expected (both theoretically and in practice) as described in the discussion. The exact values evaluated from the Triaxial test in extension could therefore not be used in the final analyses. However, all laboratory tests were initially considered during the process of retrieving input data.

When considering anisotropy in slope stability Creep-SCLAY1S is a good model to use since the number of different results retrieved in output are valuable. The factor of safety is important information, but for projects where the general mapping of slope stability along Göta Älv valley is in question, Creep-SCLAY1S a model which gives a bigger picture of the soil characteristics. Considering the ethical aspects is still a factor of safety important to fulfil the guarantee to anticipate any landslides of the slope.

Further refinements and recommendations for future work are listed below.

- It is important to analyse how the calculation of the factor of safety in Creep-SCLAY1S can be improved. Since the variation is very large in the analyses, the factor of safety is still uncertain in comparison to the calculation performed in Geostudio SLOPE/W.

- The laboratory method of performing Triaxial test in extension could be analysed to see if the test method, such as the membrane effects, affects the high values of M_e.

- The modelling of pore pressures in Creep-SCLAY1S can be refined for a more accurate pore water pressure distribution.

- The comparison between the soil test in PLAXIS 2D and the evaluated data from laboratory test is an important aspect, to analyse the quality of the performed laboratory tests.

- The input data are based on sample points located in the slope section represented by today's geometry. A recommendation could be to take more samples further away from the slope, where the conditions are more similar to the time before the erosion appeared. In that way could the stress history and initial values become more accurate.

Bibliography

[1] Abed, A., Korkiala-Tanttu, L., (2018) Stability analysis for road-cutting: Review, recommendations and examples. *Research reports of the Finnish Transport Agency 49/2018*. DOI: 10.13140/RG.2.2.10562.02244

[2] Andree, L. (2006-12-13). Få varningssystem längs Göta älv. *Göteborgs-Posten*. Retrieved 2020-04-13 from: https://www.gp.se/nyheter/g%C3%B6teborg/f%C3%A5-varningssystem-l%C3%A4ngs-g%C3%B6ta-%C3%A4lv-1.1176030

[3] Bentley (a). (2019). *PLAXIS 2D Manual: General Information*. Retrieved 2020-02-06 from: https://www.plaxis.com/support/manuals/plaxis-2d-manuals/

[4] Bentley (b). (2019). *PLAXIS 2D Manual: Reference Manual*. Retrieved 2020-04-15 from: https://www.plaxis.com/support/manuals/plaxis-2d-manuals/

[5] Bergström, F. Alaydi, K. (2020). *Projekterings-PM, Stabilitetsutredning: Smådala*. WSP Samhällsbyggnad. WSP Sverige AB.

[6] Eniro. (2020). [Online map]. Retrieved 2020-05-04 from: https://kartor.eniro.se/

[7] Geological Survey of Sweden, SGU. (2019). *SGUs map viewer*. Retrieved 2020-01-23 from: https://www.sgu.se/en/products/maps/map-viewer/

[8] Geological Survey of Sweden, SGU. (n.d.)(a). *Jord*. Retrieved 2020-02-05 from: https://www.sgu.se/om-geologi/jord/

[9] Geological Survey of Sweden, SGU. (n.d.)(b). *The Bedrock of Sweden*. Retrieved 2020-02-06 from: https://www.sgu.se/en/geology-of-sweden/the-bedrock-of-sweden/

[10] Geological Survey of Sweden, SGU. (n.d.)(c). *Maps generator*. Retrieved 2020-05-04 from: http://apps.sgu.se/kartgenerator/maporderen.html

[11] Google Maps. (2020). [Online map]. Retrieved 2020-04-16 from:

https://www.google.se/maps/@57.7026129,11.9728919,14z

[12] Gras, J. P., Sivasithamparam,N., Karstunen, M., Dijkstra, J., (2017). Strategy for consistent model parameter calibration for soft soils using multi-objective optimisation. *Computers and Geotechnics, Volume(90), 164-175.* DOI: 10.1016/j.compgeo.2017.06.006

[13] Gras,J. P., Sivasithamparam,N., Karstunen, M., Dijkstra, J., (2018). Permissible range of model parameters for natural fine-grained materials. *Acta Geotechnica, Volume(13), 387-398.* DOI: 10.1007/s11440-017-0553-1

[14] Holm, D., (2016) *Influence of strain rate in CRS tests. A laboratory study of three Swedish clays.* (Master's thesis, Royal Institute of Technology, KTH, Department of Civil and Architectural Engineering)

[15] Karstunen, M. and Amavasai, A. (2017). *BEST SOIL: Soft soil modelling and parameter determination.* Chalmers Univeristy of Technology, Gothenburg, Sweden. ISBN: 978-91-984301-0-3.

[16] Knappett, J. A., Craig R. F. (2012). *Craig's Soil Mechanics.* London and New York: Spon Press.

[17] Krahn, J., (2003). The 2001 R.M. Hardy Lecture: The limits of limit equilibrium analyses. *Canadian Geotechnical Journal, Volume(40), Issue 3, 643-660.* DOI: 10.1139/t03-024

[18] Morgenstern, N., Price, V., (1965). The Analysis of the Stability of General Slip Surfaces. *Géotechnique, Volume(15), 79-93.* DOI: 10.1680/geot.1965.15.1.79

[19] Persson, H. Bengtsson, P-E. Lundström, K. Karlsson, P. (2011). *Bedömning av grundvattenförhållanden för slänter längs Göta älv.* Retrieved 2020-02-06 from: https://www.swedgeo.se/en/samhallsplanering–sakerhet/skredriskkartering/skredrisk-gota-alv/rapporter/

[20] Petalas, A. L., Karlsson, M., Karstunen M., (2019), Modelling of undrained shearing of soft natural clays, *E3S Web Conf., Volume (92)* DOI: https://doi.org/10.1051/e3sconf/20199215001

[21] Royal Swedish Academy of Engineering Science, IVA. (1995). *Commission on Slope Stability (Report 3:95).* Retrieved 2020-01-23 from: https://www.swedgeo.se/sv/kunskapscentrum/publikationsserier/i-samverkan-med-andra/skredkommissionen/

[22] Seequent Solutions. (n.d.). *SLOPE/W Features.* Retrieved 2020-04-15 from: https://www.geoslope.com/products/slopew/features

[23] Sellin, C., Karlsson, M., and Karstunen, M., (2021). Advantages and challenges of advanced slope stability analyses. *Unpublished.* Chalmers University of Technology, Gothenburg, Sweden.

[24] Sivasithamparam, N. (2012). Modelling Creep Behaviour of Soft Soils. *Internal report. Unpublished.* Plaxis B. V. and University of Strathclyde.

[25] Sivasithamparam, N., Karstunen, M., Bonnier, P., (2015). Modelling creep behaviour of anisotropic soft soils. *Computers and Geotechnics, Volume(69), 46-57.* DOI: 10.1016/j.compgeo.2015.04.015

[26] Swedish Geotechnical Institute, SGI. (2012). *Landslide risks in the Göta River valley in a changing climate*, Final report part 2 - Mapping. Retrieved 2020-01-23 from: https://www.swedgeo.se/sv/kunskapscentrum/publikationsserier/utredningar

[27] Sällfors, G. (2013). *Geoteknik.* Göteborg: Cremona Förlag vid Chalmers tekniska högskola.

[28] Turesson, A. (2020). *Fördjupad stabilitetsutredning, Smådala: Markteknisk undersökningsrapport, Geoteknik.* WSP Samhällsbyggnad. WSP Sverige AB.

[29] Wheeler, S. J., Näätänen, A., Karstunen, M., and Lojander, M., (2003), An anisotropic elastoplastic model for soft clays, *Canadian Geotechnical Journal, 2003, Volume 40(2): 403-418*, DOI: https://doi.org/10.1139/t02-119

[30] Yu, H. S., Salgado, R., Sloan S. W., Kim, J. M., (1998). Limit Analysis versus Limit Equilibrium for Slope Stability. *Journal of Geotechnical and Geoenvironmental Engineering, Volume (124), Issue 1.* DOI: https://doi.org/10.1061/(ASCE)1090-0241(1998)124:1(1)

A

Maps

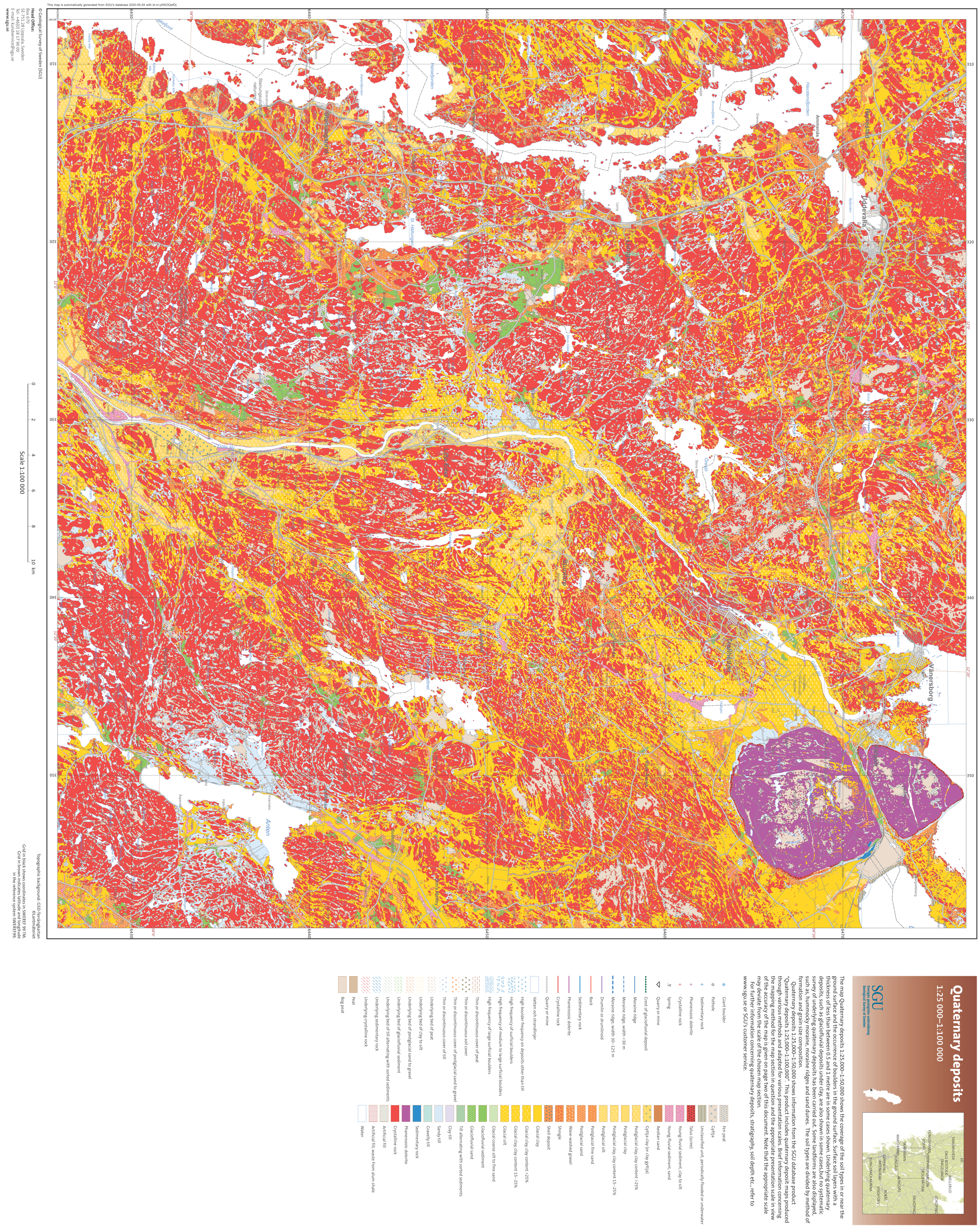

Figure A.1: *Quarternary map from Lilla Edet to Vänersborg (SGU (c), n.d.).*

B

Model parameters

Table B.1: *Data used for pore water pressures in Geostudio SLOPE/W calculation.*

X (m)	Y (m)	Water pressure head (m)
-62	6.6	0
-45	6.6	0
57.6	6.6	0
77.3	8.9	0
122.1	20.9	0
148.2	23.7	0
159.7	24.6	0
209.1	26.4	0
247.7	28.3	0
302.2	29.2	0
-45	-13.4	20
57.6	-13.4	20
77.3	5.1	3.8
77.3	-0.2	8.7
77.3	-4.9	13.7
77.3	-13.2	20.9
122.1	18.4	2.6
122.1	13.4	4.9
122.1	8.4	8.2
122.1	-1.6	13.8
-45	-23.4	30
57.6	-23.4	30
93	10.3	0
0	6.6	0
25	6.6	0
0	-23.4	30
25	-23.4	30
105	15	0

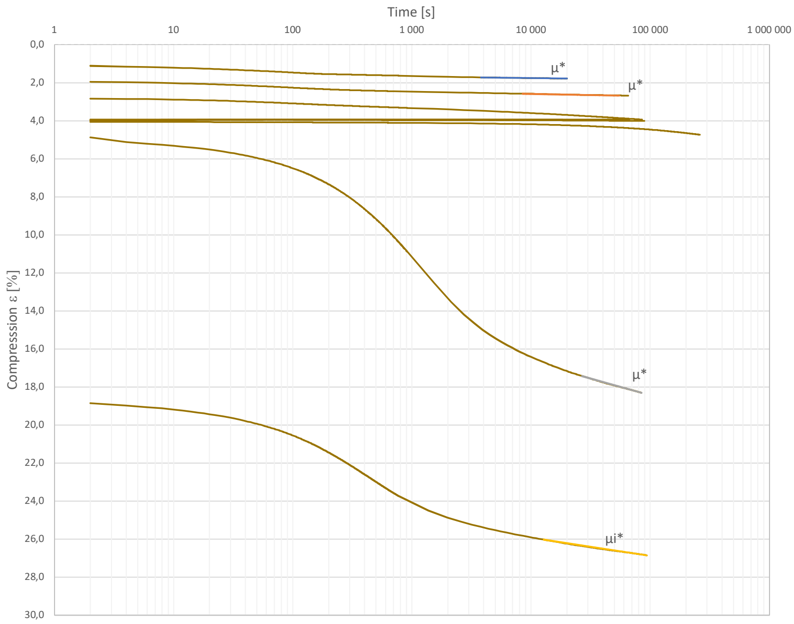

Figure B.1: *Evaluation of creep parameter from Odeometer test. This graph is from oedometer test at point 19WS58 depth 13 meters.*

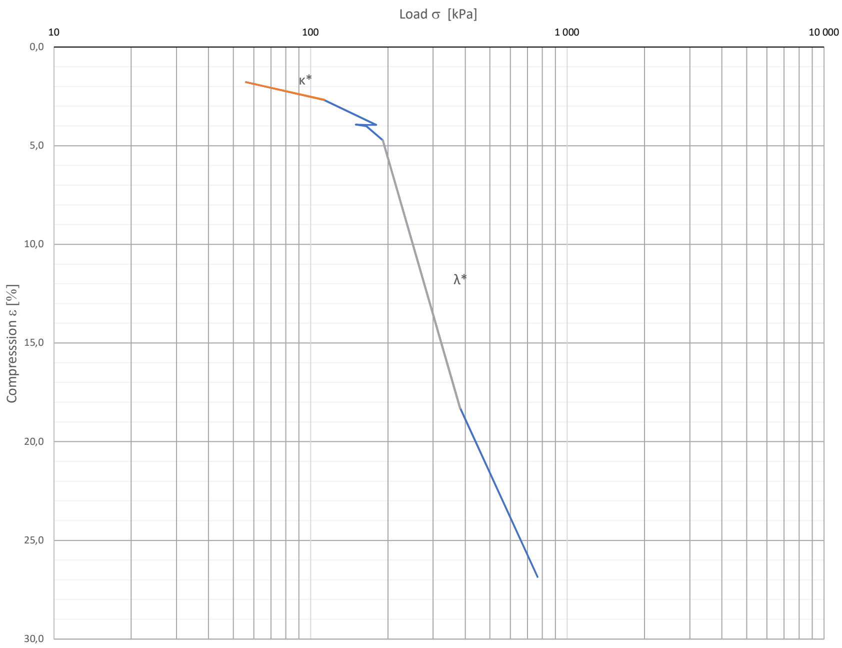

Figure B.2: *Evaluation of modified swelling and compression index from Odeometer test. This graph is from oedometer test at point 19WS58 depth 13 meters.*

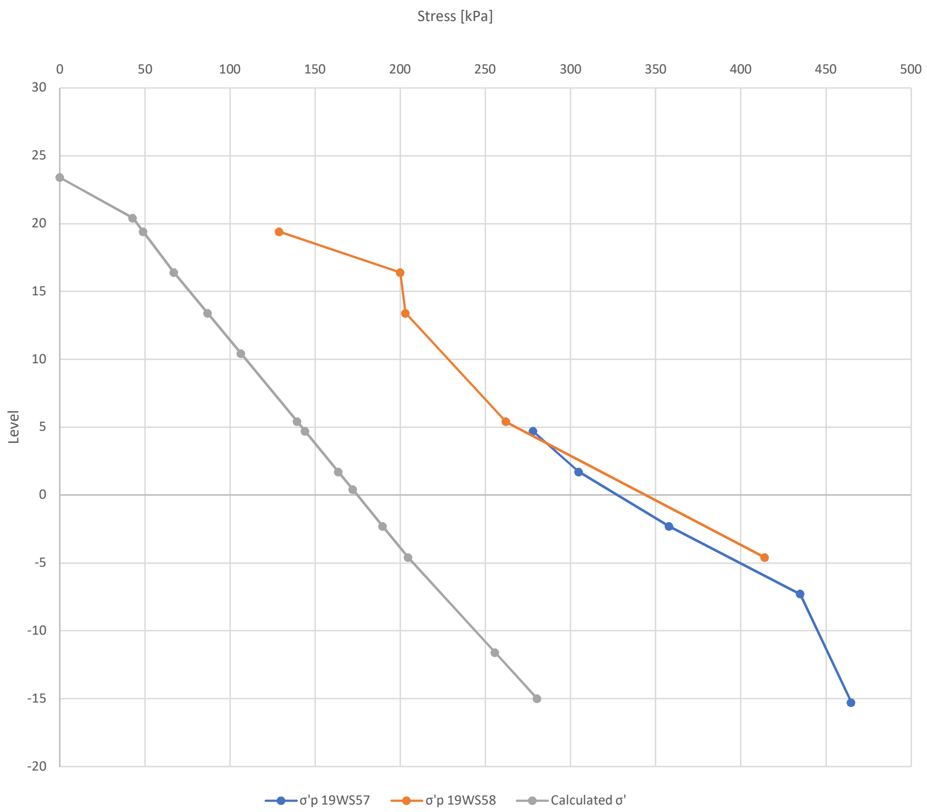

Figure B.3: *Calculated effective stress in grey and preconsolidation stress from laboratory test for poit 19WS57 and 19WS58 in orange and blue with depth.*

C

Results Geostudio SLOPE/W

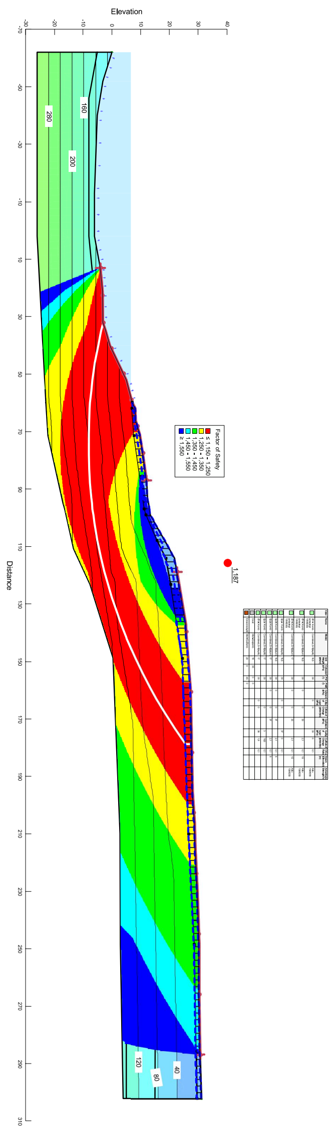

Figure C.1: *Results from GeoStudio SLOPE/W with combined analysis and anisotropy.*

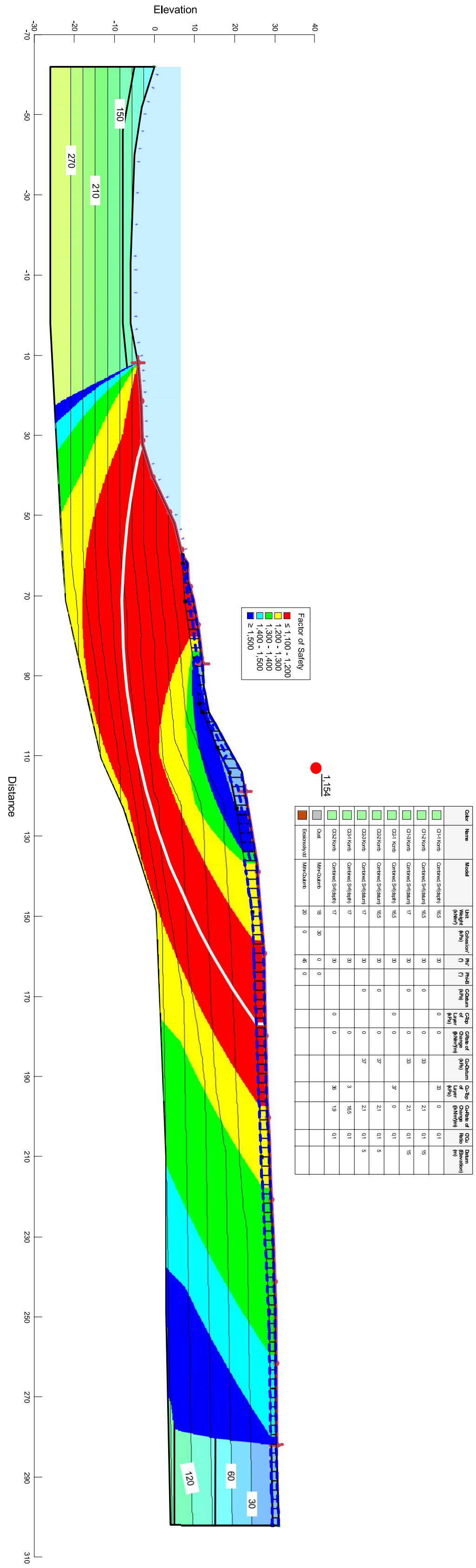

Figure C.2: *Results from GeoStudio SLOPE/W with combined analysis.*

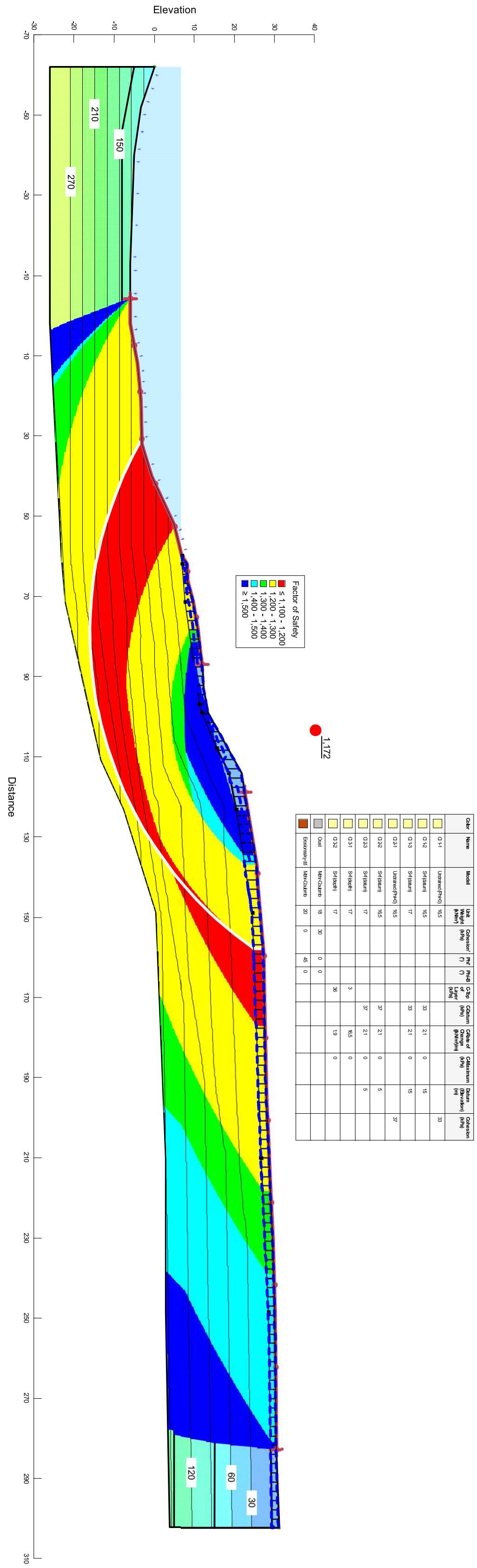

Figure C.3: *Results from GeoStudio SLOPE/W with undrained analysis.*

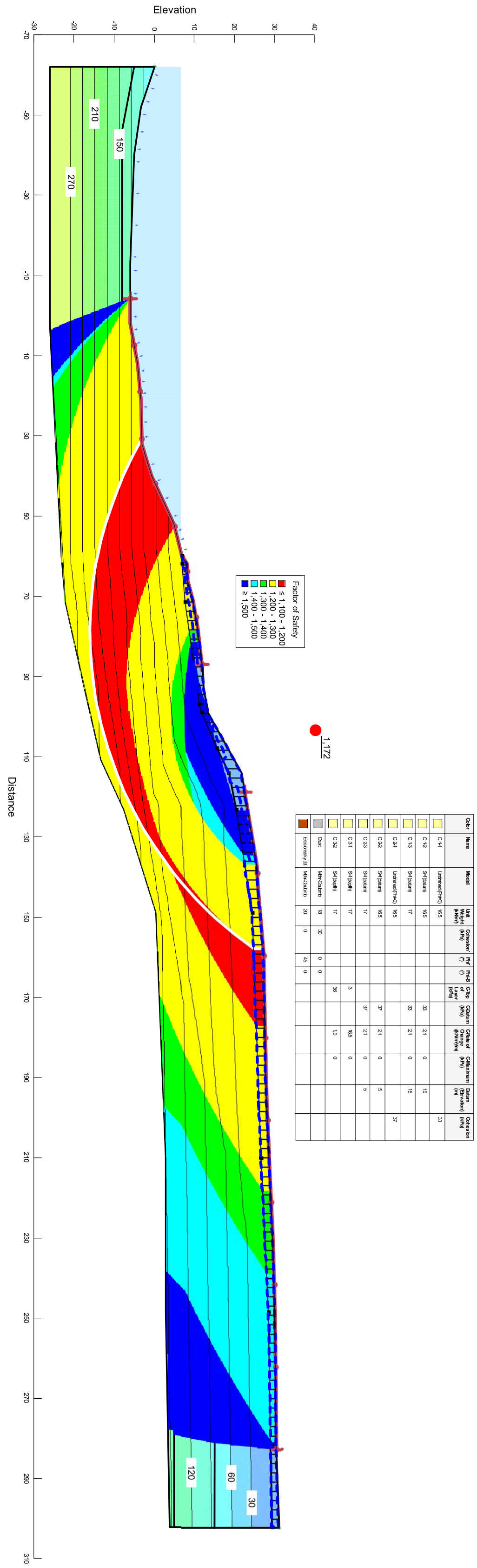

Figure C.4: *Results from GeoStudio SLOPE/W with undrained analysis.*

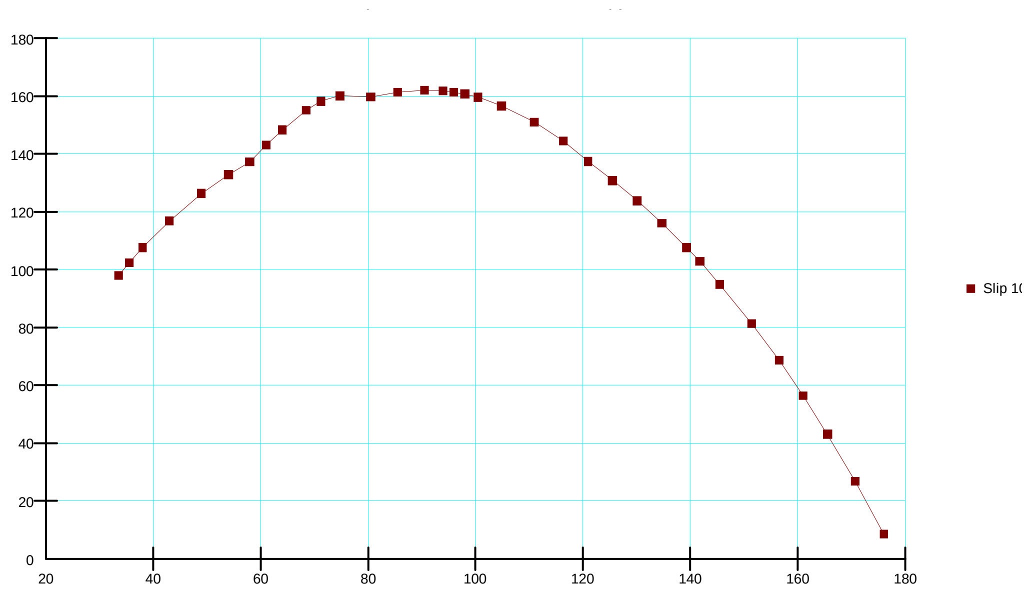

Figure C.5: *Pore pressures along the slip surface for combined analysis with consideration for anisotropy.*

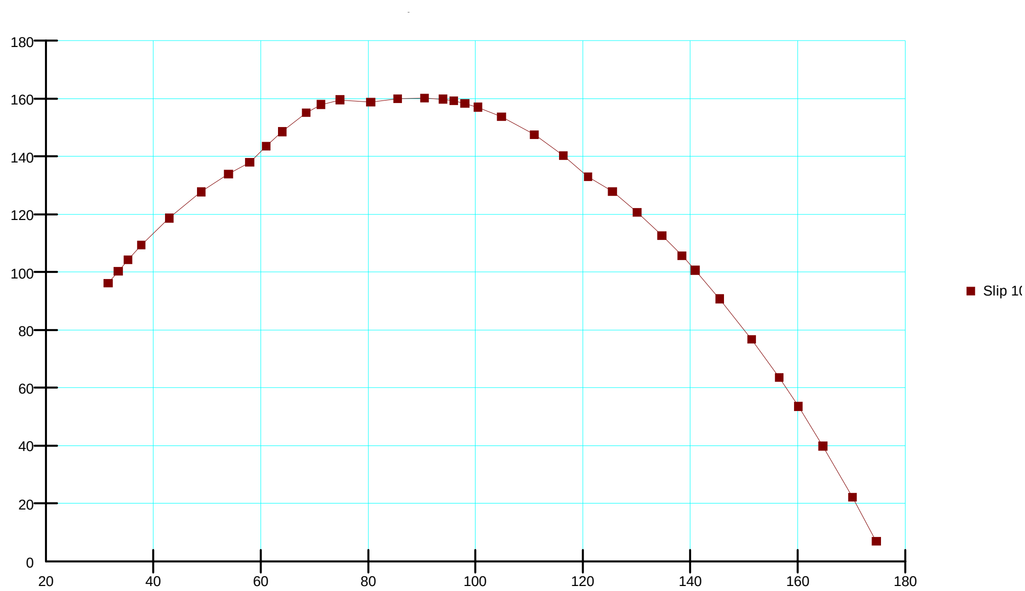

Figure C.6: *Pore pressures along the slip surface for combined analysis.*

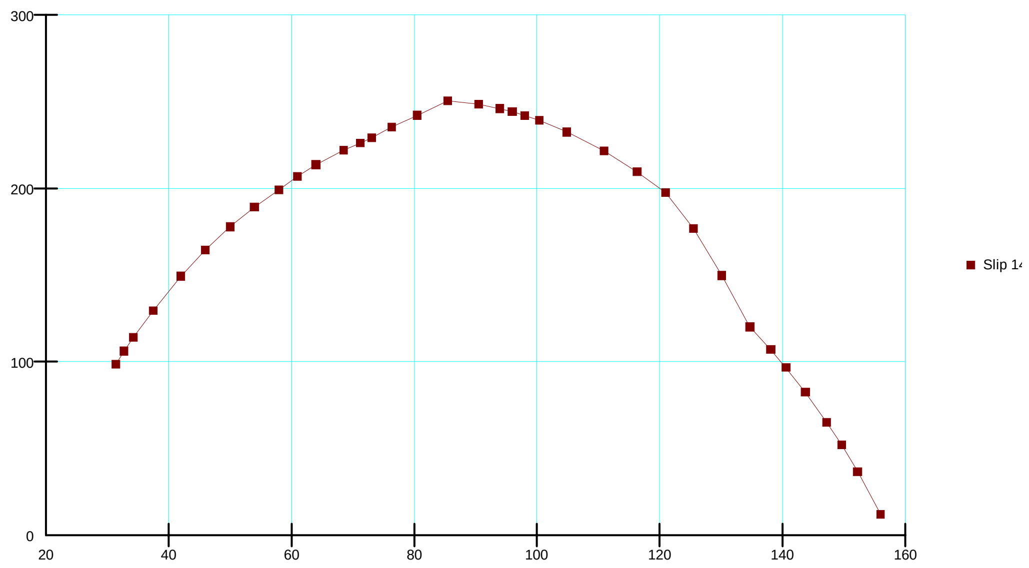

Figure C.7: *Pore pressures along the slip surface for undrained analysis.*

D

Soil test

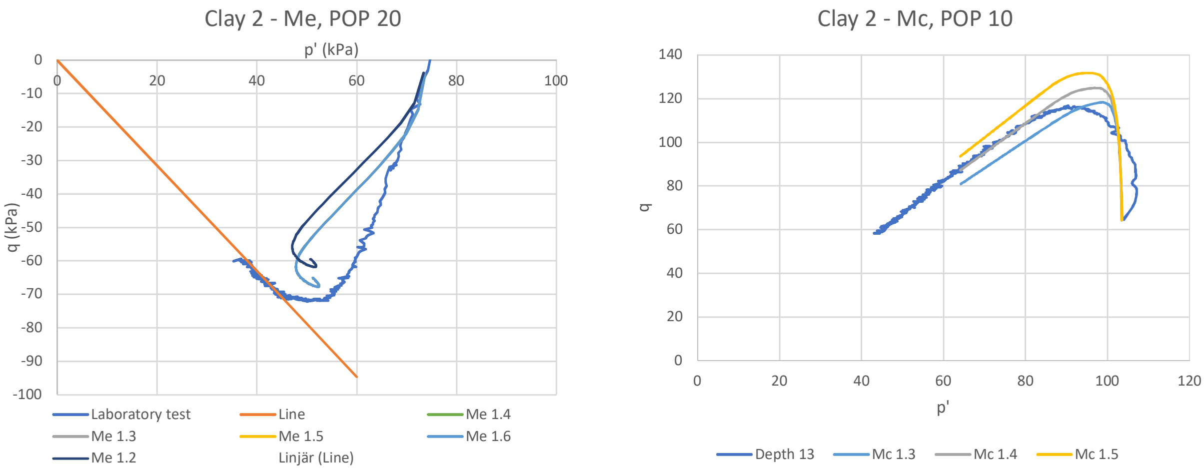

Figure D.1: *Triaxial test: Data from soil test in PLAXIS 2D in comparison with laboratory results of triaxial test for Clay 2. Left graph represents test for M_e and right graph represents test for M_e.*

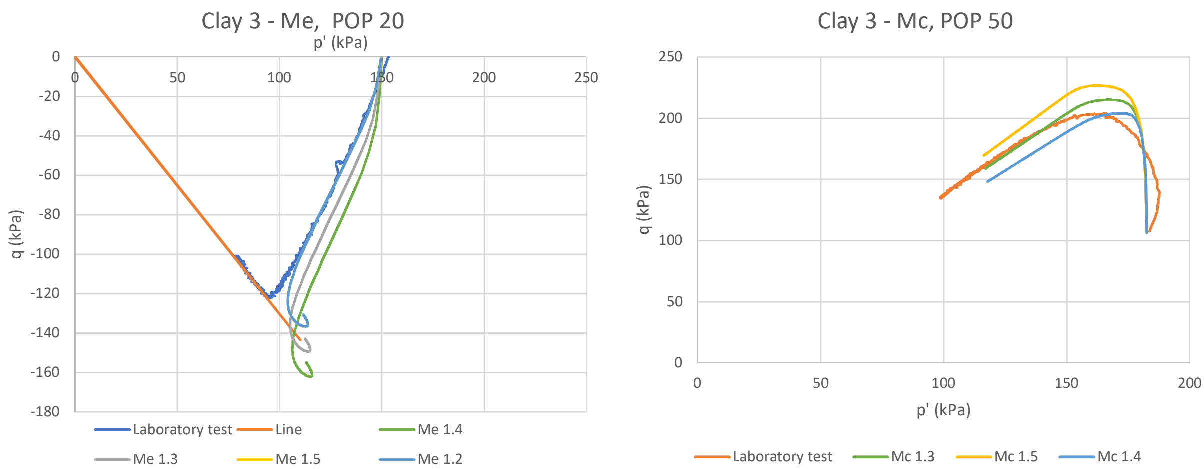

Figure D.2: *Triaxial test: Data from soil test in PLAXIS 2D in comparison with laboratory results of triaxial test for Clay 3. Left graph represents test for M_e and right graph represents test for M_e.*

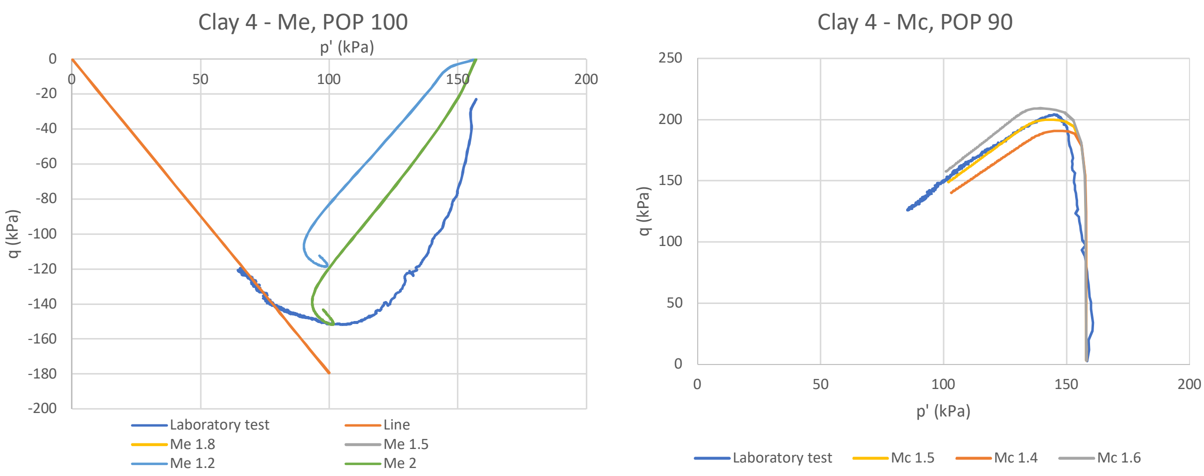

Figure D.3: *Triaxial test: Data from soil test in PLAXIS 2D in comparison with laboratory results of triaxial test for Clay 4. Left graph represents test for M_e and right graph represents test for M_e.*

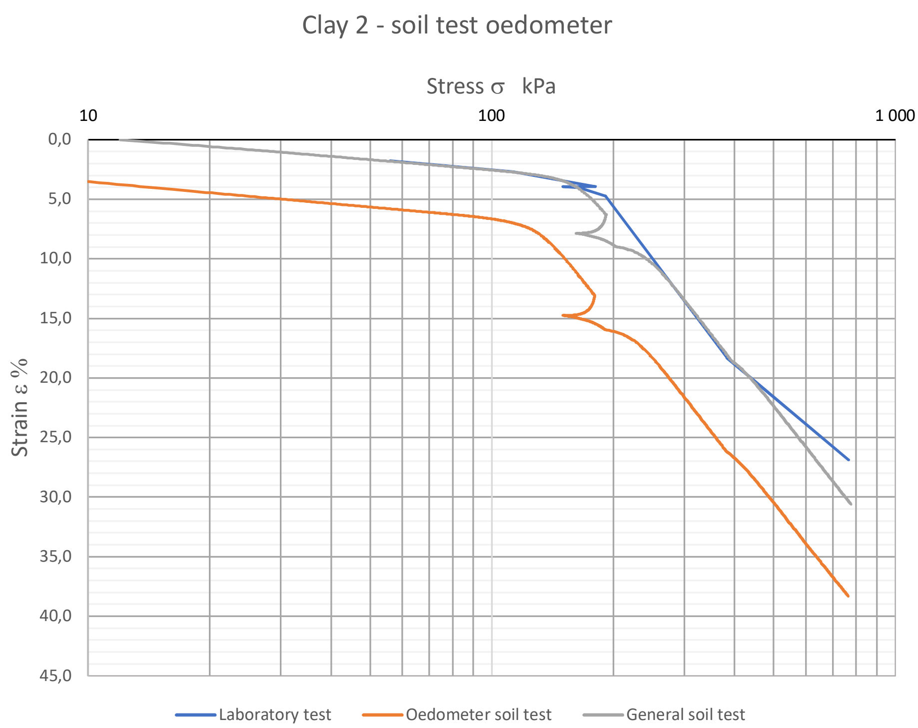

Figure D.4: *Oedometer test: Data from soil test in PLAXIS 2D using both oedometer function and general function in comparison with laboratory results of oedometer test for Clay 2.*

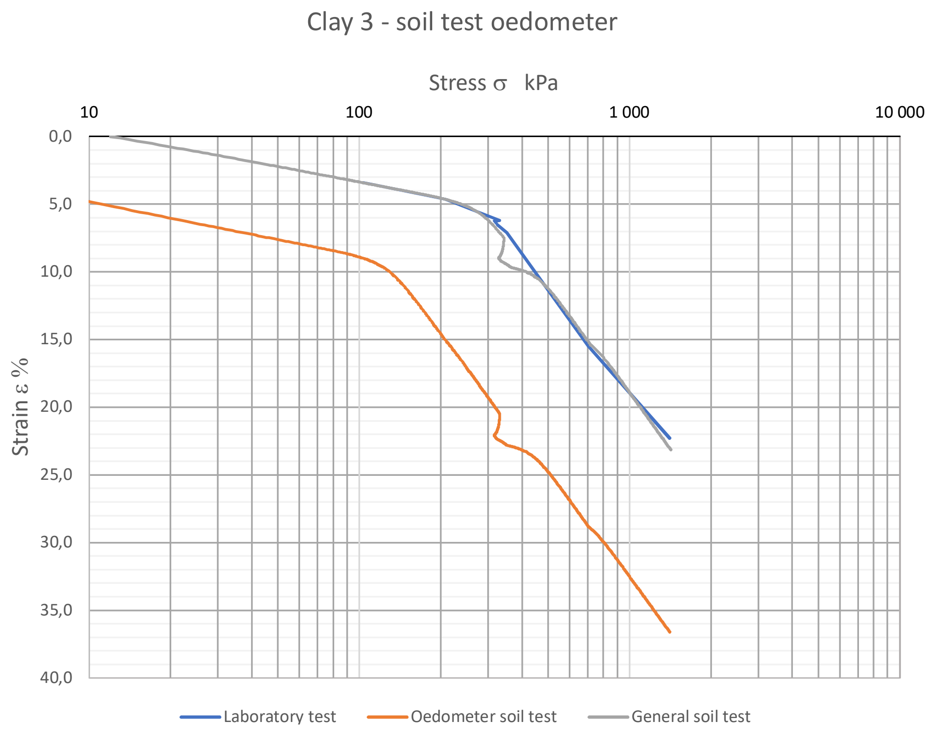

Figure D.5: *Oedometer test: Data from soil test in PLAXIS 2D using both oedometer function and general function in comparison with laboratory results of oedometer test for Clay 3.*

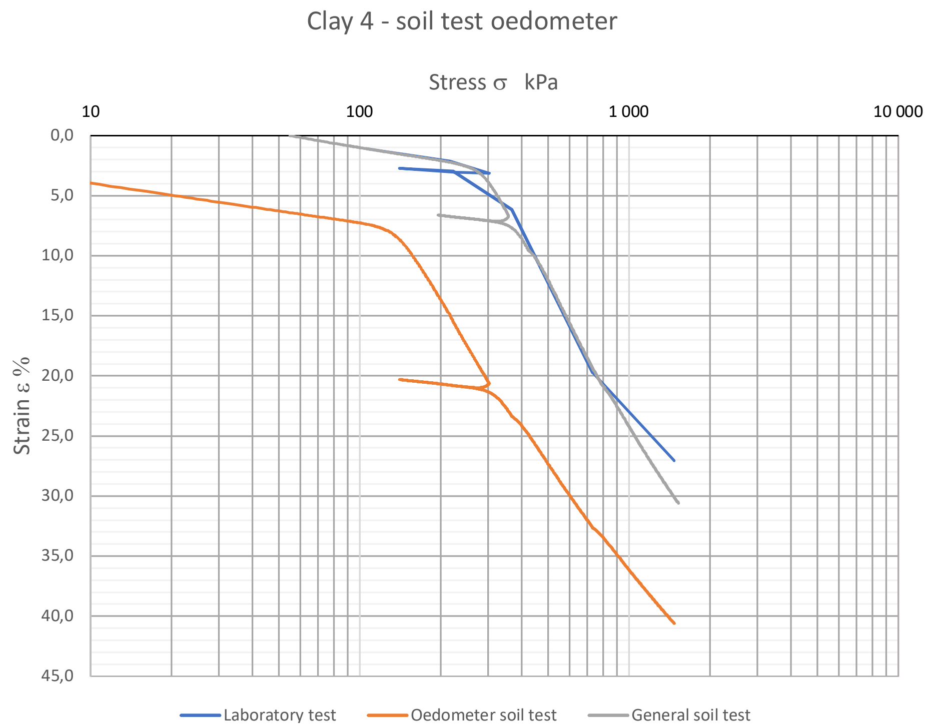

Figure D.6: *Oedometer test: Data from soil test in PLAXIS 2D using both oedometer function and general function in comparison with laboratory results of oedometer test for Clay 4.*

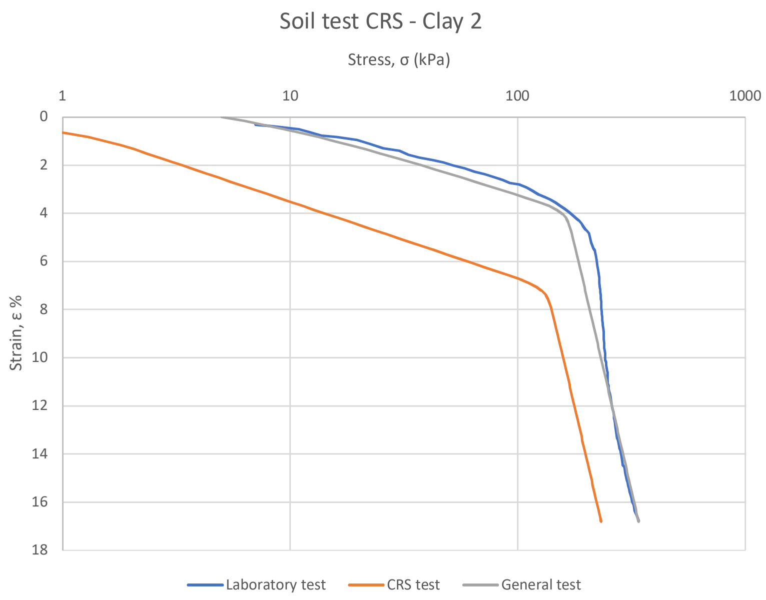

Figure D.7: *CRS test: Data from soil test in PLAXIS 2D using both CRS function and general function in comparison with laboratory results of CRS test for Clay 2.*

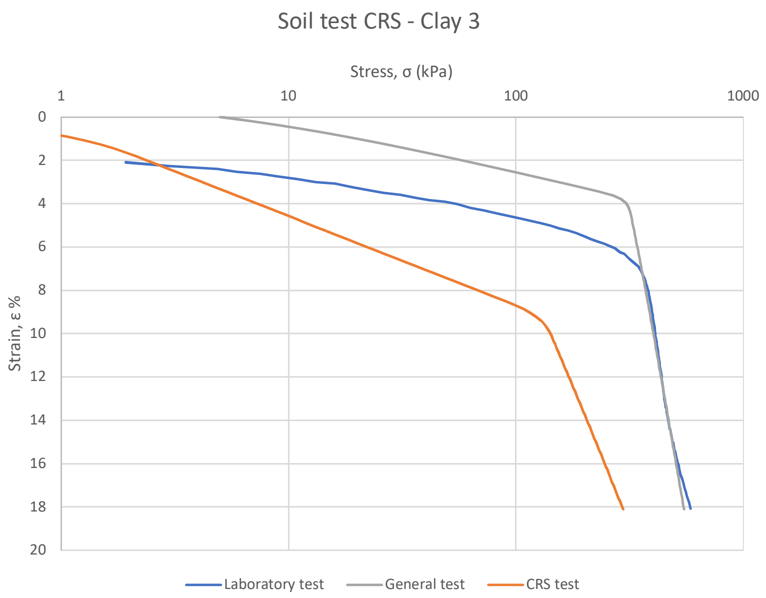

Figure D.8: *CRS test: Data from soil test in PLAXIS 2D using both CRS function and general function in comparison with laboratory results of CRS test for Clay 3.*

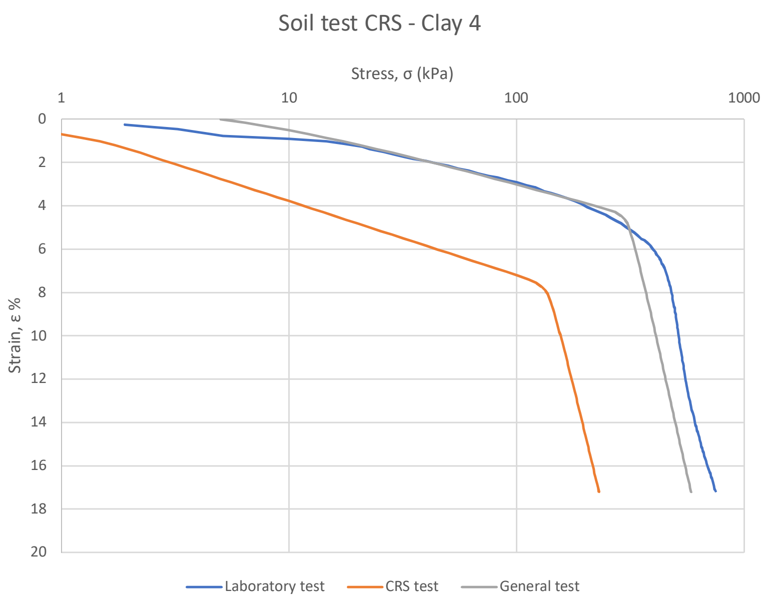

Figure D.9: *CRS test: Data from soil test in PLAXIS 2D using both CRS function and general function in comparison with laboratory results of CRS test for Clay 4.*

E

Results PLAXIS 2D

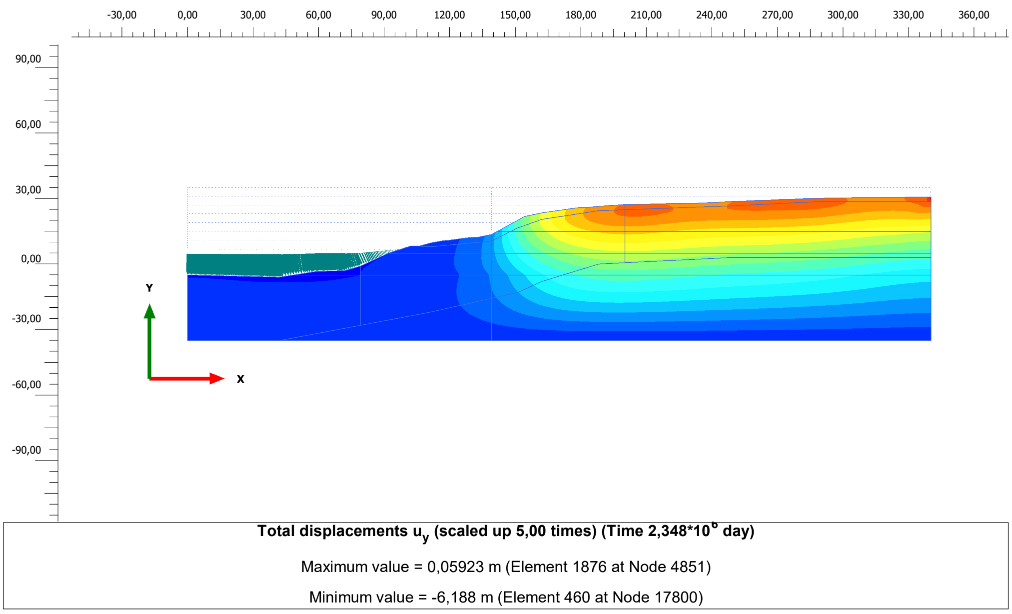

Figure E.1: *Contour of vertical deformations for the original calculation after erosion.*

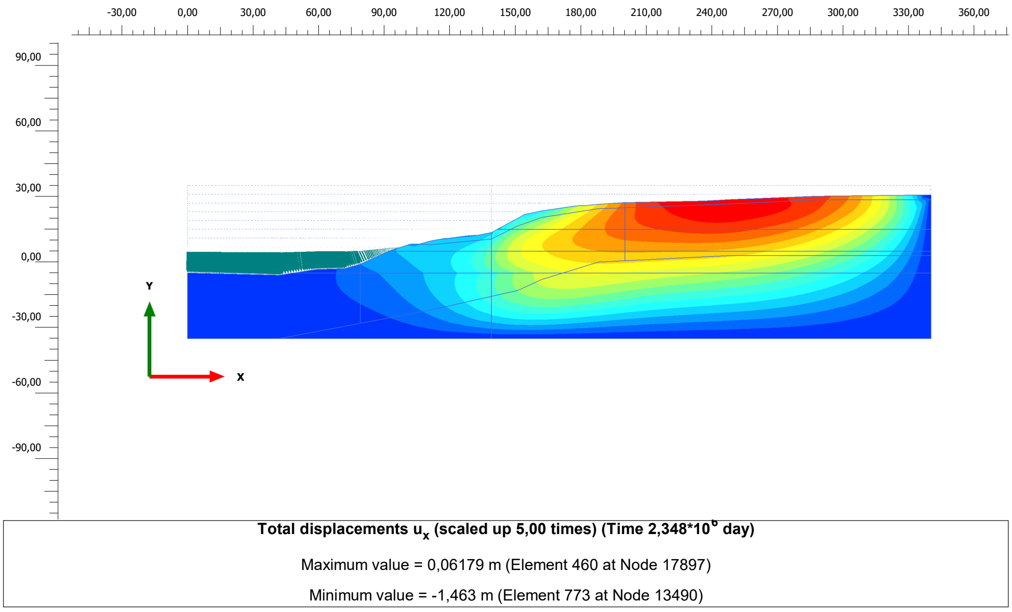

Figure E.2: *Contour of horizontal deformations for the original calculation after erosion.*

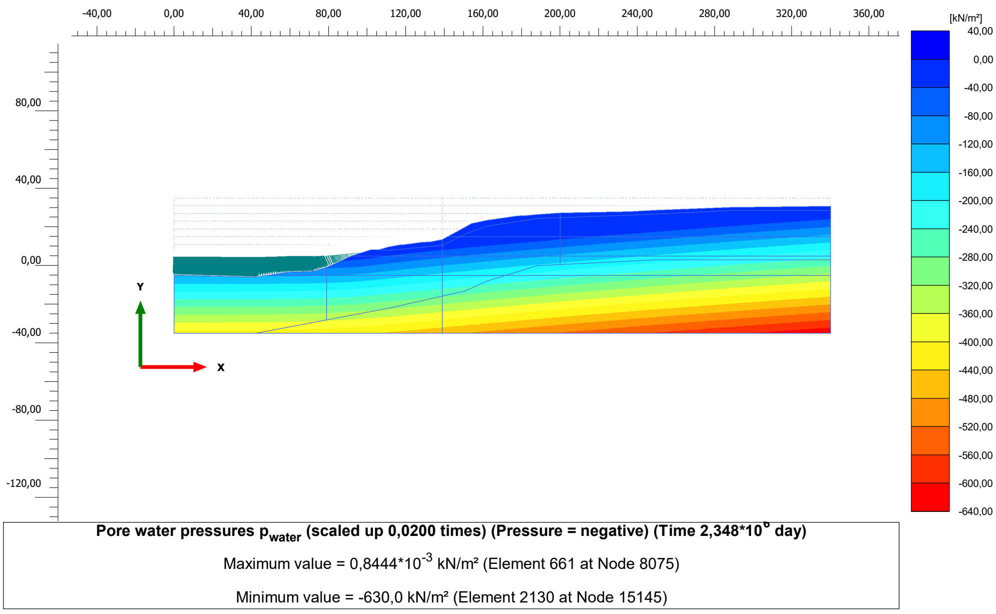

Figure E.3: *Contour of pore pressure distribution for the original calculation after erosion.*

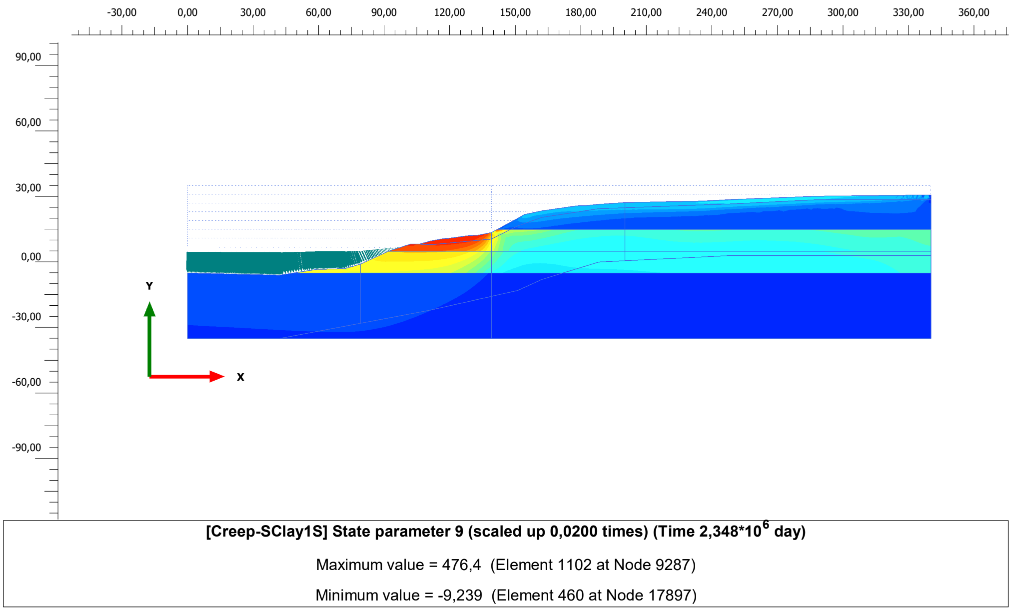

Figure E.4: *Contour of amount of bonding for the original calculation after erosion.*

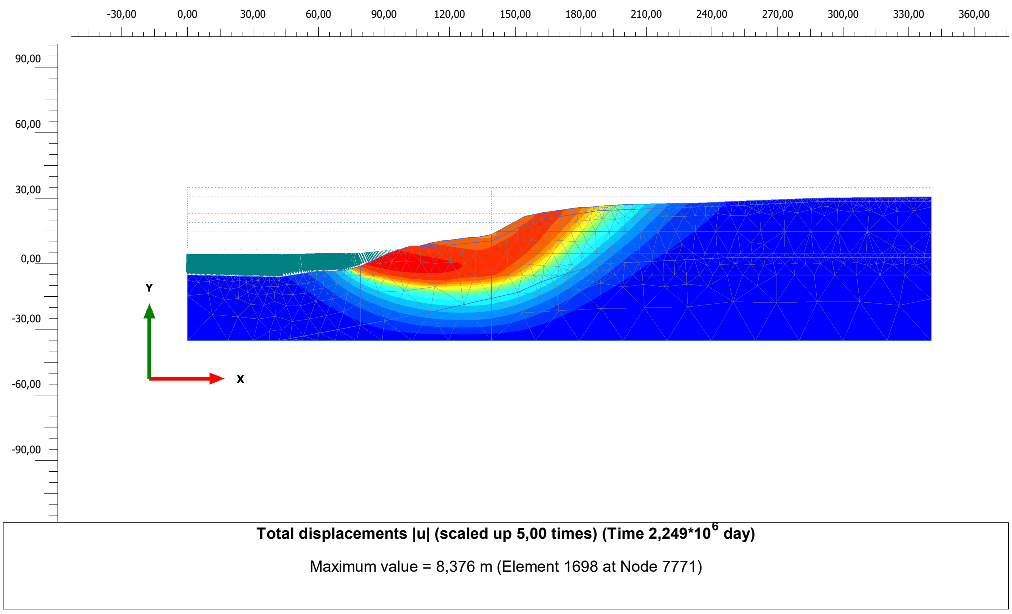

Figure E.5: *Contour of deformation for the case with lowered sensitivity in the soil layers.*

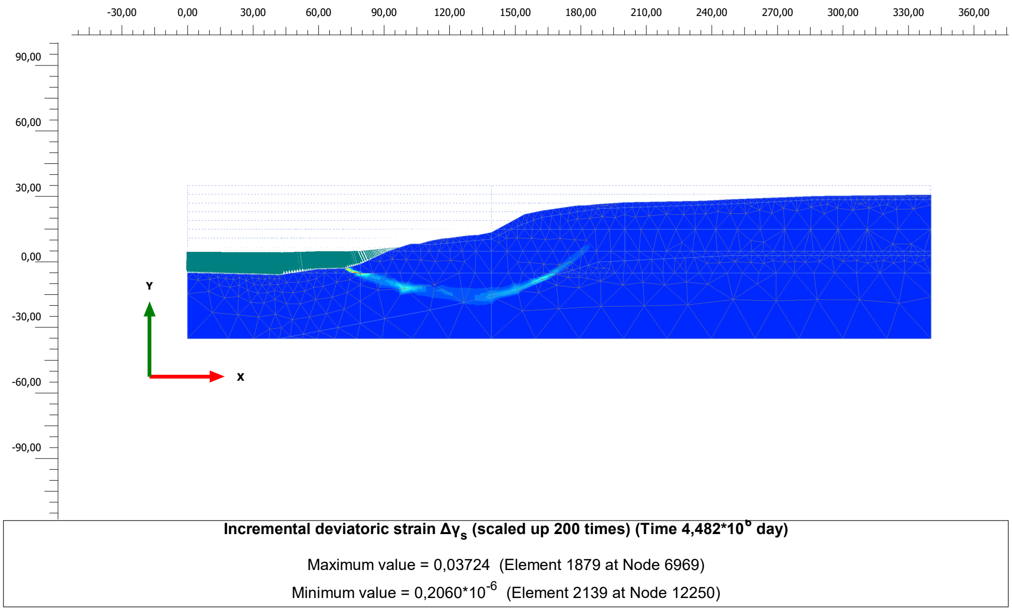

Figure E.6: *Contour of incremental deviatoric strain for the case with longer time per erosion phase.*

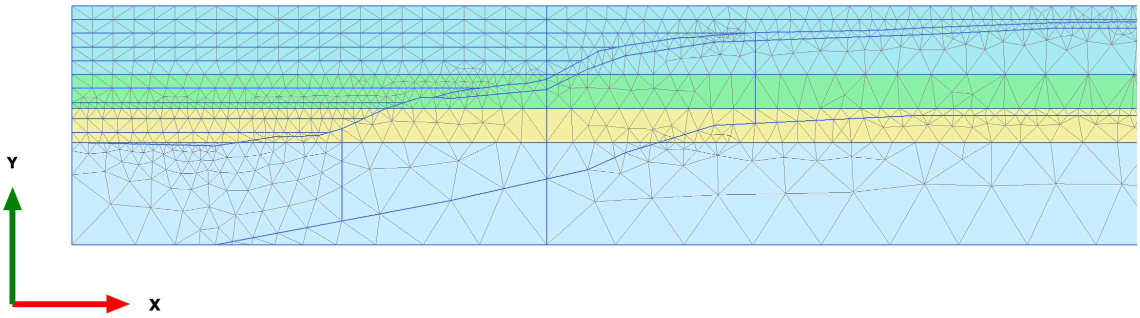

Figure E.7: *Mesh analysis: Mesh density for medium mesh with refinement in the central part of the slope.*

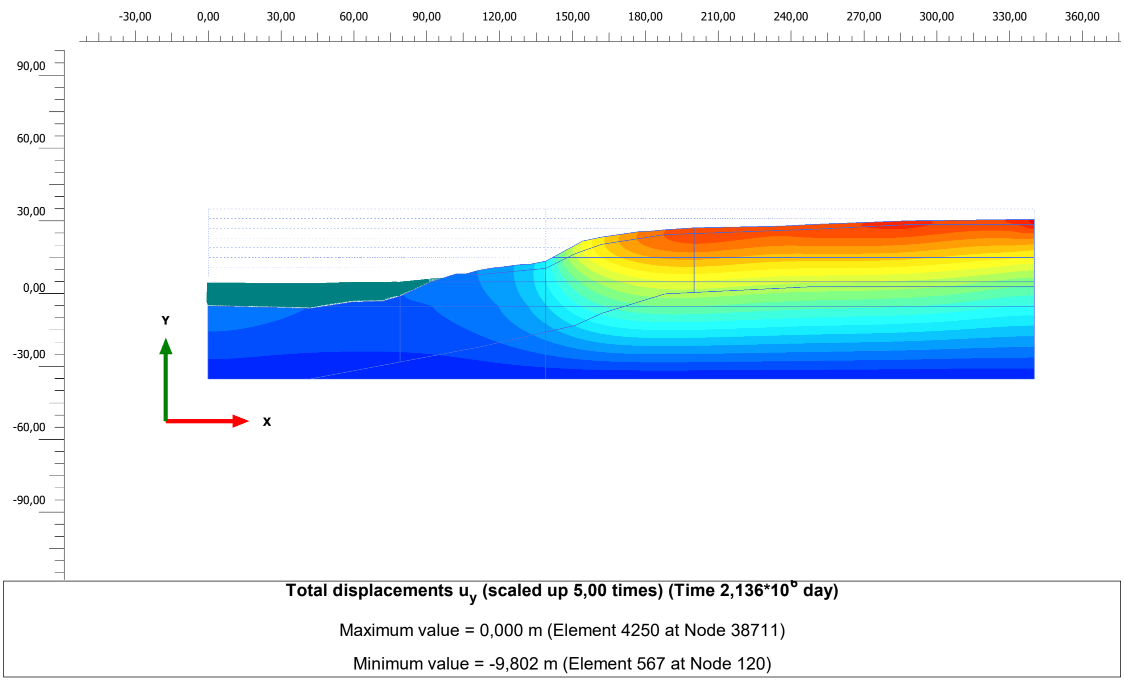

Figure E.8: *Contour of total vertical deformations after erosion of the final result.*

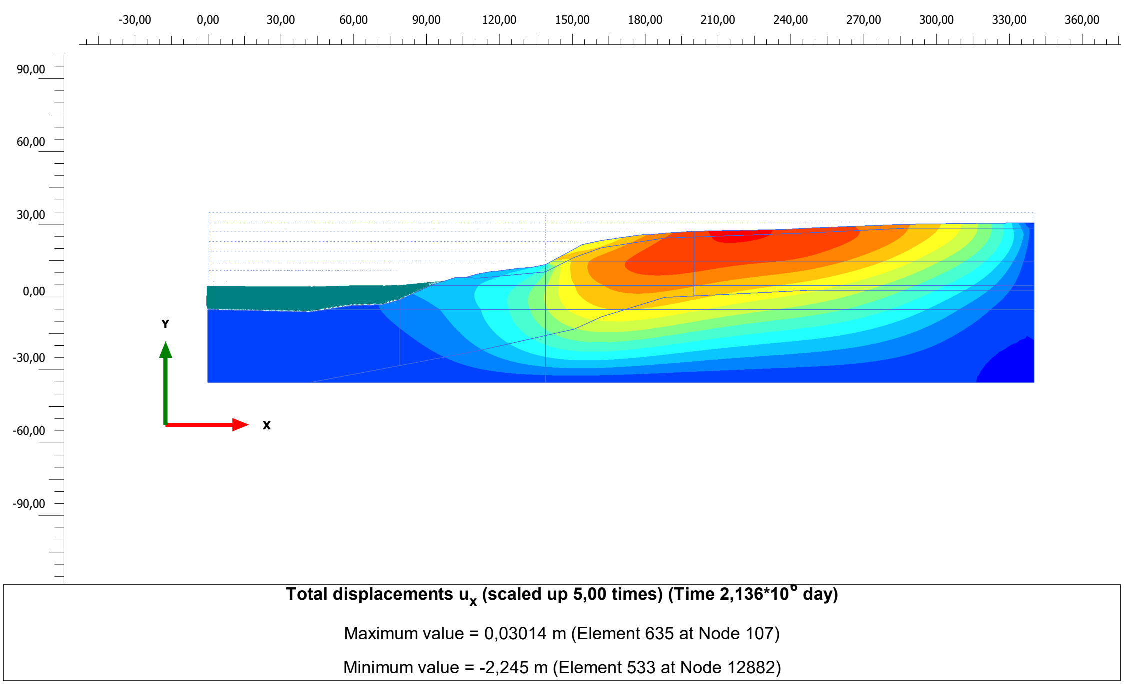

Figure E.9: *Contour of total horizontal deformations after erosion of the final result.*

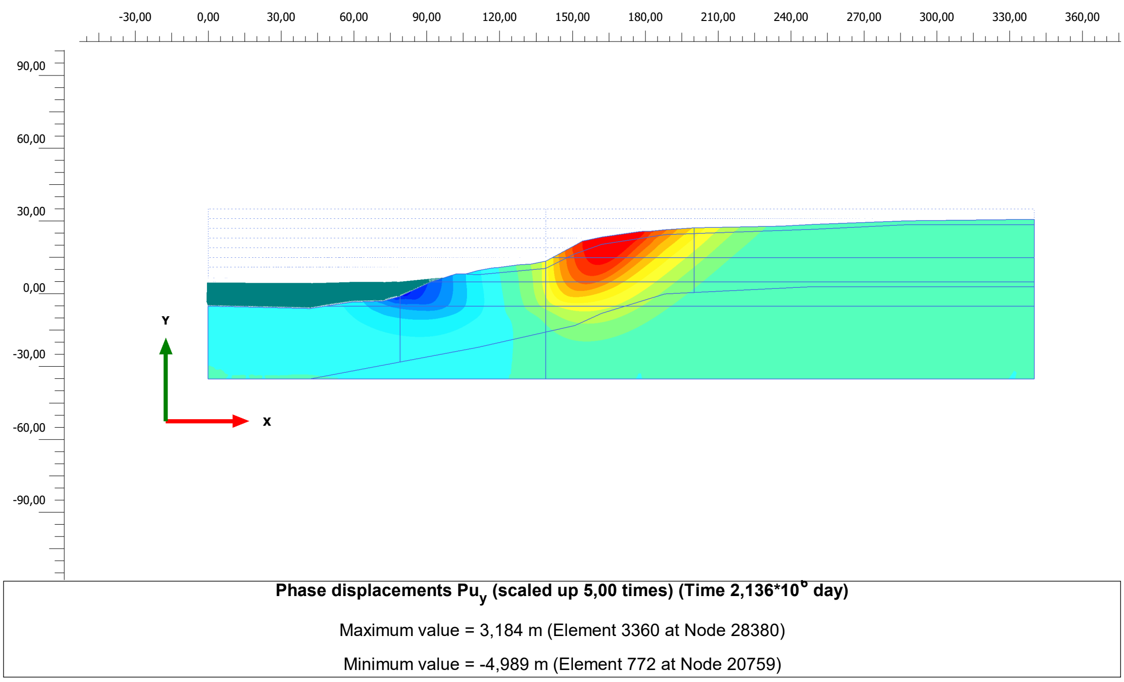

Figure E.10: *Contour of vertical deformations during failure of the final result.*

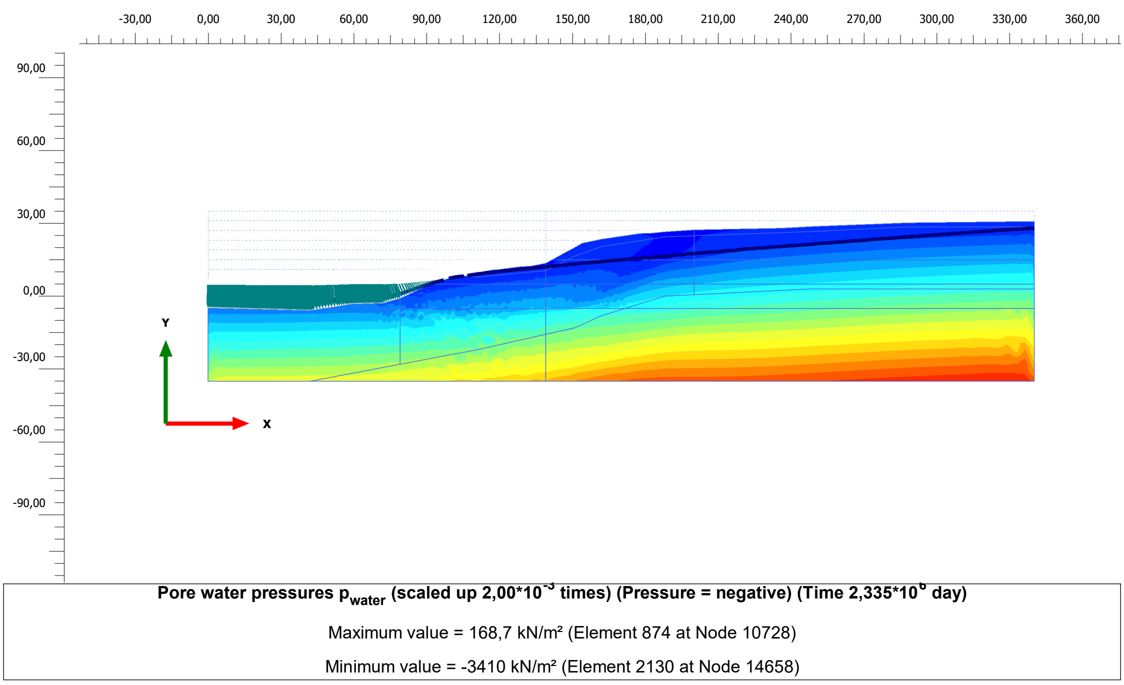

Figure E.11: *Contour of pore pressures and the phreatic line of the final result.*

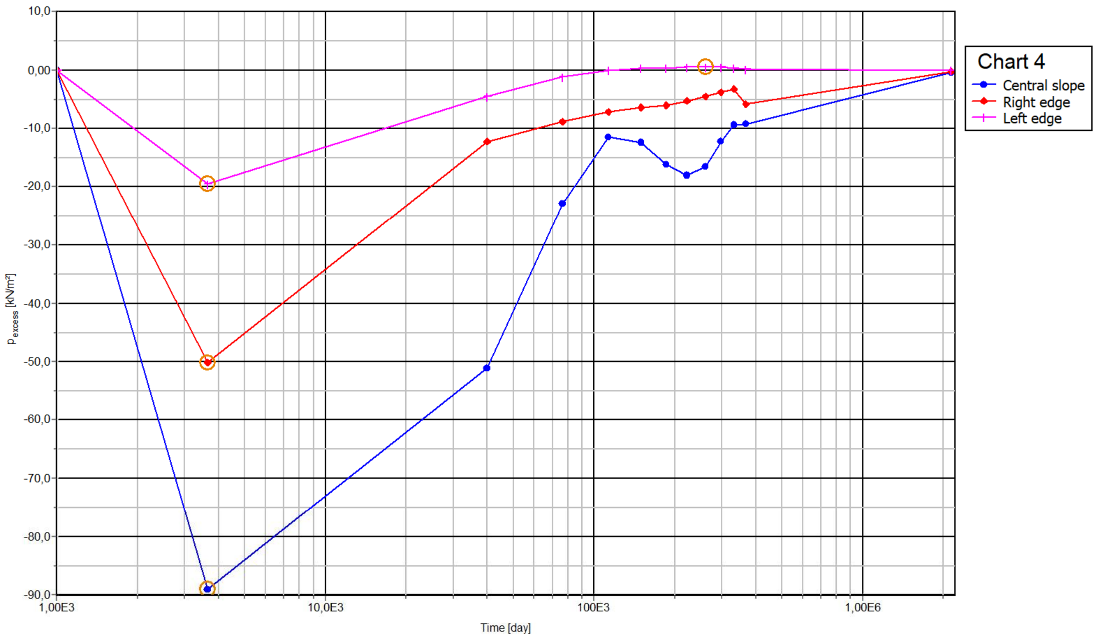

Figure E.12: *Excess pore pressures during erosion of the slope of the final result.*

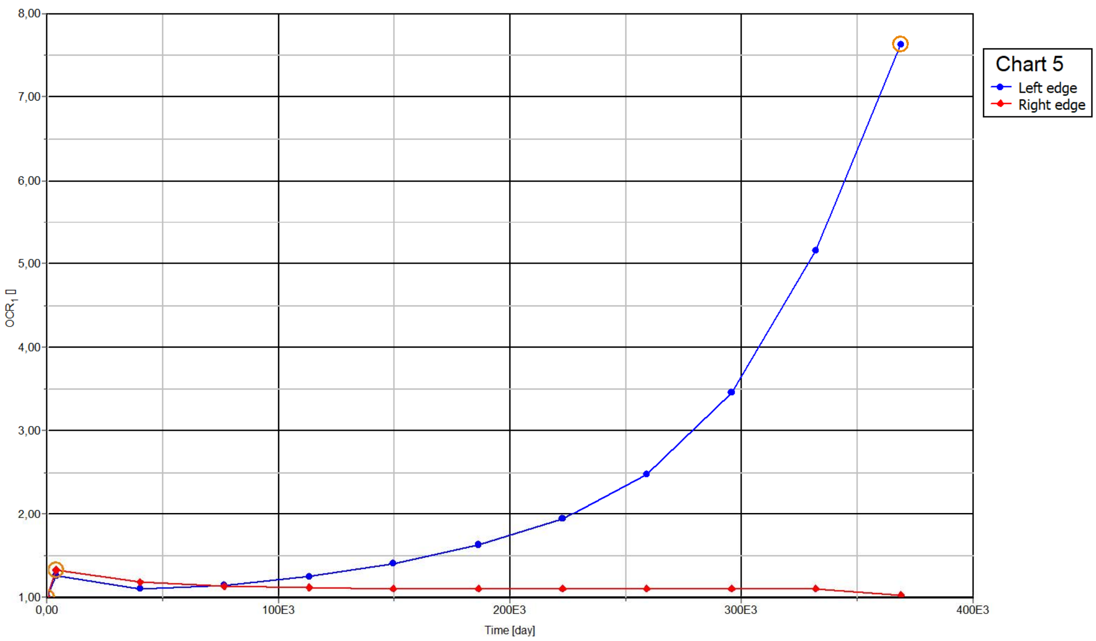

Figure E.13: *Evolution of OCR with time below the river in comparison with at the top of the slope for the final result.*

DEPARTMENT OF ARCHITECTURE AND
CIVIL ENGINEERING
CHALMERS UNIVERSITY OF TECHNOLOGY
Gothenburg, Sweden
www.chalmers.se

CHALMERS
UNIVERSITY OF TECHNOLOGY